Global Instability in Hamiltonian Systems

Thesis presented to obtain the Ph. D. in Applied Mathematics by
Universitat Politècnica de Catalunya

Rodrigo Gonçalves Schaefer

Supervisor: Amadeu Delshams

June 4, 2018

Contents

Acknowledgments

Agraeixo especialment al meu tutor, Amadeu Delshams, per haver acceptat treballar amb mi, per la solidaritat, la paciència i la dedicació.

Agraeixo també a en José Tomás Lázaro per la simpatia infinita i la somriure cada vegada que ens trobem al departament. A l'Eva Miranda per l'interès i la seva disponibilitat. Als professors Arturo Vieiro i Carles Simó pels comentaris després dels seminaris. I també a en Albert Granados per acceptar en entrar al projecte i per la seva ajuda amb la part numèrica.

Me gustaría agradecer a Alberto, mi compañero de despacho por estos 4 años, siempre una buena compañía en los cafés y congresos.

Quero agradecer aos meus amigos de Cabo Frio que se mantiveram sempre presentes apesar da distância, Gabriel, Paulo, Lucas, Marcus, Rhenan, Guilherme e Jonathas. Aos amigos do "Regent Mendieta" que fizeram possível a sobrevivência no primeiro ano de doutorado, Marcos, João e Danilo. Aos colegas de Cerdanyola Murilo, Leonardo, e Jackson. A Juliana pela companhia no período que esteve em Barcelona. E claro, ao Otávio e ao Gladston, serei eternamente grato pela amizade de vocês...vocês sabem o quão difícil foi.

Gostaria de agradecer também a Stefanella Boatto, por ter me dado a primeira oportunidade para que esse doutorado se tornasse realidade. Seu apoio e sua amizade.

Gostaria também de agradecer a minha família pelo apoio e amor que me transmitem a cada momento, meus pais Selma e Luiz, minhas irmãs Juliana e Ana Carolina e aos meus sobrinhos Caio e Camila.

I agraeixo molt especialment a la Núria i a la seva família, que ja considero com meva. Sense tu, res d'això seria possible. Encara tenim moltes coses per conquerir junts.

Thanks to the referees to read this thesis. I was supported by the PhD grant CNPq-Conselho Nacional de Desenvolvimento Científico e Tecnológico.

Chapter 1

Introduction

This thesis concerns about *global instability* in *nearly-integrable* Hamiltonian systems, also called "Arnold diffusion". In [Arn64], V.I. Arnold proposed an example of a nearly-integrable Hamiltonian with $2 + 1/2$ degrees of freedom

$$H(q, p, \varphi, I, t) = \frac{1}{2}\left(p^2 + I^2\right) + \varepsilon(\cos q - 1)\left(1 + \mu(\sin\varphi + \cos t)\right),$$

and asserted that given any $\delta, K > 0$, for any $0 < \mu \ll \varepsilon \ll 0$, there exists a trajectory of this Hamiltonian system such that

$$I(0) < \delta \text{ and } I(T) > K \qquad \text{for some time } T > 0.$$

Notice that this a *global* instability result for the variable I, since

$$\dot{I} = -\frac{\partial H}{\partial \varphi} = -\varepsilon\mu(\cos q - 1)\cos\varphi$$

is zero for $\varepsilon = 0$, so I remains constant, whereas I can have a drift of finite size for *any* $\varepsilon > 0$ small enough.

Arnold's Hamiltonian can be written as a nearly-integrable Hamiltonian with 3 degrees of freedom

$$H^*(q, p, \varphi, I, s, A) = \frac{1}{2}\left(p^2 + I^2\right) + A + \varepsilon(\cos q - 1)\left(1 + \mu(\sin\varphi + \cos s)\right),$$

which for $\varepsilon = 0$ is an integrable Hamiltonian $h(p, I, A) = \frac{1}{2}\left(p^2 + I^2\right) + A$. Since h satisfies the (Arnold) *isoenergetic non-degeneracy*

$$\begin{vmatrix} D^2h & Dh \\ Dh^\top & 0 \end{vmatrix} = -1 \neq 0,$$

by the KAM theorem proven by Arnold in [Arn63], the 5D phase space of H is filled, up to a set of relative measure $\mathcal{O}(\sqrt{\varepsilon})$, with 3D-invariant tori $\mathcal{T}_\omega$ with *Diophantine* frequencies $\omega = (\omega_1, \omega_2, 1)$:

$$|k_1\omega_1 + k_2\omega_2 + k_0| \geq \gamma/|k|^\tau \text{ for any } 0 \neq (k_1, k_2, k_0) \in \mathbb{Z},$$

where $\gamma = \mathcal{O}(\sqrt{\varepsilon})$, and $\tau \geq 2$.

Since the 3D KAM invariant tori do not separate the 5D phase space, there can exist irregular orbits 'traveling' between tori. Arnold conjectured in the KAM theorem in 1963 that this was the general case.

In the first part of this thesis we consider an *a priori unstable* Hamiltonian with $2+1/2$ degrees of freedom

$$H_\varepsilon(p, q, I, \varphi, s) = \pm \left(\frac{p^2}{2} + \cos q - 1 \right) + \frac{I^2}{2} + \varepsilon h(q, \varphi, s) \tag{1.1}$$

consisting of a pendulum and a rotor plus a time periodic perturbation $h(q, \varphi, s)$.

A priori unstable Hamiltonian systems like the above one were introduced by [Loc92, CG94]. They consist on a rotor in the variables (I, φ) as an integrable Hamiltonian in action-angle variables, a pendulum in the variables (p, q) which carries out a separatrix associated to a saddle point, plus a small perturbation of size ε. For $\varepsilon = 0$, Hamiltonian (1.1) is integrable and, in particular, the action I is constant. We want to describe the global instability in the variable I for $|\varepsilon|$ non-zero but otherwise arbitrary small.

For simplicity, we refer to global instability in this paper simply as Arnold diffusion. Nevertheless, it is worth remarking that *originally* the term Arnold diffusion was coined for a *priori stable* Hamiltonian systems, which are perturbations of integrable Hamiltonian systems written in action-angle variable. See [Ber10] for a careful exposition of a priori unstable and a priori stable Hamiltonian systems. For instance, replacing $V(q)$ by $\varepsilon V(q)$, our Hamiltonian (1.1) becomes a priori stable. In that case, Arnold diffusion would consisting on finding trajectories with large deviations $(p(T), I(T)) - (p(0), I(0))$. This would be a much more difficult problem that the one considered here, because one has to confront to exponentially small splitting of invariant manifolds with respect to the parameter ε as well as to the passage through double resonances in the action variables p, I. In particular, exponential large estimates of the time of diffusion with respect to ε due to Nekhoroshev [Nek77, LM05, BM11] would apply.

The main characteristic of an *a priori unstable* Hamiltonian system with $2+1/2$ degrees of freedom is that there exists a 3D *Normally Hyperbolic Invariant Manifold* (NHIM) which is a large invariant object with 4D unstable and stable invariant manifolds.

Inside this NHIM there exists an inner dynamics given by a Hamiltonian system with $1 + 1/2$ degrees of freedom. This Hamiltonian possesses 2D invariant tori which prevent global instability inside the 3D NHIM.

For $\varepsilon = 0$, the stable and unstable invariant manifold coincide along a huge separatrix filled with homoclinic orbits to the NHIM.

For small $|\varepsilon| \neq 0$, the unstable and stable manifolds of the NHIM in general do not coincide, but otherwise intersect transversely along 3D homoclinic invariant manifolds. Through each point on each 3D homoclinic manifold, there exists a homoclinic orbit which begins in a point of the NHIM and finishes on another point of the NHIM, not necessarily the same one. This assignment between an initial and the final point on the NHIM is called the *scattering map*. In practice, one must select an adequate domain for any scattering map.

Under the action of a scattering map, the variable I can increase (or decrease). The geometric mechanism of global instability consists on looking for trajectories of the scattering map with a large change on the variable I. Standard shadowing arguments provide the existence of nearby trajectories of Hamiltonian (1.1) with a large change on the variable I.

We are going to assume that the perturbation $h(q, \varphi, s)$ depends on two harmonics in the variables (φ, s):

$$\begin{aligned} h(q,\varphi,s) &= f(q)g(\varphi,s), \\ f(q) = \cos q, \qquad g(\varphi,s) &= a_1\cos(k_1\varphi + l_1 s) + a_2\cos(k_2\varphi + l_2 s), \end{aligned} \tag{1.2}$$

with k_1, k_2, l_1, $l_2 \in \mathbb{Z}$.

One of the main goals of this thesis is to prove that for *any* non-trivial perturbation $a_1 a_2 \neq 0$ depending on *any* two *independent* harmonics $\begin{vmatrix} k_1 & k_2 \\ l_1 & l_2 \end{vmatrix} \neq 0$, there is global instability of the action I for any $\varepsilon > 0$ small enough.

Our first result is that the global instability happens for any arbitrary perturbation (1.2).

Theorem 1. *Assume that $a_1 a_2 \neq 0$ and $k_1 l_2 - k_2 l_1 \neq 0$ in Hamiltonian (1.1)-(1.2). Then, for any $I^* > 0$, there exists $\varepsilon^* = \varepsilon^*(I^*, a_1, a_2) > 0$ such that for any ε, $0 < \varepsilon < \varepsilon^*$, there exists a trajectory $(p(t), q(t), I(t), \varphi(t))$ such that for some $T > 0$*

$$I(0) \leq -I^* < I^* \leq I(T).$$

Remark 2. For a rough estimate of $\varepsilon^* \sim \exp(-\pi I^*/2)$ at least for $|a_1/a_2| < 0.625$, $k_1 = l_2 = 1$ and $l_1 = k_2 = 0$, and $T = T(\varepsilon^*, I^*, a_1, a_2) \sim (\mathrm{T}_s(I^*, a_1, a_2)/\varepsilon)\log(C(I^*, a_1, a_2)/\varepsilon)$ for the diffusion time, see 2.4. Analogous estimates could be obtained for all the other values of the parameters.

The proof is based on the geometrical method introduced in [DLS06] and relies on the concrete computation of several *scattering maps*. A scattering map is a map of transverse homoclinic orbits to a NHIM. For Hamiltonian (1.1), the NHIM turns out to be simply

$$\tilde{\Lambda}_\varepsilon = \tilde{\Lambda} = \left\{(0, 0, I, \varphi, s) : (I, \varphi, s) \in \mathbb{R} \times \mathbb{T}^2\right\}. \tag{1.3}$$

In the unperturbed case, i.e., $\varepsilon = 0$, for any $I^* > 0$ the NHIM $\tilde{\Lambda}$ possesses a 4D *separatrix*, that is to say, coincident stable and unstable invariant manifolds

$$W^0\tilde{\Lambda} = \left\{(p_0(\tau), q_0(\tau), I, \varphi, s) : \tau \in \mathbb{R}, I \in [-I^*, I^*], (\varphi, s) \in \mathbb{T}^2\right\},$$

where (p_0, q_0) are the separatrices to the saddle equilibrium point of the pendulum

$$(p_0(t), q_0(t)) = \left(\frac{\pm 2}{\cosh t}, 4\arctan \mathrm{e}^{\pm t}\right).$$

In the perturbed case, i.e., for small $\varepsilon > 0$, $W^u(\tilde{\Lambda}_\varepsilon)$ and $W^s(\tilde{\Lambda}_\varepsilon)$ do not coincide (this is the so-called splitting of separatrices), and every local transversal intersection between

them gives rise to a (local) scattering map which is simply the correspondence between a past asymptotic motion in the NHIM to the corresponding future asymptotic motion following a homoclinic orbit. Since the NHIM has also an inner dynamics, an adequate combination of these two dynamics on the NHIM, the inner one and the outer one provided by the scattering map, generates the Arnold diffusion as long as the outer dynamics does not preserve the invariant objects of the inner dynamics.

Necessity of the assumptions

If the determinant $\Delta := k_1 l_2 - k_2 l_1$ or some coefficient a_1, a_2 vanishes, for instance, if there is only one harmonic in g, there is no global instability for the action I. Indeed, looking at the equations associated to Hamiltonian (1.1)

$$\begin{aligned} \dot{q} &= \pm p & \dot{p} &= [\pm 1 + \varepsilon\,(a_1 \cos(k_1\varphi + l_1 s) + a_2 \cos(k_2\varphi + l_2 s))] \sin q \\ \dot{\varphi} &= I & \dot{I} &= \varepsilon \cos q\,(k_1 a_1 \sin(k_1\varphi + l_1 s) + k_2 a_2 \sin(k_2\varphi + l_2 s)) \\ \dot{s} &= 1 \end{aligned} \tag{1.4}$$

this is clear for $k_1 = k_2 = 0$, since in this case I is a constant of motion. If k_1 or $k_2 \neq 0$, say $k_1 \neq 0$, the change of variables

$$\bar{\varphi} = k_1\varphi + l_1 s, \qquad r\bar{\varphi} - \bar{s} = k_2\varphi + l_2 s, \qquad \bar{I} = k_1 I + l_1,$$

where $r = k_2/k_1$ can be assumed to satisfy $0 \leq r \leq 1$ without loss of generality, casts system (1.4) into

$$\begin{aligned} \dot{q} &= \pm p & \dot{p} &= [\pm 1 + \varepsilon\,(a_1 \cos\bar{\varphi} + a_2 \cos(r\bar{\varphi} - \bar{s}))] \sin q \\ \dot{\bar{\varphi}} &= \bar{I} & \dot{\bar{I}} &= \varepsilon k_1^2 \cos q\,(a_1 \sin\bar{\varphi} + r a_2 \sin(r\bar{\varphi} - \bar{s})) \\ \dot{\bar{s}} &= \Delta/k_1 \end{aligned}$$

which is a Hamiltonian system with the Hamiltonian given by

$$\begin{aligned} \bar{H}_\varepsilon(p, q, \bar{I}, \bar{\varphi}, \bar{s}) = \pm \left(\frac{p^2}{2} + \cos q - 1\right) + \frac{\bar{I}^2}{2} \\ + \varepsilon k_1^2 \cos q\,(a_1 \cos\bar{\varphi} + a_2 \cos(r\bar{\varphi} - \bar{s}))\,. \end{aligned} \tag{1.5}$$

If $\Delta = 0$ Hamiltonian (1.5) is autonomous with 2 degrees of freedom, and therefore a global drift for the action I is not possible. Only drifts of size $\sqrt{\varepsilon}$ are possible due to KAM theorem. Analogously one easily checks that for $a_1 a_2 = 0$ Hamiltonian (1.1) is integrable or autonomous.

Reduction of the harmonic types

Under the hypothesis $(k_1 l_2 - k_2 l_1)\, a_1 a_2 \neq 0$ of Theorem 1, the case $k_2 = 0$ of Theorem 1 is proved in Chapter 2. Indeed, $k_2 = 0$ implies $r := k_2/k_1 = 0$ and it turns out from (1.5)

that Hamiltonian (1.1) is equivalent to the one with $k_1 = 1, k_2 = 0, l_1 = 0, l_2 = 1$:

$$H_\varepsilon(p, q, I, \varphi, t) = \pm \left(\frac{p^2}{2} + \cos q - 1 \right) + \frac{I^2}{2} + \varepsilon \cos q \left(a_1 \cos \varphi + a_2 \cos s \right), \tag{1.6}$$

which is just the Hamiltonian studied in Chapter 2. In Chapter 3 we prove Theorem 1 for $k_1 k_2 \neq 0$ or equivalently for $r \in (0, 1]$. For the sake of clarity we will explain in full detail and prove Theorem 1 along Section 3.3 just for $r = 1$, which by (1.5) is equivalent to the case $k_1 = 1, k_2 = 1, l_1 = 0, l_2 = -1$:

$$H_\varepsilon(p, q, I, \varphi, t) = \pm \left(\frac{p^2}{2} + \cos q - 1 \right) + \frac{I^2}{2} + \varepsilon \cos q \left(a_1 \cos \varphi + a_2 \cos(\varphi - s) \right). \tag{1.7}$$

To finish the proof of Theorem 1, in Section 3.3 we will sketch the modifications needed for the case $r \in (0, 1)$.

Scattering map types

By the definition given at Section 2.2.2, a scattering map is in principle only *locally* defined, that is, for a small ball of values of the variables (I, φ, s) or $(I, \theta = \varphi - Is)$, since it depends on a non-degenerate critical point $\tau^* = \tau^*(I, \varphi, s)$ of a real function (2.6), depending smoothly on the variables (I, φ, s), already introduced in [DLS06]. In the study carried out in Section 3.2, it will be described whether, in terms of the parameter $\mu := a_1/a_2$ and the variable I, a local scattering map can or cannot be smoothly defined for all the values of the angles (φ, s) or $\theta = \varphi - Is$, becoming thus a *global* or *extended* scattering map. This description will depend essentially on a geometrical characterization of the function $\tau^*(I, \varphi, s)$ in terms of the intersection of *crests* and *NHIM lines*, following [DH11]. Any degeneration of the critical point $\tau^* = \tau^*(I, \varphi, s)$ may give rise to more non-degenerate critical points and a bifurcation to *multiple* local scattering maps or to a non global scattering map. Different critical points $\tau^* = \tau^*(I, \varphi, s)$ give rise to different local scattering maps, and putting together different local scattering maps, one can sometimes obtain *piecewise smooth* global scattering maps, which are very useful to design paths of instability for the action I, and are simply called diffusion paths.

For instance, in Chapter 2 devoted to the Hamiltonian (1.6), it will be proven that for $0 < \mu = a_1/a_2 < 0.625$, there exist two different global scattering maps. Among the different kinds of associated orbits of these scattering maps, there will appear two of them called *highways*, where the drift of the action I was very fast and simple. As will be described in Section 3.2, such highways do not appear for Hamiltonian (1.7). Nevertheless, as will be proven in Section 3.4, there exist piecewise smooth global scattering maps, and the possible diffusion along the discontinuity sets opens the possibility of applying the theory of piecewise smooth dynamical systems [Fil88].

About the model chosen and related work

Hamiltonian (1.1) is a standard example of an *a priori unstable* Hamiltonian system [CG94] formed by a pendulum, a rotor and a perturbation. It is usual in the literature

to choose a perturbation depending periodically only on the positions—which turn out to be angles in our case—and time. Our perturbation $h(q, \varphi, s)$ (1.2) is a little bit special since it is a product of a function $f(q)$ times a function $g(\varphi, s)$. This choice makes easier the computations of the Poincaré-Melnikov potential (3.11), which is based on the Cauchy's residue theorem. Theorem 1 can be easily generalized to any trigonometric polynomial or meromorphic function $f(q)$, although the computations of poles of high order become more complicated. In the same way, it could also be generalized to more general perturbations $h(q, \varphi, s)$, as long that h is a trigonometric polynomial or meromorphic in q. The dependence on more than two harmonics gives rise to the appearance of more resonances in the inner dynamics, which requires more control of their sizes, see for instance [DH09, DS97]. Apart from more difficulty in the computations of the Poincaré-Melnikov potential and the inner Hamiltonian, we do not foresee substantial changes, so we believe that Hamiltonian (1.1) could be considered as a paradigmatic example of an *a priori unstable* Hamiltonian system.

Chapter 3 is a natural culmination of Chapter 2, which deals with the simpler Hamiltonian (1.6), and where a detailed description of NHIM lines and crests is carried out. An "optimal" estimate of the diffusion time close to some special orbits of the scattering map, called *highways*, is also given there. The study in Chapter 3 of Hamiltonian (1.7) is more complicated, due to a greater complexity of the evolution of the NHIM lines and crests with respect to the action I and the parameters of the system. In particular, the absence of highways prevents us of showing an estimate of diffusion time close to them.

Let us mention that results about global instability are not new. Indeed one can find related results in [Loc92, BCV01, Cre01, CG03, Cre03, DLS06, KL08a, KL08b, CY09, DH09, BKZ11, DH11, Zha11, Mat12, Tre12, KZ15, GT14, LMS16, Mar16, Che17, GM17, LPS17] involving the geometrical method or variational methods. Our approach is very similar to [DH11], and one of the novelties of the present thesis is that we can prove the existence of global instability for *any* value of $\mu = a_1/a_2 \neq 0$, whereas in [DH11] this was only proven for $0 < |\mu| < 0.625$. Let us mention [DT16] which contains a similar approach to the function τ^* of [DLS06] and the crests of [DH11]. Nevertheless, the main purpose of this work is to describe the paths of instability that can be chosen as well as to estimate the time of diffusion for some cases.

We notice that in this thesis we stress the interaction between NHIM lines and crests, since this allows us to describe the diverse scattering maps, as well as their domains, that appear in our problem. In more complicated models of Celestial Mechanics the Melnikov potential is not available. In these cases the computations of scattering maps rely on the numerical computation of invariant manifolds of a NHIM or some of its selected invariant objects, and the search of diffusion orbits is performed in a more crafted way (see [CDMR06, DMR08, DGR13, CGL16, DGR16]).

Partial results for a case with 3 + 1/2 degrees of freedom

A natural question is whether the results presented in Chapter 2 and Chapter 3 hold for more dimensions. In Chapter 4, we consider an analogous *nearly-integrable* Hamiltonian

system with a similar perturbation but now, with $3 + 1/2$ degrees of freedom, i.e., the following Hamiltonian given by

$$H_\varepsilon(p, q, I_1, I_2, \varphi_1, \varphi_2, s) = \pm \left(\frac{p^2}{2} + \cos q - 1 \right) + h(I_1, I_2) + \varepsilon f(q)\, g(\varphi_1, \varphi_2, s),$$

where $f(q) = \cos q$, $h(I_1, I_2) = \Omega_1 I_1^2/2 + \Omega_2 I_2^2/2$ and

$$g(\varphi_1, \varphi_2, s) = a_1 \cos \varphi_1 + a_2 \cos \varphi_2 + a_3 \cos(k \cdot \varphi - s),$$

with $k = (k_1, k_2) \in \mathbb{Z}^2$ and $\varphi = (\varphi_1, \varphi_2) \in \mathbb{T}^2$.

This case is much more complicated than the case studied in Chapter 2 and Chapter 3. There are 7 parameters and to handle them it is not easy. In this thesis we present the results obtained until now for an analogous Hamiltonian studied in Chapter 2 and we expect to complete this study in a future work. We emphasize that we do not know other work with a similar approach for this dimension.

In Chapter 4, our object of study is the Hamiltonian given by

$$H_\varepsilon(p, q, I_1, I_2, \varphi_1, \varphi_2, s) = \pm \left(\frac{p^2}{2} + \cos q - 1 \right) + h(I_1, I_2) + \varepsilon f(q)\, g(\varphi_1, \varphi_2, s), \tag{1.8}$$

where $f(q) = \cos q$, $h(I_1, I_2) = \Omega_1 I_1^2/2 + \Omega_2 I_2^2/2$ and

$$g(\varphi_1, \varphi_2, s) = a_1 \cos \varphi_1 + a_2 \cos \varphi_2 + a_3 \cos s. \tag{1.9}$$

As in the previous chapters, we begin by describing the crests and its dependence with respect to the parameters $\mu_1 := a_1/a_3$ and $\mu_2 := a_2/a_3$, and the values of I_1 and I_2. We detect a new behavior for the crests, since they can form a unique surface. In consequence we restrict our study to the case where $|\mu_1| + |\mu_2| < 0.625$. In this case, the crests are *horizontal* and there is no tangency between NHIM lines and the crests. This case is very similar to the case in [DH11] and the simplest case in Chapter 2.

In Chapter 4 the main result is

Theorem 3. *Consider the Hamiltonian* (1.8)+(1.9). *Assume* $a_1 a_2 a_3 \neq 0$ *and* $|\mu_1| + |\mu_2| < 0.625$. *Then, for every* δ *there exists* $0 < \varepsilon_0$ *such that for every* $0 < |\varepsilon| < \varepsilon_0$, *given* $I_\pm \in \mathcal{I}^* \setminus \{(0, 0)\}$, *there exists an orbit* $\tilde{x}(t)$ *and* $T > 0$, *such that*

$$|I(\tilde{x}(0)) - I_-| \leq C\delta$$
$$|I(\tilde{x}(T)) - I_+| \leq C\delta$$

Besides, in Section 4.3 we explicit the symmetries of the scattering map. In Section 4.4 we show an initial study about the *Highways* with a description to a very special case and for I_1 and I_2 close to infinity. The final chapter of this thesis contains some open questions related to the problems considered in this thesis. Some of these open questions have not been solved simply by lack time, whereas other open questions require more substantial time, since they are related to deeper problems.

We finish this introduction by noticing that the first two chapters of this thesis are very based on the papers [DS17a, DS17b] and we apologize for any repetition.

Chapter 2

The first case for 2 + 1/2 degrees of freedom

2.1 The System

We consider the following *a priori unstable* Hamiltonian with $2+1/2$ degrees of freedom with 2π-periodic time dependence:

$$H_\varepsilon(p,q,I,\varphi,s) = \pm\left(\frac{p^2}{2}+\cos q-1\right)+\frac{I^2}{2}+\varepsilon f(q)g(\varphi,s), \tag{2.1}$$

where p, $I\in\mathbb{R}$, q, φ, $s\in\mathbb{T}$ and ε is small enough.

In the unperturbed case, that is, $\varepsilon=0$, the Hamiltonian H_0 represents the standard pendulum plus a rotor:

$$H_0(p,q,I,\varphi,s) = \frac{p^2}{2}+\cos q-1+\frac{I^2}{2},$$

with associated equations

$$\dot q = \frac{\partial H_0}{\partial p} = p \qquad \dot p = -\frac{\partial H_0}{\partial q} = \sin q$$
$$\dot\varphi = \frac{\partial H_0}{\partial I} = I \qquad \dot I = -\frac{\partial H_0}{\partial \varphi} = 0$$
$$\dot s = 1$$

and associated flow

$$\phi_t(p,q,I,\varphi,s) = (p(t),q(t),I,\varphi+It,s+t)\,.$$

In this case, $(0,0)$ is a saddle point on the plane formed by variables (p,q) with associated unstable and stable invariant curves. Introducing $P(p,q)=p^2/2+\cos q-1$, we have that

$P^{-1}(0)$ divides the (p, q) phase space, separating the behavior of orbits. The branches of $P^{-1}(0)$ are called *separatrices* and are parameterized by the homoclinic trajectories to the saddle point $(p, q) = (0, 0)$,

$$(p_0(t), q_0(t)) = \left(\frac{2}{\cosh t}, 4 \arctan e^{\pm t} \right). \tag{2.2}$$

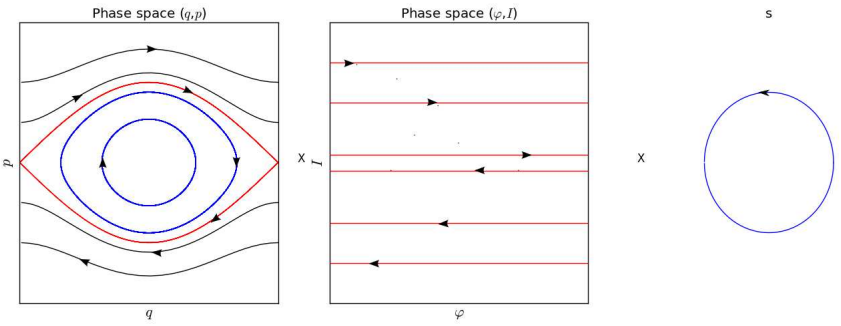

Fig. 2.1: Phase Space - Unperturbed problem

For any initial condition $(0, 0, I, \varphi, s)$, the unperturbed flow is $\phi_t(0, 0, I, \varphi, s) = (0, 0, I, \varphi + It, s + t)$, that is, any torus $\mathcal{T}_I^0 = \{(0, 0, I, \varphi, s); (\varphi, s) \in \mathbb{T}^2\}$ is an invariant set for the flow. $\mathcal{T}_I^0$ is called *whiskered torus*, and we call *whiskers* its unstable and stable manifolds, which turn out to be coincident:

$$W^0\mathcal{T}_I^0 = \{(p_0(\tau), q_0(\tau), I, \varphi, s); \tau \in \mathbb{R}, (\varphi, s) \in \mathbb{T}^2)\}.$$

For any positive value I^*, consider the interval $[-I^*, I^*]$ and the cylinder formed by an uncountable family of tori

$$\widetilde{\Lambda} = \{\mathcal{T}_I^0\}_{I \in [-I^*, I^*]} = \{(0, 0, I, \varphi, s); I \in [-I^*, I^*], (\varphi, s) \in \mathbb{T}^2\}.$$

The set $\widetilde{\Lambda}$ is a 3D-normally hyperbolic invariant manifold (NHIM) with 4D-coincident stable and unstable invariant manifolds:

$$W^0\widetilde{\Lambda} = \left\{(p_0(\tau), q_0(\tau), I, \varphi, s); \tau \in \mathbb{R}, I \in [-I^*, I^*], (\varphi, s) \in \mathbb{T}^2\right\}.$$

We now come back to the perturbed case, that is, small $|\varepsilon| \neq 0$. By the theory of NHIM (see for instance [DLS06] for more information), if $f(q)g(\varphi, s)$ is smooth enough, there exists a smooth NHIM $\widetilde{\Lambda}_\varepsilon$ close to $\widetilde{\Lambda}$ and the local invariant manifolds $W^{\mathrm{u}}_{\mathrm{loc}}(\widetilde{\Lambda}_\varepsilon)$ and $W^{\mathrm{s}}_{\mathrm{loc}}(\widetilde{\Lambda}_\varepsilon)$ are ε-close to $W^0(\widetilde{\Lambda})$. Indeed,

$$W^{\mathrm{u,s}}_{\mathrm{loc}}(\widetilde{\Lambda}_\varepsilon) = \bigcup_{\tilde{x} \in \widetilde{\Lambda}_\varepsilon} W^{\mathrm{u,s}}_{\mathrm{loc}}(\tilde{x}),$$

where $W^{\mathrm{u,s}}_{\mathrm{loc}}(\tilde{x})$ are the unstable and stable manifolds associated to a point $\tilde{x} \in \widetilde{\Lambda}_\varepsilon$ (more precise information about the differentiability of $\widetilde{\Lambda}_\varepsilon$ and $W^{\mathrm{u,s}}(\widetilde{\Lambda}_\varepsilon)$ can be found in [DLS06]). Notice that if $f'(0) = 0$, $\tilde{\Lambda}_\varepsilon = \tilde{\Lambda}$, that is, $\tilde{\Lambda}$ is a NHIM for all ε. But even in this case, in general $W^u(\tilde{\Lambda}_\varepsilon)$ and $W^s(\tilde{\Lambda}_\varepsilon)$ do not need to coincide, that is, the *separatrices* split.

Along this chapter, we are going to take

$$f(q) = \cos q \qquad \text{and} \qquad g(\varphi, s) = a_{00} + a_{10}\cos\varphi + a_{01}\cos s, \quad (a_{10}a_{01} \neq 0) \tag{2.3}$$

so that there exists a normally hyperbolic invariant manifold $\tilde{\Lambda}_\varepsilon = \tilde{\Lambda}$ in the dynamics associated to the Hamiltonian (1.1)+(1.2)

$$H_\varepsilon(p, q, I, \varphi, s) = \pm\left(\frac{p^2}{2} + \cos q - 1\right) + \frac{I^2}{2} + \varepsilon\cos q\,(a_{00} + a_{10}\cos\varphi + a_{01}\cos s)\,.$$

Remark 4. We are choosing $f(q)$ as in [DH11] and a similar $g(\varphi, s)$. Indeed, in [DH11], $g(\varphi, s) = \sum_{(k,l)\in\mathbb{N}^2} a_{k,l}\cos(k\varphi - ls - \sigma_{k,l})$ is a *full* trigonometrical series with the condition

$$\hat{\alpha}\rho^{\beta k}r^{\beta l} \leq |a_{k,l}| \leq \alpha\rho^k r^l,$$

for $0 < \rho \leq \rho^*$ and $0 < r \leq r^*$, where $\rho^*(\lambda, \alpha, \hat{\alpha}, \beta)$ and $r^*(\lambda, \alpha, \hat{\alpha}, \beta)$ are small enough. Under these hypothesis, the Melnikov potential, after ignoring terms of order greater or equal than 2, is the same Melnikov potential that we will obtain in subsection 2.2.2. However, the inner dynamics in [DH11] is different. In our case, as we will see, it is integrable, therefore it is trivial and we will not worry about KAM theory to study the perturbed dynamics inside $\widetilde{\Lambda}_\varepsilon$.

2.2 The inner and the outer dynamics

We have two dynamics associated to $\tilde{\Lambda}_\varepsilon$, the inner and the outer dynamics. For the study of the inner dynamics we use the *inner map* and for the outer one we use the *scattering map*. When it be convenient we will combine the scattering map and the inner dynamics to show the diffusion phenomenon.

2.2.1 Inner map

The inner dynamics is the dynamics in the NHIM. Since $\tilde{\Lambda}_\varepsilon = \tilde{\Lambda}$, the Hamiltonian H_ε restricted to $\tilde{\Lambda}_\varepsilon$ is

$$K(I, \varphi, s; \varepsilon) = \frac{I^2}{2} + \varepsilon\,(a_{00} + a_{10}\cos\varphi + a_{01}\cos s)\,, \tag{2.4}$$

with associated Hamiltonian equations

$$\dot{\varphi} = I \qquad \dot{I} = \varepsilon\, a_{10}\sin\varphi \qquad \dot{s} = 1. \tag{2.5}$$

Note that the first two equations just depend on the variables I and φ, thus using that

$$F(I,\varphi) := \frac{I^2}{2} + \varepsilon\, a_{10}\,(\cos\varphi - 1) = K(I,\varphi,s) - \varepsilon\,(a_{00} + a_{10}\cos s - 1)$$

is a first integral and, indeed, a Hamiltonian function for equations (2.5), one has that the inner Hamiltonian system (2.4) is integrable. Therefore, here does not appear a genuine "big gap problem", and KAM is not needed theorem to find invariant tori, since there is a continuous foliation of invariant tori simply given by F = constant. When ε is small enough we have that the solutions are close to I = constant, that is, the level curves of F are almost 'flat' or 'horizontal' in the action I (see Fig. 2.2).

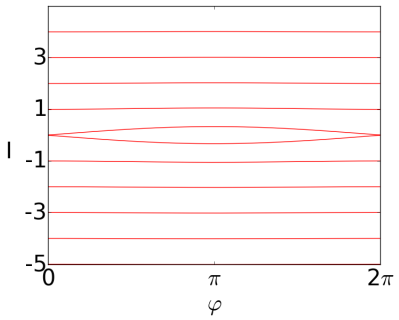

Fig. 2.2: Inner dynamics in the variables (φ, I) for $a_{10} = 0.6$ and $\varepsilon = 0.01$

2.2.2 Scattering map: Melnikov potential and crests

The scattering map was introduced in [DLS00] and is our main object of study. Let $\tilde{\Lambda}$ be a NHIM with invariant manifolds intersecting transversally along a homoclinic manifold Γ. A scattering map is a map S defined by $S(\tilde{x}_-) = \tilde{x}_+$ if there exists $\tilde{z} \in \Gamma$ satisfying

$$|\phi_t(\tilde{z}) - \phi_t(\tilde{x}_\pm)| \longrightarrow 0 \text{ as } t \longrightarrow \pm\infty$$

that is, $W^u_\varepsilon(\tilde{x}_-)$ intersects (transversally) $W^s_\varepsilon(\tilde{x}_+)$ in $\tilde{z}$.

For a more computational and geometrical definition of scattering map, we have to study the intersections between the hyperbolic invariant manifolds of $\tilde{\Lambda}_\varepsilon$. We will use the Poincaré-Melnikov theory.

Melnikov potential

We have the following proposition [DH11, DLS06].

Proposition 5. *Given $(I,\varphi,s) \in [-I^*, I^*] \times \mathbb{T}^2$, assume that the real function*

$$\tau \in \mathbb{R} \longmapsto \mathcal{L}(I, \varphi - I\,\tau, s - \tau) \in \mathbb{R} \tag{2.6}$$

has a non degenerate critical point $\tau^* = \tau^*(I, \varphi, s)$*, where*

$$\mathcal{L}(I, \varphi, s) = \int_{-\infty}^{+\infty} (f(q_0(\sigma))g(\varphi + I\sigma, s + \sigma; 0) - f(0)g(\varphi + I\sigma, s + \sigma; 0))\, d\sigma.$$

Then, for $0 < |\varepsilon|$ *small enough, there exists a unique transversal homoclinic point* $\tilde{z}$ *to* $\tilde{\Lambda}_\varepsilon$*, which is* ε*-close to the point* $\tilde{z}^*(I, \varphi, s) = (p_0(\tau^*), q_0(\tau^*), I, \varphi, s) \in W^0(\tilde{\Lambda})$*:*

$$\tilde{z} = \tilde{z}(I, \varphi, s) = (p_0(\tau^*) + O(\varepsilon), q_0(\tau^*) + O(\varepsilon), I, \varphi, s) \in W^u(\tilde{\Lambda}_\varepsilon) \pitchfork W^s(\tilde{\Lambda}_\varepsilon). \tag{2.7}$$

The function $\mathcal{L}$ is called the *Melnikov potential* of Hamiltonian (1.1). In our case, from (2.2) and (2.3)

$$\mathcal{L}(I, \varphi, s) = A_{00} + A_{10}(I)\cos\varphi + A_{01}\cos s, \tag{2.8}$$

where

$$A_{00} = 4\, a_{00}, \quad A_{10}(I) = \frac{2\,\pi\, I\, a_{10}}{\sinh(\frac{\pi I}{2})} \quad \text{and} \quad A_{01} = \frac{2\,\pi\, a_{01}}{\sinh(\frac{\pi}{2})}. \tag{2.9}$$

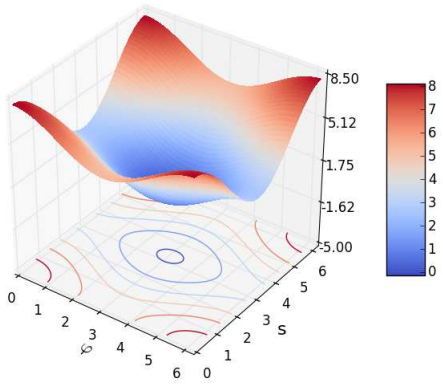

Fig. 2.3: The Melnikov potential, $\mu = a_{10}/a_{01} = 0.6$ and $I = 1$.

We now look for the critical points of (2.6) which indeed are the solutions of

$$\frac{\partial \mathcal{L}}{\partial \tau}(I, \varphi - I\tau, s - \tau) = 0.$$

Equivalently, $\tau^* = \tau^*(I, \varphi, s)$ satisfies

$$I\, A_{10}(I)\sin(\varphi - I\,\tau^*) + A_{10}\sin(s - \tau^*) = 0. \tag{2.10}$$

From a geometrical view-point, for any $(I, \varphi, s) \in [-I^*, I^*] \times \mathbb{T}^2$, finding $\tau^* = \tau^*(I, \varphi, s)$ satisfying (2.10) is equivalent to looking for the extrema of $\mathcal{L}$ on the NHIM line

$$R(I, \varphi, s) = \{(I, \varphi - I\tau, s - \tau), \tau \in \mathbb{R}\}, \tag{2.11}$$

which corresponds to the unperturbed trajectory of Hamiltonian H_0 through (I, φ, s) along the unperturbed NHIM.

Thus we can define the *scattering map* as in [DH11]. Let W be an open subset of $[-I^*, I^*] \times \mathbb{T}^2$ such that the map

$$(I, \varphi, s) \in W \mapsto \tau^*(I, \varphi, s),$$

where $\tau^*(I, \varphi, s)$ is a critical point of (2.6) or, equivalently, a solution of (2.10), is well defined and C^2. Therefore, there exists a unique $\tilde{z}$ satisfying (2.7). Let $\Gamma = \{\tilde{z}(I, \varphi, s; \varepsilon), (I, \varphi, s) \in W\}$. For any $\tilde{z} \in \Gamma$ there exist unique $\tilde{x}_{+,-} = \tilde{x}_{+,-}(I, \varphi, s; \varepsilon) \in \tilde{\Lambda}_\varepsilon$ such that $\tilde{z} \in W^s_\varepsilon(\tilde{x}_-) \cap W^u_\varepsilon(\tilde{x}_+)$. Let

$$H_{+,-} = \bigcup \{\tilde{x}_{+,-}(I, \varphi, s; \varepsilon), (I, \varphi, s) \in W\}.$$

We define the scattering map associated to Γ as the map

$$\begin{array}{rcl} S : H_- & \longrightarrow & H_+ \\ \tilde{x}_- & \longmapsto & S(\tilde{x}_-) = \tilde{x}_+. \end{array}$$

By the geometric properties of the scattering map (it is an exact symplectic map [DLS08]) we have, see [DH09] and [DH11], that the *scattering map* has the explicit form

$$S(I, \varphi, s) = \left(I + \varepsilon \frac{\partial L^*}{\partial \varphi}(I, \varphi, s) + \mathcal{O}(\varepsilon^2), \varphi - \varepsilon \frac{\partial L^*}{\partial I}(I, \varphi, s) + \mathcal{O}(\varepsilon^2), s \right), \tag{2.12}$$

where

$$L^*(I, \varphi, s) = \mathcal{L}(I, \varphi - I\,\tau^*(I, \varphi, s), s - \tau^*(I, \varphi, s)). \tag{2.13}$$

The new variable $\theta = \varphi - Is$

Notice that if $\tau^*(I, \varphi, s)$ is a critical point of (2.6), $\tau^*(I, \varphi, s) - \sigma$ is a critical point of

$$\tau \longmapsto \mathcal{L}(I, \varphi - I(\tau + \sigma), s - (\tau + \sigma)) = \mathcal{L}(I, \varphi - I\sigma - I\tau, s - \sigma - \tau). \tag{2.14}$$

Since $\tau^*(I, \varphi - I\sigma, s - \sigma)$ is a critical point of the right hand side of (2.14), by the uniqueness in W we can conclude that

$$\tau^*(I, \varphi - I\sigma, s - \sigma) = \tau^*(I, \varphi, s) - \sigma. \tag{2.15}$$

Thus, by (2.13),

$$\begin{aligned} L^*(I, \varphi - I\sigma, s - \sigma) &= \mathcal{L}(I, \varphi - I\sigma - I(\tau^* - \sigma), s - \sigma - \tau^*) \\ &= \mathcal{L}(I, \varphi - I\tau^*, s - \tau^*) = L^*(I, \varphi, s), \end{aligned}$$

and, in particular for $\sigma = s$,

$$L^*(I, \varphi - Is, 0) = L^*(I, \varphi, s).$$

Introducing the new variable

$$\theta = \varphi - Is,$$

we define *the Reduced Poincaré function*

$$\mathcal{L}^*(I, \theta) := L^*(I, \varphi - Is, 0) = L^*(I, \varphi, s). \tag{2.16}$$

We can write the scattering map on the variables (I, θ). From $(I', \varphi', s') = S(I, \varphi, s)$, we have that

$$\begin{aligned} \theta' \ = \varphi' - I's' \ &= \left(\varphi - \varepsilon \frac{\partial L^*}{\partial I}(I, \varphi, s)\right) - \left(I + \varepsilon \frac{\partial L^*}{\partial \varphi}(I, \varphi, s)\right) s + \mathcal{O}(\varepsilon^2) \\ &= \theta - \varepsilon \left(\frac{\partial L^*}{\partial I}(I, \varphi, s) + \frac{\partial L^*}{\partial \varphi}(I, \varphi, s)s\right) + \mathcal{O}(\varepsilon^2). \end{aligned}$$

Since

$$\frac{\partial L^*}{\partial I}(I, \varphi, s) = \frac{\partial \mathcal{L}^*}{\partial I}(I, \theta) - s\frac{\partial \mathcal{L}^*}{\partial \theta}(I, \theta) \qquad \text{and} \qquad \frac{\partial L^*}{\partial \varphi} = \frac{\partial \mathcal{L}^*}{\partial \theta}(I, \theta),$$

we conclude that

$$\theta' = \theta - \varepsilon \left(\frac{\partial \mathcal{L}^*}{\partial I}(I, \theta)\right) + \mathcal{O}(\varepsilon^2) \qquad \text{and} \qquad I' = I + \varepsilon \left(\frac{\partial \mathcal{L}^*}{\partial \theta}(I, \theta)\right) + \mathcal{O}(\varepsilon^2).$$

Then, in the variables (I, θ), the scattering map takes the simple form

$$\mathcal{S}(I, \theta) = \left(I + \varepsilon \frac{\partial \mathcal{L}^*}{\partial \theta}(I, \theta) + \mathcal{O}(\varepsilon^2), \theta - \varepsilon \frac{\partial \mathcal{L}^*}{\partial I}(I, \theta) + \mathcal{O}(\varepsilon^2)\right), \tag{2.17}$$

so up to $\mathcal{O}(\varepsilon^2)$ terms, $\mathcal{S}(I, \theta)$ is the $-\varepsilon$ times flow of the *autonomous* Hamiltonian $\mathcal{L}^*(I, \theta)$. In particular, the iterates under the scattering map follow the level curves of $\mathcal{L}^*$ up to $\mathcal{O}(\varepsilon^2)$.

Remark 6. We notice that the variable θ is periodic in the variable φ and quasi-periodic in the variable s. Fixing s, then θ becomes periodic.

Remark 7. Note that if for some values of (I, θ) we have that $\nabla \mathcal{L}^*(I, \theta) = \mathcal{O}(\varepsilon)$, then $\varepsilon \partial \mathcal{L}^*/\partial \theta(I, \theta) = \mathcal{O}(\varepsilon^2)$ and $\varepsilon \partial \mathcal{L}^*/\partial I(I, \theta) = \mathcal{O}(\varepsilon^2)$. In this case, the level curves of $\mathcal{L}^*(I, \theta)$ do not provide the dominant part of the scattering map $\mathcal{S}$. Therefore, we will be able to describe properly the scattering map through the level curves of the Reduced Poincaré function on the set of (I, θ) such that $\|\nabla \mathcal{L}^*(I, \theta)\| \gg \varepsilon$.

Remark 8. Using Eq.(2.15) and setting $s = \sigma$, we have that $\tau^*(I, \varphi - Is, 0) = \tau^*(I, \varphi, s) - s$. So we can define

$$\tau^*(I, \theta) := \tau^*(I, \varphi, s) - s \tag{2.18}$$

and from (2.13) and (2.16) we can write $\mathcal{L}^*$ as

$$\mathcal{L}^*(I, \theta) = \mathcal{L}(I, \theta - I\tau^*(I, \theta), -\tau^*(I, \theta)). \tag{2.19}$$

Remark 9. In the variables (I, θ), the variable s does *not* appear at all in the expression (2.17) for the scattering map, at least up to $\mathcal{O}(\varepsilon^2)$. However, s does appear in the expression (2.12) in the original variables (I, φ), so we have in (2.12) a family of scattering maps parameterized by the variable s. Playing with the parameter s, we can have scattering maps with different properties. See Lemma 14 for an application of this phenomenon.

The crests

For the computation of the scattering maps, we use an important geometrical object introduced in [DH11], the *crests*.

Definition 10. Fixed I, we define by *crests* $\mathrm{C}(I)$ the curves on $\{(I, \varphi, s), (\varphi, s) \in \mathbb{T}^2\}$, satisfying

$$I\frac{\partial \mathcal{L}}{\partial \varphi}(I, \varphi, s) + \frac{\partial \mathcal{L}}{\partial s}(I, \varphi, s) = 0.$$

In our case

$$I\, A_{10}(I) \sin\varphi + A_{01} \sin s = 0. \tag{2.20}$$

Note that a point (I, φ, s) belongs to a crest $\mathrm{C}(I)$ if it is a minimum or maximum, or more generally, a critical point of $\mathcal{L}$ along a NHIM line (2.11), that is, $\tau^*(I, \varphi, s) = 0$ in (2.10), see Fig. 2.4.

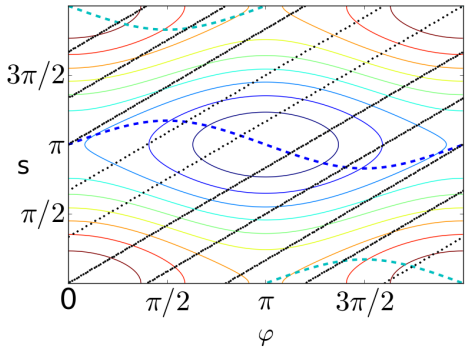

Fig. 2.4: Level curves of $\mathcal{L}$ for $\mu = a_{10}/a_{01} = 0.5$ and $I = 1.2$. Crests (dashed) in blue and green and the NHIM lines in black.

Remark 11. Note that any critical point of $\mathcal{L}(I,\cdot,\cdot)$ belongs to the crest $\mathrm{C}(I)$. In general we have two curves satisfying Eq.(2.20), the *maximum* crest $\mathrm{C_M}(I)$, and the *minimum* crest $\mathrm{C_m}(I)$. The maximum crest contains the point $(I,\varphi=0,s=0)$, and the minimum crest the point $(I,\varphi=\pi,s=\pi)$. For $a_{10}>0$, $a_{01}>0$, the Melnikov function $\mathcal{L}(I,\cdot,\cdot)$ given in (2.8) has a maximum point at the point $(I,\varphi,s)=(I,0,0)$, and a minimum at (I,π,π), and the function (2.6) has a maximum on $\mathrm{C_M}(I)$, and a minimum on $\mathrm{C_m}(I)$. For other combinations of signs of a_{10}, a_{01}, the location of maxima and minima changes, but for simplicity, we have preserved the name of maximum and minimum crest.

We now proceed to study the crests. By (2.9) we can rewrite Eq. (2.20) as

$$\mu\alpha(I)\,\sin\varphi+\sin s=0, \tag{2.21}$$

where

$$\alpha(I)=\frac{IA_{10}(I)}{\mu A_{01}}=\frac{\sinh(\frac{\pi}{2})\,I^2}{\sinh(\frac{\pi I}{2})}\qquad\text{and}\qquad \mu=\frac{a_{10}}{a_{01}}. \tag{2.22}$$

Note that if $|\mu\alpha(I)|<1$ we can write s as a function of φ for any value of φ. On the other hand, if $|\mu\alpha(I)|>1$ we can write φ as a function of s. So, we have two different kinds of crests:

- For $|\alpha(I)|<1/|\mu|$, the two crests are horizontal, see Fig. 2.5(a), with

$$\mathrm{C_{M,m}}(I)=\{(I,\varphi,\xi_{\mathrm{M,m}}(I,\varphi)):\varphi\in\mathbb{T}\},$$

$$\begin{aligned}\xi_{\mathrm{M}}(I,\varphi) &= -\arcsin(\mu\alpha(I)\sin\varphi) \qquad \mod 2\pi\\ \xi_{\mathrm{m}}(I,\varphi) &= \arcsin(\mu\alpha(I)\sin\varphi)+\pi \qquad \mod 2\pi.\end{aligned} \tag{2.23}$$

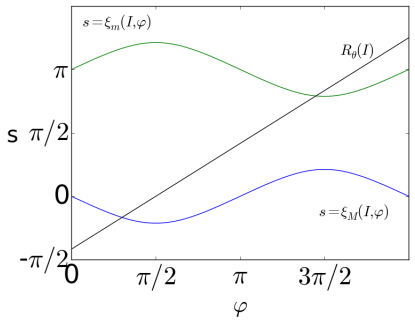

(a) Horizontal crests: $\mu=a_{10}/a_{01}=0.6$ and $I=1.2$.

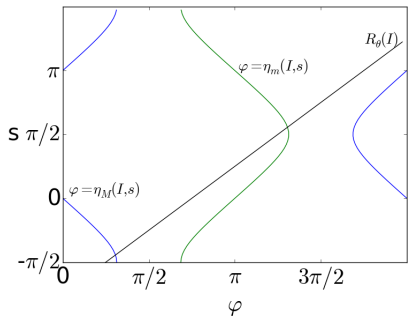

(b) Vertical crests: $\mu=a_{10}/a_{01}=1.2$ and $I=1$.

Fig. 2.5: Types of crests.

- For $|\alpha(I)|>1/|\mu|$, the two crests are vertical, see Fig. 2.5(b), with

$$\mathrm{C}_{M,m}(I)=\{(I,\eta_{M,m}(I,s),s):s\in\mathbb{T}\},$$

$$\begin{aligned}\eta_M(I,s) &= -\arcsin(\sin s/(\mu\alpha(I))) \qquad \mod 2\pi\\ \eta_m(I,s) &= \arcsin(\sin s/(\mu\alpha(I)))+\pi \qquad \mod 2\pi.\end{aligned} \tag{2.24}$$

Remark 12. The case $|\alpha(I)| = 1/|\mu|$ is singular, since both crests are piecewise NHIM lines and they touch each other at the points $(\varphi, s) = (\pi/2, 3\pi/2)$, $(3\pi/2, \pi/2)$. See Fig. 2.6.

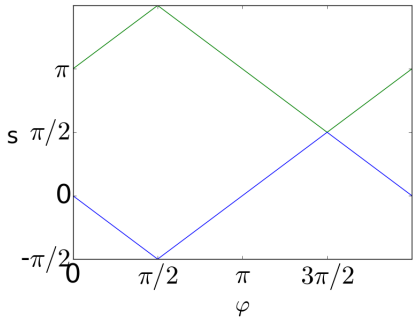

Fig. 2.6: Singular case: Crests for $I = 1$ and $\mu = 1$.

We can describe the relation between the crests $\mathrm{C}(I)$ and the NHIM lines $R(I, \varphi, s)$ through the following Proposition:

Proposition 13. *Consider the crest $C(I)$ defined by* (2.21) *and the NHIM line $R(I, \varphi, s)$ defined in* (2.11).

a) For $|\mu| < 0.625$ the crests are horizontal and the intersections between any crest and any NHIM line is transversal.

b) For $0.625 \leq |\mu| \leq 0.97$ the two crests $C(I)$ are still horizontal, but for some values of I there exist two NHIM lines $R(I, \varphi, s)$ which are quadratically tangent to the crests.

c) For $|\mu| > 0.97$, the same properties as stated in b) hold, except that for $|\mu\alpha(I)| > 1$, the crests $C(I)$ are vertical.

Proof. The "horizontality" of a) and b) and the "verticality" of c) are due the upper bound of $|\mu|$. Since $|\alpha(I)| < 1/0.97$ (see Fig.2.7), for $|\mu| \leq 0.97$, the crests are horizontal, that is, they can be expressed by equations (2.23).

The condition of transversality is proved in [DH11]. Essentially, the proof is to observe that $|I\alpha(I)| < 1.6$ and that there exists a φ such that $\partial\xi(I, \varphi)/\partial\varphi = 1/I$ if, only if, $|I\alpha(I)| < 1/|\mu|$(we will prove it in a slightly different context, see the proof of Proposition 20.)

About the amount of NHIM lines tangents to $\mathrm{C}(I)$, the proof is given in subsection 2.2.2. □

In Figs. 2.5(a) and 2.5(b) we have displayed a segment of the the NHIM line $R(I, \varphi, s)$, $|\tau| < \pi$, and we see that it intersects each crest $\mathrm{C_M}(I)$ and $\mathrm{C_m}(I)$ transversally, giving rise to two values τ^*_{M} and τ^*_{m} , therefore to two different scattering maps. We denote by τ^*_{M} the τ with minimum absolute value such that given (I, φ, s), $(I, \varphi - I\tau, s - \tau) \in \mathrm{C_M}(I)$ and τ^*_{m} is defined analogously when $(I, \varphi - I\tau, s - \tau) \in \mathrm{C_m}(I)$ (see [DH11]).

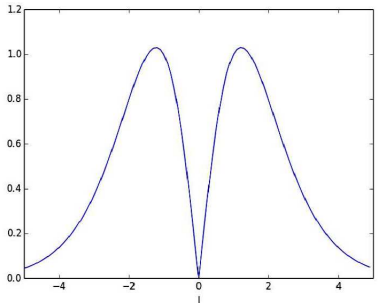

Fig. 2.7: Graph of $|\alpha(I)|$

Scattering maps and crests

Note that $\tau_{\rm m}^*$ and $\tau_{\rm M}^*$ are associated to different homoclinic points to the NHIM $\tilde{\Lambda}$, and consequently, to different homoclinic connections. From this we build different scattering maps. The most natural way is to associate one scattering map to each crest. And we will do this on the variables (I, φ, s) and (I, θ), where $\theta = \varphi - Is$.

Before, we make some considerations about the NHIM lines defined in (2.11). Note that

$$\theta := \varphi - Is = (\varphi - I\tau) - I\,(s - \tau)\,,$$

that is, θ is constant on each NHIM line $R(I, \varphi, s)$, so we will also introduce another notation for a NHIM line $R(I, \varphi, s)$, namely

$$R_\theta(I) := \{(I, \varphi, s) : \varphi - Is = \theta\}.$$

Since $(\varphi, s) \in \mathbb{T}^2$, $R(I, \varphi, s)$ is a closed line if $I \in \mathbb{Q}$, whereas it is a dense line on $\mathbb{T}^2$ if $I \notin \mathbb{Q}$. In this case, $R(I, \varphi, s)$ intersects the crests $\mathrm{C}(I)$ along an infinite number of points.

Recall (see Remark 6) that θ is quasi-periodic in the variable $s \in \mathbb{T}$. To avoid monodromy with respect to this variable, we are going to consider from now on, in this Chapter, s as a real variable in an interval of length 2π, $-\pi/2 < s \leq 3\pi/2$. Under this restriction, the NHIM line $R(I, \varphi, s)$ defined in (2.11) becomes a *NHIM segment*

$$R(I, \varphi, s) = \{(I, \varphi - I\tau, s - \tau)\,; -\pi/2 < s - \tau \leq 3\pi/2\}, \tag{2.25}$$

as well as $R_\theta(I)$, which can be written as

$$R_\theta(I) = \{(I, \varphi, s) : \varphi - Is = \theta, (\varphi, s) \in \mathbb{T} \times (-\pi/2, 3\pi/2]\}. \tag{2.26}$$

From now on, when we refer to $R(I, \varphi, s)$ and $R_\theta(I)$, they will be these line segments. Notice that $\theta \in \mathbb{T}$.

We begin to consider the *primary* scattering map $\mathcal{S}_{\rm M}$ associated to the maximum crest $\mathrm{C}_{\rm M}$, that is, we look only at the intersections between the segment $R(I, \varphi, s)$ given in (2.25) and $\mathrm{C}_{\rm M}(I)$, parameterized by $\tau_{\rm M}^*(I, \varphi, s) = \tau_{\rm M}^*(I, \theta) + s$ (see (2.18)):

$$\begin{aligned} \mathrm{C}_{\rm M}(I) \cap R(I, \varphi, s) &= \{(I, \varphi - I\tau_{\rm M}^*(I, \varphi, s), \xi_{\rm M}(I, \varphi - I\tau_{\rm M}^*(I, \varphi, s)))\} & (2.27)\\ &= \{(I, \varphi - I\tau_{\rm M}^*(I, \varphi, s), s - \tau_M^*(I, \varphi, s))\} & (2.28) \end{aligned}$$

Equation (2.27) motivates us to introduce a new variable $\psi = \varphi - I\tau^*_{\rm M}(I,\varphi,s)$ that will be useful in many contexts.

The variable ψ: a variable on the crest.

Let $\mathrm{C}(I)$ be a crest such that it can be parameterized by $\xi(I,\varphi)$ as in (2.23). Since $\tau^*(I,\varphi,s)$ is the value of τ such that $R(I,\varphi,s)$, given in (2.25), intersects $\mathrm{C}(I)$, we define

$$\psi := \varphi - I\tau^*(I,\varphi,s). \tag{2.29}$$

By (2.18) we can also write ψ in terms of the variable θ:

$$\psi = \varphi - I\left(\tau^*(I,\theta) + s\right) = \theta - I\tau^*(I,\theta). \tag{2.30}$$

By (2.27) and (2.28),

$$s - \tau^*(I,\varphi,s) = \xi(I,\varphi - I\tau^*(I,\varphi,s)) = \xi(I,\psi). \tag{2.31}$$

In particular, for $s=0$, $\xi(I,\psi) = -\tau^*(I,\varphi,0) = -\tau^*(I,\theta)$ again by (2.18) and from (2.30) we have the expression of θ in terms of ψ:

$$\theta = \psi - I\xi(I,\psi). \tag{2.32}$$

All the relations between the variables (φ,s), θ and ψ are written in Table 2.1 and are displayed in Fig. 2.8. By the definitions of $L^*(I,\varphi,s)$ in (2.13), and $\mathcal{L}^*(I,\theta)$ in (2.16) and (2.19), we have that

$$\mathcal{L}^*(I,\theta) = L^*(I,\varphi,s) = \mathcal{L}(I,\psi,\xi(I,\psi)), \tag{2.33}$$

So we can define the reduced Poincaré function in terms of (I,ψ) simply as the restriction of the Melnikov potential $\mathcal{L}(I,\varphi,s)$ on the crest $C(I) = \{(I,\psi,\xi(I,\psi),\psi\in\mathbb{T})\}$, i.e.,

$$\mathfrak{L}^*(I,\psi) := \mathcal{L}(I,\psi,\xi(I,\psi)), \tag{2.34}$$

which in our case takes the simple and computable form

$$\mathfrak{L}^*(I,\psi) = A_{00} + A_{10}(I)\cos\psi + A_{01}\cos\xi(I,\psi), \tag{2.35}$$

for a horizontal crest (3.21).

Therefore, as $(I,\psi,\xi(I,\psi))$ are points on the crest, the domain of $L^*(I,\cdot,\cdot)$ is a subset of $C(I)$. So, if there exist different subsets where $L^*(I,\cdot,\cdot)$ can be well defined, we can build different scattering maps associated to $C(I)$.

Denote $\mathcal{L}^*_i(I,\theta) = L(I,\varphi - I\tau^*_i(I,\varphi,s), s - \tau^*_i(I,\varphi,s))$, $i = \mathrm{m},\mathrm{M}$, and $\mathfrak{L}^*_i(I,\psi) = \mathcal{L}(I,\psi,\xi_i(I,\psi))$ from (2.33) and (2.34). We state the following lemma

Lemma 14. *a) The Poincaré Reduced functions $\mathfrak{L}^*_M(I,\psi)$ and $\mathcal{L}^*_M(I,\theta)$ are even functions in the variable I, that is, $\mathfrak{L}^*_M(I,\psi) = \mathfrak{L}^*_M(-I,\psi)$ and $\mathcal{L}^*_M(I,\theta) = \mathcal{L}^*_M(-I,\theta)$, and consequently $\mathcal{S}_M(I,\theta)$ is symmetric in this variable I. The same happens for $\mathcal{S}_m(I,\theta)$, that is, for the scattering map associated to $C_m(I)$.*

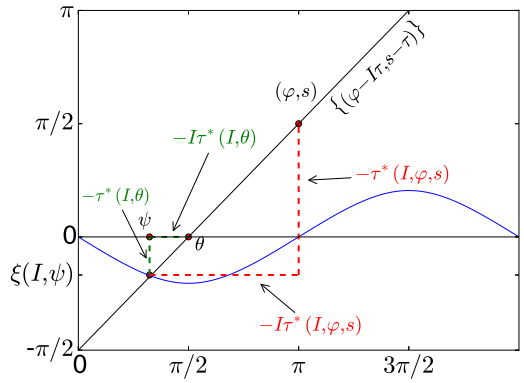

Fig. 2.8: The three variables on the plane (φ, s): φ, θ and ψ.

$\theta = \psi - I\xi(I,\psi)$	$\psi = \theta - I\tau^*(I,\theta)$
$\theta = \varphi - Is$	$\varphi = \theta + Is$
$\psi = \varphi - I\tau^*(I,\varphi,s)$	$\varphi = \psi + I\,(s - \xi(I,\psi))$

Table 2.1: Relation between variables.

b) The scattering map for a value of μ and $s = \pi$, associated to the intersection between $R_\theta(I)$ and $C_m(I)$ has the same geometrical properties as the scattering map for $-\mu$ and $s = 0$, associated to the intersection between $R_\theta(I)$ and $C_M(I)$, i.e.,

$$S_{\mu,m}(I,\varphi,\pi) = S_{-\mu,M}(I,\varphi,0) = \mathcal{S}_{-\mu,M}(I,\theta)$$

Proof. a) This is an immediate consequence of the fact that function $A_{10}(I)$ is even and $\xi_{\rm M}(I,\varphi)$ is odd in the variable I, see (2.9) and (2.23).

b) First, we look for $\tau^*_{\rm m}$ such that the NHIM segment $R_\theta(I)$ intersects the crest $C_{\rm m}(I)$. If we fix $s = \pi$, we have by (2.13) and (2.8):

$$L^*_{\mu,{\rm m}}(I,\varphi,\pi) = A_{00} + A_{10}(I)\cos(\varphi - I\tau^*_{\rm m}(I,\varphi,\pi)) + A_{01}\cos(\pi - \tau^*_{\rm m}(I,\varphi,\pi)). \quad (2.36)$$

Besides, we have by (2.10)

$$IA_{10}(I)\sin(\varphi - I\tau^*_{\rm m}) + A_{01}\sin(\pi - \tau^*_{\rm m}) = 0,$$

which, introducing μ (2.22), is equivalent to

$$\mu\alpha(I)\sin(\varphi - I\tau^*_{\rm m}) + \sin(\pi - \tau^*_{\rm m}) = 0, \quad (2.37)$$

or

$$-\mu\alpha(I)\sin(\varphi - I\tau^*_{\rm m}) + \sin(-\tau^*_{\rm m}) = 0. \quad (2.38)$$

By (2.31) and (2.23) we have that $\pi - \tau^*_{\rm m} = \xi_{\rm m}(I, \varphi - I\tau^*_{\rm m})$ for $\pi/2 \le \xi_{\rm m} \le 3\pi/2$ and therefore $-\pi/2 \le -\tau^*_{\rm m} \le \pi/2$.

By looking at (2.37) and (2.38), $\tau^*_{\rm m}(I,\varphi,\pi)$ for μ is solution of the same equation as $\tau^*_{\rm M}(I,\varphi,0)$ for $-\mu$, and lies in the same interval $-\pi/2 \le -\tau^*_{\rm M} \le \pi/2$. Therefore $\tau^*_{\rm m}(I,\varphi,\pi)$ for μ is equal to $\tau^*_{\rm M}(I,\varphi,0)$ for $-\mu$. From (2.36), $L^*_{\mu,{\rm m}}(I,\varphi,\pi)$ satisfies

$$\begin{aligned} L^*_{\mu,{\rm m}}(I,\varphi,\pi) &= A_{00} + A_{10}(I)\cos(\varphi - \tau^*_{\rm M}(I,\varphi,0)) + (-A_{01})\cos(-\tau^*_{\rm M}(I,\varphi,0)) \\ &= L^*_{-\mu,{\rm M}}(I,\varphi,0). \end{aligned}$$

Since $L^*_{\mu,\mathrm{m}}(\cdot,\cdot,\pi)$ and $L^*_{-\mu,\mathrm{M}}(\cdot,\cdot,0)$ coincide, their derivatives too and this implies that $S_{\mu,\mathrm{m}}(I,\varphi,\pi) = S_{-\mu,\mathrm{M}}(I,\varphi,0) = \mathcal{S}_{-\mu,\mathrm{M}}(I,\theta)$.

□

The importance of the part b) of this lemma is that, concerning diffusion, the study for a positive μ using $\mathcal{S}_{\mathrm{M}}(I,\theta)$ is equivalent to the study for $-\mu$ using $S_{\mathrm{m}}(I,\varphi,\pi)$, i.e., if we ensure the diffusion for a positive μ, we can ensure it for a negative one (just changing the scattering map). Besides, since $\mathcal{S}_{\mathrm{M}}(I,\theta)$ symmetric in the variable I (from the first part of the lemma), from now on we will consider always $I \geq 0$, $\mu > 0$ and $\mathcal{S}_{\mathrm{M}}$.

Now we are going to describe the influence of the intersections between the crests and the NHIM segments with respect to the parameter μ described in Proposition 13 on the scattering map associated to such crests.

Single scattering map: $\mu < 0.625$

As in [DH11], assuming $\mu < 1/1.6 = 0.625$, the crests are horizontal and there is no tangency between $R_\theta(I)$ and $\mathrm{C}_{\mathrm{M}}(I)$, so that $\tau^*_{\mathrm{M}}(I,\theta)$ is well defined and by (2.19) and (3.11) the reduced Poincaré function takes the form

$$\mathcal{L}^*_{\mathrm{M}}(I,\theta) = A_{00} + A_{10}(I)\cos(\theta - I\tau^*_{\mathrm{M}}(I,\theta)) + A_{01}\cos(-\tau^*_{\mathrm{M}}(I,\theta)), \tag{2.39}$$

and therefore $\mathcal{S}_{\mathrm{M}}(I,\theta)$ takes the form (2.17).

Example To illustrate this construction, we fix $\mu = 0.6$. In this case the crests are horizontal for all I, and we display $C_{\mathrm{M}}(I)$ parametrized by ξ_{M} (see (3.21)) in Fig.2.9 for $I = 1.2$. We can see how $R_\theta(I)$ intersects transversally $\mathrm{C}_{\mathrm{M}}(I)$, as well as the phase space of scattering map $\mathcal{S}_{\mathrm{M}}$ generated by this intersection given by the level curves of $\mathcal{L}^*_{\mathrm{M}}(I,\theta)$.

Remark 15. Recall from Remark 9 that s does not appear in the expression (2.17) for $\mathcal{S}(I,\theta)$ and is a parameter in the expression (2.12) for $S(I,\varphi,s)$. Computationally, one difference is that in expression (2.12), once fixed a value of s, one throws from any "initial point" (φ,s) the NHIM segment $R(I,\varphi,s)$ until it touches the crest $\mathrm{C}(I)$ after a time $\tau^*(I,\varphi,s)$, obtaining a value for $L^*(I,\varphi,s)$ given by (2.13), while in expression (2.17), s is fixed equal to 0 or, equivalently, the initial point to throw the NHIM segment $R_\theta(I)$ is of the form $(\theta,0)$ (see Fig. 2.8).

Multiple scattering maps: $0.625 \leq \mu \leq 0.97$

As said before, for $\mu < 1/1.6 = 0.625$ and any value of I, the two crests $C_{\mathrm{M}}(I)$ and $C_{\mathrm{m}}(I)$ are horizontal, and the NHIM segment $R_\theta(I)$ intersects transversely each of them, giving rise to a unique scattering map $\mathcal{S}_{\mathrm{M}}$ and $\mathcal{S}_{\mathrm{m}}$ associated to each crest. We will now explore larger values of μ to detect tangencies between $C(I)$ and $R_\theta(I)$, that is, when there exists (φ,I) such that

$$\frac{\partial \xi}{\partial \varphi}(I,\varphi) = 1/I,$$

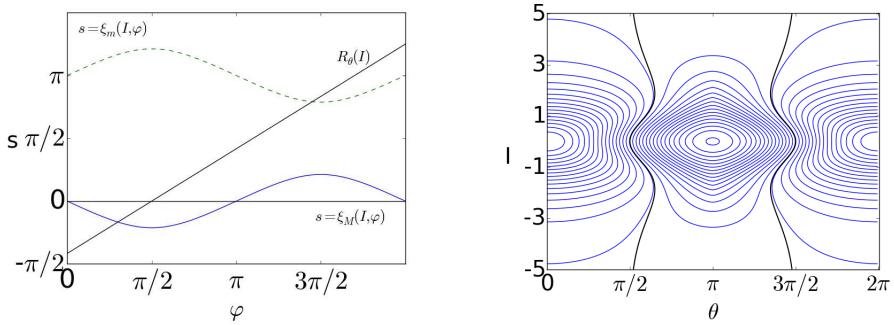

(a) Intersection between $R_\theta(I)$ and $\mathrm{C_M}(I)$ (in blue) for $\mu = 0.6$ and $I = 1.2$.

(b) The level curves of $\mathcal{L}^*_{\mathrm{M}}(I,\theta)$.

Fig. 2.9: $R_\theta(I) \cap \mathrm{C_M}(I)$ and $\mathcal{S}_{\mathrm{M}}(I,\theta)$.

where $\xi(I,\varphi)$ is the parameterization (3.21) of the crest.

Tangencies between $\mathbf{C}(I)$ and $R_\theta(I)$ and multiple scattering maps

We take $\mathrm{C_M}(I)$ parameterized by ξ_{M} as in (3.21). For the other crest $\mathrm{C_m}(I)$ is analogous. Suppose that there exists a tangency point between $\mathrm{C_M}(I)$ and $R_\theta(I)$. This is equivalent to the existence of ψ such that $\partial\xi_{\mathrm{M}}/\partial\psi(I,\psi) = 1/I$. Using (3.21), this condition is equivalent to

$$-\frac{\mu\alpha(I)\cos\psi}{\sqrt{1-\mu^2\alpha(I)^2\sin^2\psi}} = \frac{1}{I}, \tag{2.40}$$

where $\alpha(I)$ is introduced in (2.22). Therefore

$$\psi = \pm\arctan\left(\sqrt{\frac{I^2\mu^2\alpha(I)^2-1}{1-\mu^2\alpha(I)^2}}\right) + \pi,$$

where the expression under the square root is non-negative for $0.625 \le \mu \le 0.97$ for some values of I by Proposition 13. We are considering just these values of I.

Equation (2.40) implies $\cos\psi < 0$, say $\psi \in (\pi/2, 3\pi/2)$. Denote the two tangent points by ψ_1 and ψ_2 and, without loss of generality, $\psi_1 \le \psi_2$ with $\psi_1 \in (\pi/2,\pi]$ and $\psi_2 = 2\pi - \psi_1 \in [\pi, 3\pi/2)$.

We consider the function relating the variables θ and ψ (see Table 2.1)

$$\theta(\psi) = \psi - I\xi_{\mathrm{M}}(I,\psi), \tag{2.41}$$

and define

$$\theta_1 = \psi_1 - I\xi_{\mathrm{M}}(I,\psi_1) \qquad \text{and} \qquad \theta_2 = \psi_2 - I\xi_{\mathrm{M}}(I,\psi_2).$$

The function $\theta(\psi)$ has only two critical points, ψ_1 and ψ_2, except for the case where $\psi_1 = \psi_2 = \pi$. Besides, we have

$$I\frac{\partial\xi_M}{\partial\psi}(I,\psi) = -\frac{I\mu\alpha(I)\cos\psi}{\sqrt{1-\mu^2\alpha(I)^2\sin^2\psi}} < 0, \quad \forall\psi \in (0,\pi/2)\cup(3\pi/2,2\pi)$$

Therefore, $-I\partial\xi_M/\partial\psi > 0$, thus $d\theta/d\psi = 1 - I\partial\xi_M/\partial\psi > 0 \quad \forall\psi \in (0,\pi/2)\cup(3\pi/2,2\pi)$.

By continuity of $d\theta/d\psi$ and since $\theta(\psi)$ has only two critical points, we have

$$\begin{aligned}\frac{d\theta}{d\psi} &> 0 \quad \forall\psi \in (0,\psi_1)\cup(\psi_2,2\pi)\\ \frac{d\theta}{d\psi} &< 0 \quad \forall\psi \in (\psi_1,\psi_2)\,.\end{aligned}$$

Therefore $\theta_1 = \theta(\psi_1) \geq \theta_2 = \theta(\psi_2)$. Note that $\theta([\psi_2, 2\pi]) = [\theta_2, 2\pi]$. As $\theta_1 \in [\theta_2, 2\pi]$, there is a $\tilde{\psi}_1 \in [\psi_2, 2\pi]$ such that $\theta(\tilde{\psi}_1) = \theta_1$. As $d\theta/d\psi$ is positive, $\tilde{\psi}_1$ is unique in that interval. Analogously, we have $\tilde{\psi}_2 \in (0,\psi_1)$ such that $\theta(\tilde{\psi}_2) = \theta_2$. We have $\tilde{\psi}_2 \leq \psi_1 \leq \psi_2 \leq \tilde{\psi}_1$. We can build, at least, three bijective functions:

$$\begin{aligned}\theta_A: &\qquad D_A := \left[0,\tilde{\psi}_2\right]\cup(\psi_2,2\pi] &&\longrightarrow [0,2\pi]\\ \theta_B: &\qquad D_B := [0,\psi_1)\cup\left[\tilde{\psi}_1,2\pi\right] &&\longrightarrow [0,2\pi]\\ \theta_C: &\quad D_C := \left[0,\tilde{\psi}_2\right]\cup(\psi_1,\psi_2)\cup\left[\tilde{\psi}_1,2\pi\right] &&\longrightarrow [0,2\pi]\end{aligned} \tag{2.42}$$

If $\psi_1 < \psi_2$, that is, the tangency point is different from $\psi = \pi$, we have, at least, three scattering maps associated to C_{M}, the scattering map associated to $\mathcal{L}^*(I,\theta_j)$, $j = A, B, C$.

Remark 16. Those three scattering maps appear because the NHIM line $R_\theta(I)$ intersects $C_{\mathrm{M}}(I)$ three times for θ in the interval (θ_1,θ_2).

Definition 17. We call *tangency locus* the set

$$\left\{(I,\theta(\psi)) : \frac{\partial\xi}{\partial\psi}(I,\psi) = \frac{1}{I} \text{ and } I \in [-I^*, I^*]\right\}.$$

Fixed I such that there exist tangencies, as we have seen before, there exist $\theta_1 \leq \theta_2$ such that $(I,\theta_1),(I,\theta_2)$ belong to the tangency locus. We have that for any $\theta \notin (\theta_1,\theta_2)$ there is only one scattering map. But we have three different scattering maps for $\theta \in (\theta_1,\theta_2)$. We can see this behavior on the example below.

Example We illustrate the scattering maps of $C_{\mathrm{M}}(I)$ for $\mu = 0.9$ in Fig. 2.10. We can see the three scattering maps and we emphasize their difference showing a zoom around the tangency locus. In this zoom, we can see curves with three different colors. Each color represents a different scattering map.

The scattering maps "with holes": $\mu > 0.97$

We study now the case when μ is large enough such that $\mu\alpha(I) > 1$ for some I, that is, for $\mu > 0.97$. In this case, the horizontal crests become vertical crests for some values of I. But locally, the structure of the parameterizations ξ_{M} and ξ_{m} are preserved, that is,

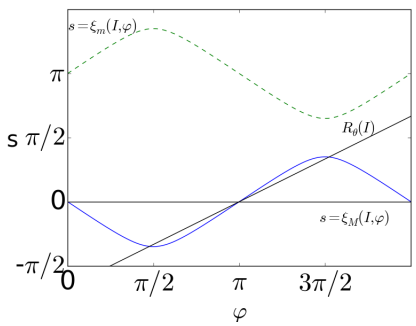

(a) The three intersections between $R_\theta(I)$ and $C_{\mathrm{M}}(I)$ for $\mu = 0.9$, $I = 1.5$.

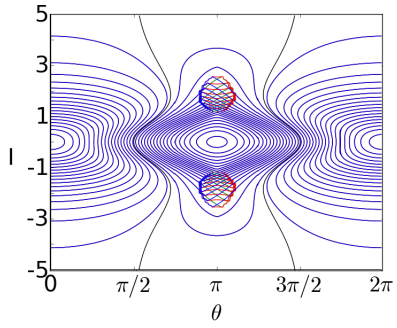

(b) Level curves of $\mathcal{L}^*_{\mathrm{M}}(I,\theta)$.

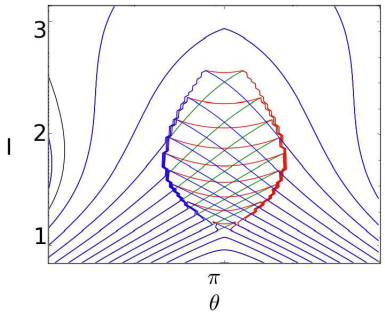

(c) Zoom around the tangency locus

Fig. 2.10: Tangencies: Multiple scattering maps.

even if the crests are vertical from a global view-point, these crests are formed by pieces of horizontal crests. So, some intersections between $R_\theta(I)$ and $C(I)$ parameterized by the vertical parameterization η, given in (2.24), can be seen, indeed, as intersections between $R_\theta(I)$ and $C(I)$ parameterized by ξ, given in (3.21). Using this idea, we can extend the scattering map associated to the reduced Poincaré function, given in (2.34), for the values of (I,φ) such that $\mu\alpha(I) > 1$ but $|\mu\alpha(I)\sin\varphi| < 1$. For some values of φ like $\varphi = \pi/2, 3\pi/2$, this is not possible, and for those values of φ some "holes" appear in the definition of the scattering map when the horizontal parameterization ξ is used.

Remark 18. For the diffusion, a priori, the existence of such values can be a problem. However, one can avoid these holes using the inner map, or using another scattering map associated to the vertical parameterization η given in (2.24).

Example We illustrate this case in Fig. 2.11. We display in (a) an example of intersection between $R_\theta(I)$ and $C_{\mathrm{M}}(I)$ and in (b) the level curves of $\mathcal{L}^*_{\mathrm{M}}(I,\theta)$ (recall that they provide an approximation to the orbits of the scattering map $\mathcal{S}_{\mathrm{M}}(I,\theta)$). The green region in (b) is the region where the scattering map is not defined, that is, for a point (I,θ) in this region, $R_\theta(I)$ does not intersect $C_{\mathrm{M}}(I)$.

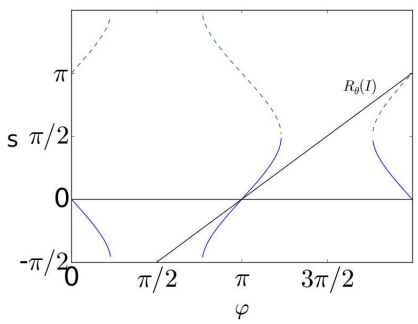

(a) Intersection between $C_{\mathrm{M}}(I)$ and $R_\theta(I)$. $\mu = 1.5$ and $I = 1$.

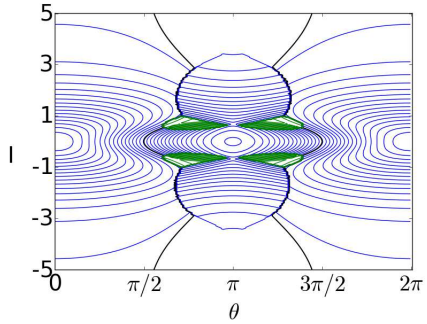

(b) Level curves of $\mathcal{L}^*_{\mathrm{M}}(I, \theta)$. In green, the region which the level curves are not defined.

Fig. 2.11: Scattering map with holes

Summary of the scattering maps

Taking into account the results of the last three sub-subsections 2.2.2–2.2.2 on the primary scattering map $\mathcal{S}_{\mathrm{M}}$, $\mathcal{S}_{\mathrm{m}}$ for $\mu > 0$ as well as Lemma 54 we can complete Proposition 13.

Theorem 19. *Consider the crests $C(I)$ defined in* (2.21) *and the NHIM lines $R(I, \theta)$ defined in* (2.26)

- *For $0 < |\mu| < 0.625$ the two crests are horizontal and the intersection between any crest and any NHIM lines is transversal. There exist two primary scattering maps $\mathcal{S}(I, \theta)$ defined on the whole range of $\theta \in \mathbb{T}$.*
- *For $0.625 \leq |\mu| \leq 0.97$ the two crests are still horizontal, but for some values of I there exist two NHIM lines $R_{\theta_1}(I)$, $R_{\theta_2}(I)$ which are geometrically tangent to the crests. There exist two or six scattering maps defined for $\theta \neq \theta_1, \theta_2$.*
- *For $|\mu| > 0.97$, the same properties stated in b) hold, except that for some bounded interval of $|I|$ there exists a sub-interval of $\theta \in \mathbb{T}$ such that the scattering maps are not defined.*

2.3 Arnold diffusion

In the rest of the chapter, our goal will be the study of Arnold diffusion using adequately chosen scattering maps. For this diffusion, it will be important to describe the level curves of the reduced Poincaré function $\mathcal{L}^*(I, \theta)$, since the scattering map is up to an error $\mathcal{O}(\varepsilon^2)$, the $-\varepsilon$ time flow of the Hamiltonian $\mathcal{L}^*(I, \theta)$. Among the level curves of $\mathcal{L}^*(I, \theta)$, we will first describe two candidates for fast diffusion, namely the ones of equation $\mathcal{L}^*(I, \theta) = A_{00} + A_{01}$, that will be called "highways". Indeed, such highways will be taken into account in the two theorems about the existence of diffusion that will be proven in this section.

In the next proposition we prove that $\mathcal{L}^*(I,\theta) = A_{00} + A_{01}$ is a union of two "vertical" curves in a rectangle $\mathbb{T} \times B$, that is, it can be written as $\mathrm{H_l} \cup \mathrm{H_r}$ where $\mathrm{H}_k = \{(I, \theta_k(I)) : I \in B\}$, $\theta_k(I)$ is a smooth function, and the index k takes the value l for left ($0 < \theta_{\mathrm{l}}(I) < \pi$) o r for right ($\pi < \theta_{\mathrm{r}}(I) < 2\pi$). To prove this, we only need to prove that

$$\frac{\partial \mathcal{L}^*_{\mathrm{M}}}{\partial \theta}(I,\theta) \neq 0 \quad \forall (I,\theta) \in \{(I,\theta) : \mathcal{L}^*_{\mathrm{M}}(I,\theta) = A_{00} + A_{01} \text{ and } I \in B\}\,.$$

2.3.1 A geometrical proposition: The level curves of $\mathcal{L}^*(I,\theta)$

Proposition 20. *Assuming $a_{10}\, a_{01} \neq 0$, the level curve $\mathcal{L}^*(I,\theta) = A_{00} + A_{01}$ of the reduced Poincaré function* (2.16) *is a union of two "vertical" curves on a cylinder $(\theta, I) \in \mathbb{T} \times B$, where the set B is given by*

- *for $|\mu| < 0.625$, B is the real line.*
- *for $0.625 \leq |\mu|$, $B = (-\infty, -I_{++}) \cup (-I_+, I_+) \cup (I_{++}, +\infty)$, where*

$$I_{++} = \max\left\{ I > 0 : \frac{I^3 \sinh(\pi/2)}{\sinh(I\pi/2)} = \frac{1}{|\mu|} \right\}$$

and

  - $I_+ = \min\left\{ I > 0 : I^3 \sinh(\pi/2)/\sinh(I\pi/2) = 1/|\mu| \right\}$, *for* $|\mu| \leq 1$
  - $I_+ = \min\left\{ I > 0 : I^2 \sinh(\pi/2)/\sinh(I\pi/2) = 1/|\mu| \right\}$, *for* $|\mu| \geq 1$

Proof. Consider the real set A:

$$A = \left\{ I \geq 0 : |\alpha(I)| \leq \frac{1}{|\mu|} \right\}. \tag{2.43}$$

For $I \in A$, the maximum crest $\mathrm{C_M}(I)$ is horizontal and can be parameterized by the expression (3.21) and $\xi_{\mathrm{M}}(I,0) = \xi_{\mathrm{M}}(I,\pi) = \xi_{\mathrm{M}}(I,2\pi) = 0$.

Consider now the subset of A

$$B = \{I \in A : \text{there is no tangency between } \mathrm{C_M}(I) \text{ and } R_\theta(I)\}. \tag{2.44}$$

As already mentioned, for $I \in B$ one has $\partial \xi_{\mathrm{M}}/\partial \psi(I,\psi) \neq 1/I, \quad \forall \psi \in [0, 2\pi]$. In particular, for $I \in B$ the change (2.32) $\psi \in \mathbb{T} \mapsto \theta = \psi - I\xi(I,\psi) \in \mathbb{T}$ is smooth with inverse

$$\psi = \theta - I\tau^*_{\mathrm{M}}(I,\theta) \qquad \forall \theta \in \mathbb{T}. \tag{2.45}$$

Then we can rewrite for $I \in B$ and $\theta \in \mathbb{T}$ the reduced Poincaré function $\mathcal{L}^*_{\mathrm{M}}(I,\theta)$ of (2.39) in terms of this variable ψ as

$$\mathfrak{L}^*_{\mathrm{M}}(I,\psi) = A_{00} + A_{10}(I)\cos\psi + A_{01}\cos\xi_{\mathrm{M}}(I,\psi).$$

Notice that $\mathfrak{L}^*_{\mathrm{M}}(I,\psi)$ is well defined for all $(I,\psi)\in A\times\mathbb{T}$ and it is immediate to see that for any $I\in A$ there exists exactly one $\psi_0\in(0,\pi)$ and another one $\psi_1\in(\pi,2\pi)$ such that $\mathfrak{L}^*_{\mathrm{M}}(I,\psi_0)=\mathfrak{L}^*_{\mathrm{M}}(I,\psi_1)=A_{00}+A_{01}$. Restricting now to $I\in B$, the same property holds for $\mathcal{L}^*(I,\theta)$, since the relation between θ and ψ is a change of variables sending $\theta=0,\,\pi$ to $\psi=0,\,\pi$ respectively. In other words, introducing the projection $\Pi:\mathbb{R}\times\mathbb{T}\to\mathbb{R}$, $\Pi(I,\theta)=I$, $B\subset\Pi\left(\mathcal{L}^{*-1}_{\mathrm{M}}(A_{00}+A_{01})\right)$.

We can characterize B defined in (2.44) by the following property

$$I\in B\Leftrightarrow\beta(I):=I\alpha(I)<\frac{1}{|\mu|}. \tag{2.46}$$

Indeed, by definition (2.43), A is characterized by $I\in A\Leftrightarrow\alpha(I)\leq 1/|\mu|$, where $\alpha(I)\geq 0$ is defined in (2.22), and it satisfies $\lim_{I\to 0^+}\alpha(I)=0=\lim_{I\to+\infty}\alpha(I)$ and it has a unique positive critical point $I_\alpha\approx 1.219$ which is a global maximum, see Fig.2.12. Therefore

$$\alpha(I)\leq\alpha(I_\alpha)=\frac{1}{0.97}\sim 1.03. \tag{2.47}$$

On the other hand, for $I\in A$ there exist tangencies between $\mathrm{C}_{\mathrm{M}}(I)$ and $R_\theta(I)$ as long as the condition (2.40) holds, which can only take place for $|I\alpha(I)|\geq 1/\mu$, which justifies the characterization (2.46) for B.

The function $\beta(I)$ is very similar to $\alpha(I)$, that is, $\beta(I)$ is always positive for $I>0$, it has a unique positive critical point $I_\beta=1.9$ and $\beta(I)\to 0$ as $I\to 0$ and $I\to+\infty$. This positive critical point is a global maximum point,

$$\beta(I)\leq\beta(I_\beta)=1.6. \tag{2.48}$$

Besides, by (2.46), for $I<1$, $\beta(I)<\alpha(I)$, $\beta(1)=\alpha(1)=1$ and for $I>1$, $\beta(I)>\alpha(I)$. See Fig. 2.12.

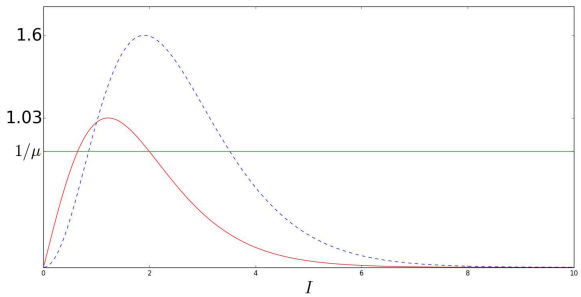

Fig. 2.12: Graph of $\alpha(I)$, in red, and $\beta(I)$, in blue (dashed).

Now we consider the three case of the proposition, that is, **1)** $|\mu|<0.625$, **2)** $0.625\leq|\mu|\leq 1$ and **3)** $|\mu|\geq 1$.

- **Case 1** $|\mu| < 0.625$, that is, $1/|\mu| > 1.6$. Then, by (2.47) and (2.48),

$$\alpha(I) \leq 1.03 < \frac{1}{\mu} \quad \text{and} \quad \beta(I) \leq 1.6 < \frac{1}{|\mu|},$$

for all I, that is, for $I > 0$, $B = [0, +\infty)$.

- **Case 2** Note that for $0.625 \leq |\mu| < 0.97$

$$\alpha(I) \leq 1.03 = 1/0.97 < \frac{1}{|\mu|} \leq 1.6 = \beta(I_\beta),$$

and by (2.47), $A = [0, +\infty)$. But, now $\beta(I_b) \geq 1/|\mu|$. Then there exist two values $I \in A$ such that $\beta(I) = 1/|\mu|$. Define

$$I_+ = \min\{I : \beta(I) = 1/|\mu|\} \qquad \text{and} \qquad I_{++} = \max\{I : \beta(I) = 1/|\mu|\}. \tag{2.49}$$

By the characterization (2.46) of the set B we have $B = [0, I_+) \cup (I_{++}, +\infty)$.

For $0.97 \leq |\mu| \leq 1$, there exist $I_a < I_{\bar{a}}$ such that $\alpha(I_j) = 1/|\mu|$, $j \in \{a, \bar{a}\}$ and $A = [0, I_a) \cup (I_{\bar{a}}, +\infty)$. Analogously, there exist $I_b < I_{\bar{b}}$ such that $\beta(I_j) = 1/|\mu|$, $j \in \{b, \bar{b}\}$. As $I_b \leq I_a$ and $I_{\bar{a}} < I_{\bar{b}}$, we have $B = [0, I_b) \cup (I_{\bar{b}}, +\infty)$, see Fig. 2.12. But this the equivalent to $B = [0, I_+) \cup (I_{++}, +\infty)$, where I_+ and I_{++} are given by (2.49).

- **Case 3** This case is similar to the **Case 2** for $0.97 \leq |\mu| \leq 1$. But now, as $|\mu| \geq 1$, we have $I_a \leq I_b$. So, in this case we have $B = [0, I_a) \cup (I_{\bar{b}}, \infty)$, or $B = [0, I_+) \cup (I_{++}, +\infty)$, where $I_+ = \min\{I : \alpha(I) = 1/|\mu|\}$ and $I_{++} = \max\{I : \beta = 1/|\mu|\}$.

Finally, we see that $\mathcal{L}^*_{\mathrm{M}}(I, \theta) = A_{00} + A_{01}$ is composed by two curves in rectangles $(\theta, I) \in ((0, \pi) \cup (\pi, 2\pi)) \times B$. This is equivalent to prove that the derivative of this curve with respect to the variable θ is different from 0 for all I in B. For any $I \in B$, we compute the expression for $\partial \mathcal{L}^*_{\mathrm{M}} / \partial \theta(I, \theta)$ which using (2.10) and the change of variables (2.45) takes the form

$$\frac{\partial \mathcal{L}^*_{\mathrm{M}}}{\partial \theta}(I, \theta) = -A_{10}(I) \sin(\psi), \tag{2.50}$$

and never vanishes for $\psi \in (0, \pi) \cup (\pi, 2\pi)$, or equivalently, for $\theta \in (0, \pi) \cup (\pi, 2\pi)$. Then $\mathcal{L}^*_{\mathrm{M}}(I, \theta) = A_{00} + A_{01}$ is composed by two vertical curves on B.

As we have seen in Lemma 54, $\mathcal{L}^*(-I, \theta) = \mathcal{L}^*(I, \theta)$. Then, the level curve $\mathcal{L}^*_{\mathrm{M}}(I, \theta) = A_{00} + A_{01}$ is also defined for $I < 0$, which concludes the proof. □

Remark 21. Using the expressions above for I_+ and I_{++} one can check that

$$I_+ \sim \frac{\pi}{2|\mu| \sinh(\pi/2)} \quad \text{and} \quad I_{++} \sim \left(\frac{2}{\pi}\right) \log(|2 \sinh(\pi/2)\mu|), \text{ as } |\mu| \to +\infty.$$

Definition 22. We call *highways* the two curves $H_{\rm l} \subset (0,\pi)\times\mathbb{T}$ and $H_{\rm r} \subset (\pi,2\pi)\times\mathbb{T}$ such that $\mathcal{L}^*(I,\theta) = A_{00} + A_{01}$. By Proposition 20, they exist at least for $I \in (-\infty,-I_{++}) \cup (-I_+,I_+) \cup (I_{++},+\infty)$ for $|\mu| \geq 0.615$ and for any value I for $|\mu| < 0.625$. If $a_{10} > 0$, by (2.50), $\partial\mathcal{L}^*/\partial\theta$ is positive (respectively negative) along the highway $H_{\rm r}$ (resp. $H_{\rm l}$). If $a_{10} < 0$, change $H_{\rm l}$ to $H_{\rm r}$.

Proposition 23. *Consider the Hamiltonian*

$$H_\varepsilon(p,q,I,\varphi,s) = \pm\left(\frac{p^2}{2} + \cos q - 1\right) + \frac{I^2}{2} + \varepsilon\cos q\,\left(a_1\cos\varphi + a_2\cos s\right),$$

$a_1 a_2 \neq 0$. *The highways take the form*

$$\theta_h(I) = \begin{cases} \arccos\left(\frac{A_2(1-f(I))}{A_1(I)}\right) + I\arccos(f(I)), & I \leq 0; \\ \arccos\left(\frac{A_2(1-f(I))}{A_1(I)}\right) - I\arccos(f(I)), & I > 0; \end{cases}$$

and

$$\theta_H(I) = \begin{cases} -\arccos\left(\frac{A_2(1-f(I))}{A_1(I)}\right) - I\arccos(f(I)), & I \leq 0; \\ -\arccos\left(\frac{A_2(1-f(I))}{A_1(I)}\right) + I\arccos(f(I)), & I > 0; \end{cases}$$

where $\theta_h \in (0,\pi)$ *and* $\theta_H \in (\pi,2\pi)$.

Proof. From (2.20), (2.33) and the definition of the highways, we have the following two equations

$$\begin{aligned} A_1(I)\cos(\theta - I\tau^*) + A_2\cos(-\tau^*) &= A_2 \\ IA_1(I)\sin(\theta - I\tau^*) + A_2\sin(-\tau^*) &= 0. \end{aligned} \tag{2.51}$$

Multiplying by I the first equation we obtain

$$\begin{aligned} IA_1(I)\cos(\theta - I\tau^*) + IA_2\left(\cos(-\tau^*) - 1\right) &= 0 \\ IA_1(I)\sin(\theta - I\tau^*) + A_2\sin(-\tau^*) &= 0. \end{aligned}$$

or equivalently

$$\begin{aligned} IA_1(I)\cos(\theta - I\tau^*) &= -IA_2\left(\cos(-\tau^*) - 1\right) \\ IA_1(I)\sin(\theta - I\tau^*) &= -A_2\sin(-\tau^*). \end{aligned}$$

We sum these two equations squared and we obtain

$$I^2A_1^2(I) = \left[IA_2\left(\cos(-\tau^*) - 1\right)\right]^2 + A_2^2\sin^2(-\tau^*).$$

After some arithmetical manipulations we obtain the following equation of second degree in $\cos(-\tau^*)$

$$(I^2-1)A_2^2\cos^2(-\tau^*) - 2I^2A_2^2\cos(-\tau^*) + A_2^2(I^2+1) - I^2A_1^2(I) = 0.$$

Solving this equation we have

$$\cos(-\tau^*) = \frac{2I^2A_2^2 \pm \sqrt{4I^4A_2^4 - 4(I^2-1)A_2^2\left[A_2^2(I^2+1) - I^2A_1^2(I)\right]}}{2(I^2-1)A_2^2}.$$

After more arithmetical manipulation and considering that $-1 \leq \cos(-\tau^*) \leq 1$ we have

$$\cos(-\tau^*) = \frac{I^2A_2 - \sqrt{A_2^2 + (I^2-1)I^2A_1^2(I)}}{(I^2-1)A_2}.$$

In order to simplify the notation we define

$$f(I) := \frac{I^2A_2 - \sqrt{A_2^2 + (I^2-1)I^2A_1^2(I)}}{(I^2-1)A_2}$$

And therefore,

$$\Rightarrow -\tau^*(I,\theta) = \pm\arccos(f(I)).$$

Remember that we have two highways. This explains why we have found two different values for the function τ^*. Then we can rewrite the first equation of (2.51) as

$$A_1(I)\cos(\theta \pm I\arccos(f(I))) + A_2f(I) = A_2.$$

This immediately implies

$$\theta = \pm\arccos\left(\frac{A_2\left(1-f(I)\right)}{A_1(I)}\right) \mp I\arccos(f(I)).$$

From the four possibilities, by comparing with numerical results we obtain

$$\theta_{\mathrm{h}}(I) = \begin{cases} \arccos\left(\frac{A_2(1-f(I))}{A_1(I)}\right) + I\arccos(f(I)), & I \leq 0; \\ \arccos\left(\frac{A_2(1-f(I))}{A_1(I)}\right) - I\arccos(f(I)), & I > 0; \end{cases}$$

and

$$\theta_{\mathrm{H}}(I) = \begin{cases} -\arccos\left(\frac{A_2(1-f(I))}{A_1(I)}\right) - I\arccos(f(I)), & I \leq 0; \\ -\arccos\left(\frac{A_2(1-f(I))}{A_1(I)}\right) + I\arccos(f(I)), & I > 0; \end{cases}.$$

□

2.3.2 Results about global instability

Now we are going to prove two results about existence of the diffusion phenomenon in our model. The first one is a direct application of the geometrical Proposition 20 just proved and describes the diffusion that takes place close to the highways. The second is a more general type of diffusion, valid also for the values of the action I where there are no highways.

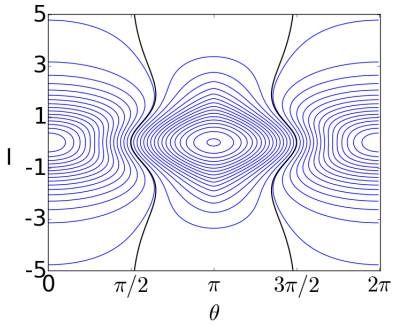

Fig. 2.13: *Highways* in black for $\mu = 0.6$.

Diffusion close to highways

Theorem 24. *Assume that* $a_{10}\, a_{01} \neq 0$ *in the Hamiltonian* (2.1)+(2.3). *Then, for any* I^* *there exists* $\varepsilon^* = \varepsilon^*(I^*) > 0$ *such that for* $0 < \varepsilon < \varepsilon^*$, *there exists a trajectory* $(p(t), q(t), I(t), \varphi(t))$ *such that for some* $T > 0$

$$I(0) \leq -I^*; \qquad I(T) \geq I^*,$$

where the admissible values for $I^* = I^*(\mu)$ *satisfy*

- *For* $|\mu| < 0.625$, I^* *is arbitrary* $I^* \in (0, +\infty)$.
- *For* $0.625 \leq |\mu| \leq 1$, $I^* \in (0, I_+)$, *where* $I_+ = \min\{I > 0 : I^3 \sinh(\pi/2)/\sinh(\pi I/2) = 1/|\mu|\}$.
- *For* $|\mu| \geq 1$, $I^* \in (0, I_+)$, *where* $I_+ = \{I > 0 : I^2 \sinh(\pi/2)/\sinh(\pi I/2) = 1/|\mu|\}$.

Proof. Recall that the reduced Poincaré function, given in (2.39), is

$$\mathcal{L}^*_{\mathrm{M}}(I, \theta) = A_{00} + A_{10}(I)\cos(\theta - I\tau^*_{\mathrm{M}}(I, \theta)) + A_{01}\cos(-\tau^*_{\mathrm{M}}(I, \theta)).$$

During this proof, we denote $\tau^*_{\mathrm{M}}(I, \theta)$ simply by τ^*_{M}. For ε small enough, the scattering map $\mathcal{S}_{\mathrm{M}}(I, \theta)$ takes the form (2.17) for $\mathcal{L}^* = \mathcal{L}^*_{\mathrm{M}}$, so that orbits under the scattering map are contained in the level curves of the reduced Poincaré function $\mathcal{L}^*_{\mathrm{M}}$, up to error of $\mathcal{O}(\varepsilon^2)$.

Proposition 20 ensures the existence of the highways as two vertical level curves $\mathcal{L}^*_{\mathrm{M}}(I, \theta) = A_{00} + A_{01}$ for I in

- $(-\infty, +\infty)$ for $|\mu| < 0.625$.
- $(-I_+, I_+)$, where
  - $I_+ = \min\{I > 0 : I^3 \sinh(\pi/2)/\sinh(\pi I/2) = 1/|\mu|\}$ for $0.625 \leq |\mu| \leq 1$;
  - $I_+ = \min\{I > 0 : I^2 \sinh(\pi/2)/\sinh(\pi I/2) = 1/|\mu|\}$ for $|\mu| \geq 1$.

Take $a_{10} > 0$. Then given $I^* > 0$ (with the restriction $I^* < I_+$ if $|\mu| > 0.625$), $\partial\mathcal{L}^*_{\rm M} > 0$ along the highway $H_{\rm r}$. Note that $(I_0, \theta_0) := (0, 3\pi/2) \in H_{\rm r}$. Taking any $(I_i, \theta_i) \in H_{\rm r}$, $I_i > 0$, its image under the scattering map $(\widetilde{I}_{i+1}, \widetilde{\theta}_{i+1}) = \mathcal{S}_{\rm M}(I_i, \theta_i)$ satisfies $\widetilde{I}_{i+1} - I_i = \mathcal{O}(\varepsilon) > 0$ and is $\mathcal{O}(\varepsilon^2)$-close to $H_{\rm r}$. Using the inner map on $\tilde{\Lambda}$, we find $(I_{i+1}, \theta_{i+1}) = \phi_{t_{i+1}}(\widetilde{I}_{i+1}, \widetilde{\theta}_{i+1}) \in H_{\rm r}$ with $I_{i+1} - I_i = \mathcal{O}(\varepsilon) > 0$. Continuing recursively in this way, we get a pseudo-orbit $\{(I_i, \theta_i), i = 0, \dots, N\} \subset H_{\rm r}$ with $I_N \geq I^*$ formed by applying successively the scattering map and the inner map. Using the symmetry of $H_{\rm r}$, introducing $I_i = -I_i$ for $i < 0$, we have the pseudo-orbit $\{(I_i, \theta_i), |i| \leq N\} \subset H_{\rm r}$. Using standard shadowing results in [FM00, FM03] based on the existence of transverse heteroclinic orbits between non-resonant tori (changing slightly I_i to obtain an irrational frequency of the inner map, if necessary) or newer results like the corollary 3.5 of [GLS14] where the recurrence property of the inner dynamics is also used, there exists a trajectory of the system such that for some T, $I_0 \leq -I^*$ and $I(T) \geq I^*$. If $a_{10} < 0$, changing $H_{\rm r}$ to $H_{\rm l}$ all the previous reasoning applies. □

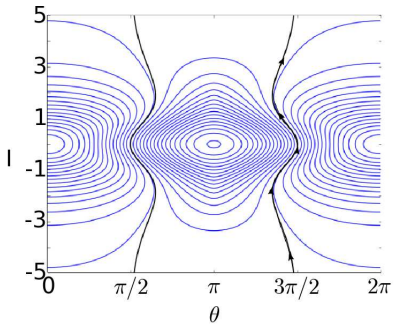

Fig. 2.14: The diffusion trajectory in $\mathcal{S}_{\rm M}$ for $\mu = 0.6$.

The general diffusion

Now we present a theorem that ensures the diffusion for all values of the parameter a_{10}, a_{01} (as long as $a_{10}a_{01} \neq 0$) and for any value of I^*. Besides, we prove it using the geometrical properties of the scattering map that we have explored up to now.

Theorem 25. *Assume that $a_{10}\, a_{01} \neq 0$ in the Hamiltonian (2.1)+(2.3). Then, for any $I^* > 0$, there exists $\varepsilon^* = \varepsilon^*(I^*) > 0$ such that for any ε, $0 < \varepsilon < \varepsilon^*$, there exists a trajectory $(p(t), q(t), I(t), \varphi(t))$ such that for some $T > 0$*

$$I(0) \leq -I^* < I^* \leq I(T).$$

Proof. Our proof consists on showing the existence of adequate orbits under several scattering maps, whose orbits will be given approximately by the level curves of the corresponding reduced Poincaré functions, in such a way the value of I will be increasing. Later on, we will combine them with orbits under the inner map to produce adequate pseudo-orbits for shadowing.

We begin with the simplest case. Assume $|\mu| < 0.625$. In this case the highways, by Proposition 20, are defined for any value of $I \in \mathbb{R}$ and Theorem 24 ensures the diffusion phenomenon.

We now assume $0.625 \leq |\mu| \leq 0.97$. In this case for some value of I there may exist tangencies between the crests $\mathrm{C_M}(I)$ and the NHIM lines $R_\theta(I)$. Again by Proposition 20, in this case the highways are defined for all $I \in (-\infty, -I_{++}) \cup (-I_+, I_+) \cup (I_{++}, +\infty)$ where $0 < I_+ \leq I_{++}$. The case $I^* \in (0, I_+)$ is contained in the result of Theorem 24. So, we are going to consider $I^* \in [I_+, +\infty)$.

As before, we have one $\mathcal{S}_\mathrm{M}$-orbit contained in one highway where I is increasing. We have to study the region of I where the highways are not defined.

Our strategy is proving the existence of a scattering map in the side of θ where the I is increasing, that is, for $\theta \in (0, \pi)$ or $\theta \in (\pi, 2\pi)$ (this depends on $\mathrm{sign}(a_{10})$) where $\partial \mathcal{L}^*_\mathrm{M}/\partial\theta$ is positive. Then, we will use the inner map (or another scattering map S') for changing of pseudo-orbit (level curve) of $\mathcal{L}^*_\mathrm{M}$. In this way, we continue the growth of I.

For any $I \in (-I_{++}, -I_+) \cup (I_+, I_{++})$, there exist tangencies between $C_\mathrm{M}(I)$ and $R_\theta(I)$, i.e., there exists ψ such that $\partial \xi_M/\partial\psi = 1/I$, and therefore there exist three different scattering maps.

Consider the case with $\mu > 0$. As we have seen in Subsection 2.2.2, $\psi \in \mathbb{T} \mapsto \theta \in \mathbb{T}$ given in (2.41) is no longer a change of variables, but we have three bijections $\theta_i : D_i(I) \to \mathbb{T}$, $i \in \{\mathrm{A}, \mathrm{B}, \mathrm{C}\}$ (see (2.42)). And for each bijection we have a scattering map associated to it. Among these three scattering maps, we will chose only one for the diffusion. Consider first the case $a_{10} > 0$ (recall that the highway H_r goes from $-I_+$ toward I_+). We chose for instance, the scattering map associated to the reduced Poincaré function $\mathcal{L}^*_{\mathrm{M,A}}(I, \theta) = \mathcal{L}^*_M(I, \theta_\mathrm{A}(\psi))$, $\psi \in D_\mathrm{A}(I)$ since

$$\frac{\partial \mathcal{L}^*_\mathrm{M}}{\partial\theta}(I, \theta_A(\psi)) = -A_{10}(I)\sin(\psi) > 0 \quad \text{for } \psi \in D_\mathrm{A}(I) \cap (\pi, 2\pi)$$

and therefore the iterates under the scattering map $\mathcal{S}_{\mathrm{M}.A}(I, \theta)$ (2.17) associated to $\mathcal{L}^*_{\mathrm{M,A}}(I, \theta)$ increase the values of I for $\theta \in (\pi, 2\pi)$. Notice that by definition of $D_A(I)$ for $\psi \in D_\mathrm{A}(I) \cap (\pi, 2\pi) = (\psi_2, 2\pi)$ with $\psi_2 \in (\pi, 3\pi/2)$ (see Subsection 2.2.2) there are no tangencies between the crest and the NHIM segment.

We can now proceed in the following way. We first construct a pseudo-orbit $\{(I_i, \theta_i) : i = 0, \ldots, N_1\} \subset H_\mathrm{r}$ with $I_0 = 0$ and $I_\mathrm{N} = I_+$, as in the proof of Theorem 24. Note that all these points lie in the same level curve of $\mathcal{L}^*_\mathrm{M}$, that is, $\mathcal{L}^*_\mathrm{M}(I_i, \theta_i) = A_{00} + A_{01}$, $i = 0, \ldots, N_1$. Applying the inner dynamics, we get $(I_{\mathrm{N}_1+1}, \theta_{\mathrm{N}_1+1}) = \phi_{t_{N_1}}(I_{\mathrm{N}_1}, \theta_{\mathrm{N}_1})$ with $\theta_{\mathrm{N}_1+1} \in (\theta_\mathrm{A}(\psi_2(I_{N_1})), 2\pi)$ and then we construct a pseudo-orbit $\{(I_i, \theta_i) : i = N_1+1, ..., N_1+M_1\} \subset \mathcal{L}^*_{\mathrm{M,A}}(I_{\mathrm{N}_1+1}, \theta_{\mathrm{N}_1+1}) = l_{\mathrm{N}_1+1}$ with $\theta_i \in (\theta_{\mathrm{N}_1+1}, 2\pi)$, $2\pi - \theta_{\mathrm{N}_1+\mathrm{M}_1} = \mathcal{O}(\varepsilon^2)$. Applying the inner dynamics, we get $(I_{\mathrm{N}_1+\mathrm{M}_1+1}, \theta_{\mathrm{N}_1+\mathrm{M}_1+1}) = \phi_{t_{\mathrm{N}_1+\mathrm{M}_1}}(I_{\mathrm{N}_1+\mathrm{M}_1}, \theta_{\mathrm{N}_1+\mathrm{M}_1})$ with $\theta_{\mathrm{N}_1+\mathrm{M}_1+1} \in \theta_\mathrm{A}(\psi_2(I_{\mathrm{N}_1+\mathrm{M}_1}), 2\pi))$. Recursively, we construct pseudo-orbit $\{(I_i, \theta_i) : i = \mathrm{N}_1 + 1, ..., \mathrm{N}_2\}$ such that $I_{\mathrm{N}_2} \geq I_{++}$. We finally follow the highway from I_{++} to I^* constructing a pseudo-orbit $\{I_i, \theta_i) : i = \mathrm{N}_2, ..., I_{\mathrm{N}_3}\} \subset H_\mathrm{r}$ with $I_{\mathrm{N}_3} = I^*$.

Using the symmetry properties (see Lemma 54) introducing $I_i = -I_i$ for $i < 0$ we have a pseudo-orbit $\{(I_i, \theta_i) : |i| \leq \mathrm{N}_3\}$ with $I_{-\mathrm{N}_3} = -I^*$, $I_{\mathrm{N}_3} = I^*$. Using now the same

shadowing techniques as in the proof of Theorem 25, there exists a diffusion trajectory. If $a_{10} < 0$, changing $H_{\rm r}$ to $H_{\rm l}$ all the previous reasoning applies. □

Remark 26. For the proof of this theorem we have chosen a simple pseudo-orbit, just choosing the scattering map $\mathcal{S}_{\mathrm{M},A}$ when it was not unique. Of course, there is a lot of freedom in choosing pseudo-orbits, and we do not claim that the one chosen here is the best one concerning minimal time of diffusion.

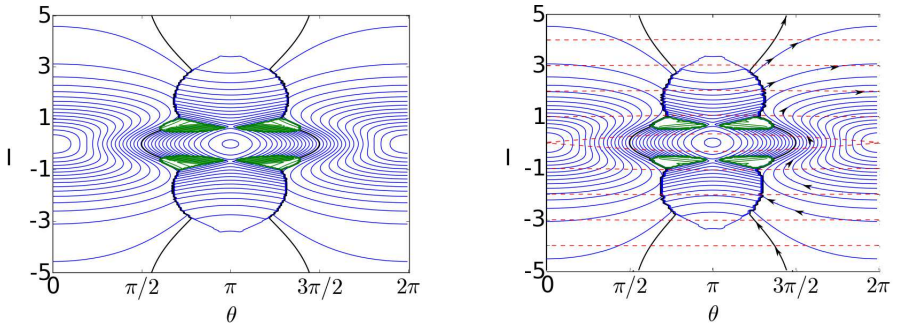

(a) $\mathcal{S}_{\rm M}$ for $\mu = 1.5$

(b) $\mathcal{S}_{\rm M}$ combined with inner map (in red)

Fig. 2.15: For $\mu = 1.5$, highways are not preserved. Inner map and scattering map can be adequately combined

Remark 27. A rough estimate for $\varepsilon^* = \varepsilon^*(I^*)$ of Theorem 25 . The scattering map $\mathcal{S}(I,\theta)$ (2.17) is the $-\varepsilon$ time map of the Hamiltonian $\mathcal{L}^*(I,\theta)$ given in (2.39), up to order $\mathcal{O}(\varepsilon^2)$. Therefore, as already noticed in Remark 7, if $|\partial\mathcal{L}^*/\partial\theta(I,\theta)| \leq \varepsilon$ or $|\partial\mathcal{L}^*/\partial I(I,\theta)| \leq \varepsilon$, the level curves of $\mathcal{L}^*(I,\theta)$ are not useful enough to describe the orbits of $\mathcal{S}$. It is easy to check that $\nabla\mathcal{L}^*(I,\theta)$ only vanishes for $I = 0$, $\theta = 0,\ \pi \mod 2\pi$ and that $\|\nabla\mathcal{L}^*(I,\theta)\| \lesssim 8\pi\,|a_{10}I|\,e^{-\pi|I|/2}$ for $|I| \to +\infty$. Thus, in general one has to avoid small neighborhoods of $(I,\theta) = (0,0)$, $(0,\pi)$ and take care in regions where $|I|$ is very large. In particular, the highways $H_{\rm l}$, $H_{\rm r}$ are far from $(I,\theta) = (0,0)$, $(0,\pi)$ and on them $\|\nabla\mathcal{L}^*(I,\theta)\| \geq A_{10}(I)(1 - \mathcal{O}(\beta(I)\mu)) \gtrsim 4\pi\,|a_{10}I|\,e^{-\pi|I|/2}$ for large $|I|$, from which we get an upper bound for $\varepsilon^*(I^*)$, which is exponentially small in $|I^*|$ for large $|I^*|$:

$$\varepsilon^*(I^*) < 4\pi\,|a_{10}|\,|I^*|\exp(-\pi\,|I^*|\,/2).$$

For smaller values of I^*, one can compute numerically the level curves of $\|\nabla\mathcal{L}^*(I,\theta)\| = \varepsilon$ and obtain $\varepsilon^* > \varepsilon^*(I^*)$ such that $\|\nabla\mathcal{L}^*(I,\theta)\| = \varepsilon^*$ implies $|I| > |I^*|$. See Table 2.2 for some values of I^*, and $\mu = 0.9$.

2.4 The time of diffusion

In this section we will provide an estimate of the diffusion time. For simplicity, we are going to estimate the time for a diffusion using a highway (see Definition 22) as a guide,

I^*	1	2	3	4
$\varepsilon^*(I^*)$	1.4	0.75	0.25	0.07

Table 2.2: Estimates of ε^* for $\mu = 0.9$

that is, we are going to construct a pseudo-orbit close a the highway. This implies to iterate the scattering map using as initial point a point on a highway. As we have seen before, see Subsection 2.2.2, one iterate of $\mathcal{S}_{\mathrm{M}}(I,\theta)$ is approximated by $-\varepsilon$ time map of the Hamiltonian $\mathcal{L}^*_{\mathrm{M}}(I,\theta)$ up to $\mathcal{O}(\varepsilon^2)$. However, if we iterate the scattering map a number n of times, it generates a propagated error with respect to the level curve of $\mathcal{L}^*_{\mathrm{M}}(I,\theta)$.

So, first we study the error generated by n iterates of the scattering map. Later, we will estimate the time of diffusion along the highway combining the scattering and the inner maps.

2.4.1 Accuracy of the scattering map

Equation (2.17) for the scattering map $\mathcal{S}$ is good enough up to an error of $\mathcal{O}(\varepsilon^2)$ for understanding one iterate of $\mathcal{S}$. But if we consider $\mathcal{S}^n$, that is, n-iterates of $\mathcal{S}$, some problems appear. These problems are related with the lack of precision of the equation (2.17):

- Equation (2.17) of the scattering map has a relative error of order $\mathcal{O}(\varepsilon)$ and an absolute error $\mathcal{O}(\varepsilon^2)$. Therefore, for n-iterates, when n is large, the error is propagated in a such way that it cannot be discarded.

- Highways are unstable, i.e., the nearby level curves of $\mathcal{L}^*$ move away from highways (see instance Fig.2.9.b).

Now, our goal is to show how we can control these errors along a region U in the phase space (I,θ) close to a highway. Basically, the control is to choose a good moment and interval to apply the inner map to come back to the highway and to maintain the errors small enough.

The propagated error

After iterating n times formula (2.17) for the scattering map, one gets for $(I_n,\theta_n) = \mathcal{S}^n(I_0,\theta_0)$:

$$I_n = I_0 + \varepsilon \sum_{j=0}^{n-1} \frac{\partial \mathcal{L}^*}{\partial \theta}(I_j,\theta_j) + \mathcal{O}(n\varepsilon^2), \quad \text{and also} \quad \theta_n = \theta_0 - \varepsilon \sum_{j=0}^{n-1} \frac{\partial \mathcal{L}^*}{\partial I}(I_j,\theta_j) + \mathcal{O}(n\varepsilon^2). \tag{2.52}$$

From now on, in this section, we will use the following notation:

- $\mathcal{S}(I,\theta)$ is the scattering map, see (2.17).
- $S_{\mathrm{T}}(I,\theta) = (I + \varepsilon\,\partial\mathcal{L}^*/\partial\theta(I,\theta), \theta - \varepsilon\,\partial\mathcal{L}^*/\partial I(I,\theta))$ is the truncated scattering map.
- $S_{0,t}(I,\theta) = (I(t),\theta(t))$ is the solution of the Hamiltonian system

$$\dot{I}(t) = \frac{\partial\mathcal{L}^*}{\partial\theta}(I(t),\theta(t)) \qquad \dot{\theta}(t) = -\frac{\partial\mathcal{L}^*}{\partial I}(I(t),\theta(t)), \tag{2.53}$$

  with initial condition $(I(0),\theta(0)) = (I,\theta)$.

Let $(I_{\mathrm{h}},\theta_{\mathrm{h}})$ be a point in the highway. The error between the scattering map and the level curve of the reduced Poincaré function after n-iterates is given by

$$\left\|\mathcal{S}^n(I_{\mathrm{h}}+\Delta I,\theta_{\mathrm{h}}+\Delta\theta) - S_{0,n\varepsilon}(I_{\mathrm{h}},\theta_{\mathrm{h}})\right\|, \tag{2.54}$$

where ΔI and $\Delta\theta$ are small. Note that we can rewrite (2.54) as

$$\begin{aligned} \|(\mathcal{S}^n(I_{\mathrm{h}}+\Delta I,\theta_{\mathrm{h}}+\Delta\theta) &- S_{\mathrm{T}}^n(I_{\mathrm{h}}+\Delta I,\theta_{\mathrm{h}}+\Delta\theta)) \\ +(S_{\mathrm{T}}^n(I_{\mathrm{h}}+\Delta I,\theta_{\mathrm{h}}+\Delta\theta) &- S_{0,n\varepsilon}(I_{\mathrm{h}}+\Delta I,\theta_h+\Delta\theta)) \\ +S_{0,n\varepsilon}(I_{\mathrm{h}}+\Delta I,\theta_h+\Delta\theta)) &- S_{0,n\varepsilon}(I_{\mathrm{h}},\theta_{\mathrm{h}}))\|. \end{aligned}$$

We now proceed to study each subtraction.

- We begin with $\mathcal{S}^n(I_{\mathrm{h}}+\Delta I,\theta_{\mathrm{h}}+\Delta\theta) - S_{\mathrm{T}}^n(I_{\mathrm{h}}+\Delta I,\theta_{\mathrm{h}}+\Delta\theta)$. From (2.52), we can readily obtain by induction that

$$\mathcal{S}^n(I_{\mathrm{h}}+\Delta I,\theta_{\mathrm{h}}+\Delta\theta) - S_{\mathrm{T}}^n(I_{\mathrm{h}}+\Delta I,\theta_{\mathrm{h}}+\Delta\theta) = \mathcal{O}(n\varepsilon^2). \tag{2.55}$$

- Now we consider $S_{\mathrm{T}}^n(I_{\mathrm{h}}+\Delta I,\theta_{\mathrm{h}}+\Delta\theta) - S_{0,n\varepsilon}(I_{\mathrm{h}}+\Delta I,\theta_h+\Delta\theta)$. By the definition of S_{T} we have that S_{T}^n is the n-step of the Euler method with step size ε in each coordinate for solving the system (2.53). It is not difficult to check the standard bound (see, for instance, [SB02])

$$\|S_{\mathrm{T}}^n(I_{\mathrm{h}}+\Delta I,\theta_{\mathrm{h}}+\Delta\theta) - S_{0,n\varepsilon}(I_{\mathrm{h}}+\Delta I,\theta_h+\Delta\theta)\| \leq \frac{L\varepsilon}{2}\left[(1+\varepsilon K)^n - 1\right], \tag{2.56}$$

  where $K := \max_{(I,\theta)\in U}\left\|\mathrm{J}\mathbf{H}(I,\theta)\,(\mathrm{J}\nabla\mathcal{L}^*(I,\theta))^T\right\|$, $L = \max_{(I,\theta)\in U}\|\nabla\mathcal{L}^*(I,\theta)\|$ and $\mathbf{H}(I,\theta)$ is the Hessian matrix of $\mathcal{L}^*(I,\theta)$.

- Now we look for the last subtraction $S_{0,n\varepsilon}(I_{\mathrm{h}}+\Delta I,\theta_h+\Delta\theta)) - S_{0,n\varepsilon}(I_{\mathrm{h}},\theta_{\mathrm{h}})$. Applying Grönwall's inequality on the variational equation associated to the Hamiltonian vector field $-\nabla\mathcal{L}^*(I,\theta)$, one gets

$$\|S_{0,\varepsilon n}(I_{\mathrm{h}}+\Delta I,\theta_h+\Delta\theta)) - S_{0,\varepsilon n}(I_{\mathrm{h}},\theta_{\mathrm{h}})\| \leq \|(\Delta I,\Delta\theta)\|\,e^{K\varepsilon n}. \tag{2.57}$$

We can now conclude from (2.55), (2.56) and (2.57), that the propagated error is

$$\|\mathcal{S}^n(I_{\rm h}+\Delta I,\theta_{\rm h}+\Delta\theta)-S_{0,n\varepsilon}(I_{\rm h},\theta_{\rm h})\|\leq\mathcal{O}(n\varepsilon^2)+\frac{L\varepsilon}{2}\left[(1+\varepsilon K)^n-1\right]+\|(\Delta I,\Delta\theta)\|\,e^{K\varepsilon n}$$

To avoid large propagated errors, one has to choose n such that $n\varepsilon\ll 1$. For instance, taking

$$n=\varepsilon^{-c}, \tag{2.58}$$

with $0<c<1$ (which implies $n\varepsilon\ll 1$) and $\|(\Delta I,\Delta\theta)\|=\varepsilon^a$, $a>0$, one gets

$$\|\mathcal{S}^n(I_{\rm h}+\Delta I,\theta_{\rm h}+\Delta\theta)-S_{0,n\varepsilon}(I_{\rm h},\theta_{\rm h})\|=\mathcal{O}(\varepsilon^{2-c},\varepsilon^a). \tag{2.59}$$

2.4.2 Estimate for the time of diffusion

In this section our goal is to estimate the time of diffusion along the highway. We have three different types of estimates associated to the time of diffusion.

- The total number of iterates $N_{\rm s}$ of the scattering map. This is the number of iterates that scattering map spends to cover a piece of a level curve of the reduced Poincaré function $\mathcal{L}^*$.
- The time under the flow along the homoclinic invariant manifolds of $\widetilde{\Lambda}$. This is the time spent by each application of the scattering map following the concrete homoclinic orbit to $\widetilde{\Lambda}$ up to a distance δ of $\widetilde{\Lambda}$. This time is denoted by $T_{\rm h}=T_{\rm h}(\delta)$.
- The time under the inner map. This time appears if we use the inner map between iterates of the scattering map (it is sometimes called ergodization time) and we denoted it by $T_{\rm i}$.

For each iterate of the scattering map we have to consider the time $T_{\rm h}$. Besides, we have seen in the previous subsection that to control the propagated error, we iterate *successively* the scattering map just a number $n=\varepsilon^{-c}$ of times, $0<c\ll 1$. From now on we denote this number n by $N_{\rm ss}$. So, after $N_{\rm ss}$ iterates of the scattering maps we apply the inner dynamics during some time $T_{\rm i}$ to come back to a distance ε^a to the highway. Therefore, the total time spent under the inner map is $\lfloor N_{\rm s}/N_{\rm ss}\rfloor\, T_{\rm i}$. We estimate that the diffusion time along the highway is thus

$$T_{\rm d}=N_{\rm s}T_{\rm h}+\lfloor N_{\rm s}/N_{\rm ss}\rfloor\, T_{\rm i}. \tag{2.60}$$

Theorem 28. *The time of diffusion T_d close to a highway of Hamiltonian (2.1)+(2.3) between $-I^*$ to I^*, for any $0<I^*<I_+$, with I_+ given in Proposition 20, satisfies the following asymptotic expression*

$$T_d=\frac{T_s}{\varepsilon}\left[2\log\left(\frac{C}{\varepsilon}\right)+\mathcal{O}(\varepsilon^b)\right],\ \textit{for } \varepsilon\to 0,\ \textit{where } 0<b<1,$$

with

$$T_s = T_s(I^*, a_{10}, a_{01}) = \int_0^{I^*} \frac{-\sinh(\pi I/2)}{\pi a_{10} I \sin\psi_h(I)} dI,$$

where $\psi_h(I)$ *is the parameterization* (2.45) *of the highway* $\mathcal{L}^*(I, \psi_h) = A_{00} + A_{01}$*, and*

$$C = C(I^*, a_{10}, a_{01}) = 16\,|a_{10}| \left(1 + \frac{1.465}{\sqrt{1-\mu^2 A^2}}\right)$$

where $A = \max_{I\in[0,I^*]} \alpha(I)$*, with* $\alpha(I)$ *given in* (2.22) *and* $\mu = a_{10}/a_{01}$*.*

The proof of this Proposition is a consequence of the following four subsections.

Number of iterates N_{s} of the scattering map

The scattering map $(I', \theta') = \mathcal{S}(I, \theta)$ given in (2.17) can be rewritten as

$$\frac{I' - I}{\varepsilon} = \frac{\partial \mathcal{L}^*}{\partial \theta}(I, \theta) + \mathcal{O}(\varepsilon) \qquad \frac{\theta' - \theta}{\varepsilon} = -\frac{\partial \mathcal{L}^*}{\partial I}(I, \theta) + \mathcal{O}(\varepsilon).$$

Hence, disregarding the $\mathcal{O}(\varepsilon)$ terms, we define

$$\frac{dI}{d\upsilon} = \frac{\partial \mathcal{L}^*}{\partial \theta}(I, \theta) \qquad \frac{d\theta}{d\upsilon} = -\frac{\partial \mathcal{L}^*}{\partial I}(I, \theta), \tag{2.61}$$

where υ is a new parameter of time. Note that $\mathcal{L}^*(I, \theta)$ is a first integral of (2.61) and that the highway has the equation $\mathcal{L}^*(I, \theta) = A_{00} + A_{01}$. Recalling formula (2.50) for $\partial \mathcal{L}^*/\partial\theta(I, \theta)$, the equation for I reads as

$$\frac{dI}{d\upsilon} = \frac{\partial \mathcal{L}^*}{\partial \theta}(I, \theta) = -A_{10}(I) \sin\psi,$$

where $\psi = \theta - I\tau^*(I, \theta)$ as given in (2.45). We choose the highway H_{r} for $a_{10} > 0$ (or H for $a_{01} < 0$) to ensure that $\partial \mathcal{L}^*/\partial\theta(I, \theta) > 0$ (see Definition 22). This implies that we can rewrite the equation above as

$$\frac{d\upsilon}{dI} = \frac{-1}{A_{10}(I) \sin\psi_{\mathrm{h}}}$$

so that

$$T_{\mathrm{s}} := \upsilon = \int_{I_0}^{I_{\mathrm{f}}} \frac{-1}{A_{10}(I) \sin\psi_{\mathrm{h}}(I)} dI = \int_{I_0}^{I_{\mathrm{f}}} \frac{-\sinh(\pi I/2)}{2\pi I a_{10} \sin\psi_{\mathrm{h}}(I)} dI$$

is the time of diffusion in the interval $[I_0, I_f]$ of values of I following the flow (2.61).

Remark 29. If we consider an interval of diffusion as in Theorem 25, that is, $[-I^*, I^*]$, the time T_{s} is

$$T_{\mathrm{s}} = \int_0^{I^*} \frac{-\sinh(\pi I/2)}{\pi I a_{10} \sin\psi_{\mathrm{h}}(I)} dI.$$

Remark 30. Observe that

$$T_{\rm s} \geq \frac{1}{2\pi a_{10}} \left(\mathrm{Shi}\left(\frac{I_f \pi}{2}\right) - \mathrm{Shi}\left(\frac{I_0 \pi}{2}\right)\right),$$

where the function $\mathrm{Shi}(x)$ is defined as

$$\mathrm{Shi}(x) := \int_0^x \frac{\sinh \sigma}{\sigma} d\sigma.$$

The time $T_{\rm s}$ has been computed from the continuous dynamics (2.61) . But the scattering map generates a discrete dynamics with a ε-step. Then for us, the important information is the number of iterations of the scattering map (2.17) from I_0 to $I_{\rm f}$ which is given by

$$N_{\rm s} = \frac{T_{\rm s}}{\varepsilon}(1 + \mathcal{O}(\varepsilon)).$$

Time of the travel $T_{\rm h}$ on the invariant manifold

Let $\tilde{x}_-$ and $\tilde{x}_+$ be on $\tilde{\Lambda}$ such that $S(\tilde{x}_-) = \tilde{x}_+$. We now estimate the time of the flow from a point δ-close to $\tilde{x}_-$ to a point δ-close to $\tilde{x}_+$.

Recall that the unperturbed separatrices (2.2) are given by

$$(p_0(t), q_0(t)) = \left(2/\cosh t, 4 \arctan e^t\right).$$

We have $(p_\varepsilon(\tau), q_\varepsilon(\tau)) = (2/\cosh \tau, 4 \arctan e^\tau) + \mathcal{O}(\varepsilon)$, where $(p_\varepsilon(\tau), q_\varepsilon(\tau)) \in \overline{\mathrm{B}_\delta(0)} \cap W^{s,u}_\varepsilon(0)$.

Note that when $\tau \to \pm\infty$,

$$p_0(\tau) = \frac{4}{e^{|\tau|}}\left(1 - e^{-2|\tau|} + e^{-4|\tau|} + \dots\right) = \frac{4}{e^{|\tau|}}\left(1 + \mathcal{O}(e^{-2|\tau|})\right).$$

Besides, as $\dot{q}_0(\tau) = \partial H_0/\partial p = p_0(\tau)$, we also have

$$q_0(\tau) = \mp \frac{4}{e^{|\tau|}}\left(1 + \mathcal{O}(e^{-2|\tau|})\right) \mod 2\pi \quad \text{when } \tau \to \pm\infty.$$

We consider starting and ending points on $\partial \mathrm{B}_\delta(0,0)$. Then, denoting by $\tau_{\rm f} = -\tau_{\rm i}$ the initial and final points, we have

$$q_0^2(\tau_{\rm i}) + p_0^2(\tau_{\rm i}) = q_0^2(\tau_{\rm f}) + p_0^2(\tau_{\rm f}) = \left[\frac{4}{e^u}\left(1 + \mathcal{O}(e^{-2u})\right)\right]^2 + \left[-\frac{4}{e^u}\left(1 + \mathcal{O}(e^{-2u})\right)\right]^2 = \delta^2,$$

where $u = |\tau_{\rm i}|\,, |\tau_{\rm f}|$. Therefore,

$$\frac{4\sqrt{2}}{e^u}\left(1 + \mathcal{O}(e^{-2u})\right) = \delta. \tag{2.62}$$

Note that by the above equation $\delta = \mathcal{O}(e^{-u})$, thus $e^{-2u} = \mathcal{O}(\delta^2)$. Hence, we can rewrite equation (2.62) as

$$e^u = \frac{4\sqrt{2}}{\delta}\left(1 + \mathcal{O}(\delta^2)\right). \tag{2.63}$$

So,

$$u = \log\left[\frac{4\sqrt{2}}{\delta}\left(1 + \mathcal{O}(\delta^2)\right)\right] = \log\left(\frac{4\sqrt{2}}{\delta}\right) + \mathcal{O}(\delta^2).$$

Since $\Delta\tau = 2u$, we finally have

$$T_{\mathrm{h}} = 2\log\left(\frac{4\sqrt{2}}{\delta}\right) + \mathcal{O}(\delta^2) + \mathcal{O}(\varepsilon). \tag{2.64}$$

It is now necessary to estimate a value for δ and we want δ small enough such that this choice does not affect significantly the scattering map (2.17), that is, that the level curves of the reduced Poincaré remain at a distance of $\mathcal{O}(\varepsilon)$. From Proposition 5 the Melnikov potential, using that $p_0^2/2 + \cos q_0 - 1 = 0$, is

$$\mathcal{L}(I,\varphi,s) = \frac{1}{2}\int_{-\infty}^{+\infty} p_0^2(\sigma)\left(a_{00} + a_{10}\cos(\varphi + I\sigma) + a_{01}\cos(s+\sigma)\right)d\sigma.$$

The reduced Poincaré function (2.16) $\mathcal{L}^*(I,\theta)$ is

$$\begin{aligned}\mathcal{L}^*(I,\theta) = \frac{1}{2}\int_{-\infty}^{+\infty} p_0^2(\sigma)\,&\left(a_{00} + a_{10}\cos(\varphi + I(\sigma - \tau^*(I,\varphi,s)))\right.\\ &\left.+a_{01}\cos(s - \tau^*(I,\varphi,s) + \sigma)\right)d\sigma.\end{aligned}$$

Considering the diffusion along the highways, recall that ψ, given in (2.29), is well defined and, as in(2.35), we can write the reduced Poincaré function on the variables (I,ψ) as

$$\begin{aligned}\mathfrak{L}^*(I,\psi) &= \frac{1}{2}\int_{-\infty}^{+\infty} p_0^2(\sigma)\left(a_{00} + a_{10}\cos(\psi + I\sigma) + a_{01}\cos(\xi(I,\psi)+\sigma)\right)d\sigma\\ &= A_{00} + A_{10}(I)\cos\varphi + A_{01}\cos\xi(I,\varphi).\end{aligned}$$

As we want to preserve the level curves of the reduced Poincaré function up to $\mathcal{O}(\varepsilon)$, we need t_{i} and t_{f} such that the integration above along all the real numbers does not change much when the interval of integration is $[t_{\mathrm{i}}, t_{\mathrm{f}}]$, more precisely, given a $\varepsilon > 0$

$$\left|\frac{\partial\mathfrak{L}^*}{\partial I}(I,\psi) - \left(\frac{\partial\mathfrak{L}^*}{\partial I}(I,\psi)\right)_\delta\right| < \varepsilon \qquad \text{and} \qquad \left|\frac{\partial\mathfrak{L}^*}{\partial\psi}(I,\psi) - \left(\frac{\partial\mathfrak{L}^*}{\partial\psi}(I,\psi)\right)_\delta\right| < \varepsilon, \tag{2.65}$$

where $\left(\frac{\partial\mathfrak{L}^*}{\partial\gamma}(I,\psi)\right)_\delta$ is given, for $\gamma \in \{\psi, I\}$ by

$$\frac{-1}{2}\int_{t_{\mathrm{i}}}^{t_{\mathrm{f}}}\frac{\partial}{\partial\gamma}\left(p_0^2(\sigma)\left(a_{00} + a_{10}\cos(\varphi + I(\sigma - \tau^*(I,\varphi,s))) + a_{01}\cos(s - \tau^*(I,\varphi,s)+\sigma)\right)\right)d\sigma.$$

Using that $|\alpha'(I)| < 1.465$, one computes for $t_{\rm i} = -t_{\rm f}$ that

$$\left|\frac{\partial \mathfrak{L}^*}{\partial \gamma}(I,\psi) - \left(\frac{\partial \mathfrak{L}^*}{\partial \gamma}(I,\psi)\right)_\delta\right| < Ce^{-t_{\rm f}} \quad \gamma \in \{\psi, I\},$$

where $C = 16\left(|a_{10}| + 1.465\,|a_{01}|\,|\mu|\,/\sqrt{1-\mu^2A^2}\right)$, $A = \max_{I\in[0,I^*]}\alpha(I)$. By (2.63) with $u = t_{\rm f}$, this is equivalent to

$$\left|\frac{\partial \mathfrak{L}^*}{\partial \gamma}(I,\psi) - \left(\frac{\partial \mathfrak{L}^*}{\partial \gamma}(I,\psi)\right)_\delta\right| < \frac{C\delta(1+\mathcal{O}(\delta^2))}{4\sqrt{2}}.$$

To satisfy Eq.(2.65) we have to take a δ such that the above right hand side is less or equal than ε. For simplicity, we take δ satisfying the equality, that is,

$$\delta = \frac{4\sqrt{2}\varepsilon}{C}(1+\mathcal{O}(\varepsilon_0^2)).$$

Inserting this value of δ in (2.64), we can conclude that

$$T_{\rm h} = 2\log\left(\frac{16\,|a_{10}|\left(1+\frac{1.465}{\sqrt{1-\mu^2A^2}}\right)}{\varepsilon}\right) + \mathcal{O}(\varepsilon).$$

Time $T_{\rm i}$ under the inner map

To build of the pseudo-orbit which shadows the real diffusion orbit, we need, after each $N_{\rm ss}$-iterates of the scattering map ($N_{\rm ss} = \lceil \varepsilon^{-c} \rceil$, see (2.58)), to apply the inner flow to return to the same level curve of $\mathcal{L}^*$ (or close enough). The time spent by the inner flow is the time $T_{\rm i}$, which we are going to estimate.

Recall that $\widetilde{\Lambda}_\varepsilon = \widetilde{\Lambda}$, where $\widetilde{\Lambda}$ is a NHIM of the unperturbed case (see Section 2.1). We will calculate the time for the flow of the unperturbed case because in our case it is a good approximation, that is, along NHIM lines $(I, \varphi + It, s + t)$ (see Section 2.1).

Given $\varepsilon > 0$ small enough, our goal is to calculate $t > 0$ such that

$$|(I, \varphi + It, s + t) - (I, \varphi, s)| < \varepsilon^a, \tag{2.66}$$

that is, $|I(2\pi k) - 2\pi l| < \varepsilon^a$ for some integer k, l, or equivalently

$$\left|I - \frac{l}{k}\right| < \frac{\varepsilon^a}{2\pi k}. \tag{2.67}$$

We now recall the Dirichlet Box Principle:

Proposition 31. ***(Dirichlet Box Principle)*** *Let N be a positive integer and let α be any real number. Then there exists positive integers $k \le N$ and $l \le \alpha N$ such that*

$$\left|\alpha - \frac{l}{k}\right| \le \frac{1}{k(N+1)}.$$

Define $N := \lceil 2\pi/\varepsilon^a - 1 \rceil$, the smaller natural number such that it is greater or equal than $2\pi/\varepsilon^a - 1$. Then from the Dirichlet Box Principle, there exist k, l satisfying the condition (2.67) such that $k \leq N$ and $l \leq IN$. Then $T_{\rm i} = 2\pi k$ is the time required for (2.66), called the ergodization time. Note that for any φ,

$$T_{\rm i} \leq 2\pi N = 2\pi \left\lceil \frac{2\pi}{\varepsilon^a} - 1 \right\rceil,$$

So that $T_{\rm i} = \mathcal{O}(\varepsilon^{-a})$.

Dominant time and the order of diffusion time

We finally put together the estimates of $N_{\rm s}$, $T_{\rm h}$ and $T_{\rm i}$, jointly with $N_{\rm ss} = \varepsilon^{-c}$ in the formula for the time of diffusion (2.60). If we look just at the order of the time of diffusion we have

$$T_{\rm d} = N_{\rm s} T_{\rm h} + \lfloor N_{\rm s}/N_{\rm ss} \rfloor \, T_{\rm i} = \mathcal{O}(\varepsilon^{-1} \log \varepsilon^{-1}) + \mathcal{O}(\varepsilon^{c-a-1}).$$

Choosing $0 < a < c$ the term containing the time $T_{\rm i}$ under the inner map is negligible compared with the term containing the time of travel $T_{\rm h}$ along the homoclinic orbit: $\varepsilon^{c-a-1} \ll (1/\varepsilon) \log 1/\varepsilon$. We finally obtain the desired estimate for the time of diffusion

$$T_{\rm d} = \frac{T_{\rm s}}{\varepsilon} \left[2 \log \frac{C}{\varepsilon} + \mathcal{O}(\varepsilon^b) \right],$$

where $b = c - a$. Since $c < 1$, $0 < b < 1$. Notice that by the choice of the parameter $0 < a < c \ll 1$, the accuracy of the scattering map given in (2.59) is $\mathcal{O}(\varepsilon^a)$.

Chapter 3

Second case for 2+1/2 degrees of freedom

This Chapter, as explained in the Introduction, concerns about the case given by Hamiltonian

$$H_\varepsilon(p,q,I,\varphi,t) = \pm\left(\frac{p^2}{2}+\cos q-1\right)+\frac{I^2}{2}+\varepsilon\cos q\left(a_1\cos\varphi+a_2\cos(\varphi-s)\right). \tag{3.1}$$

We notice that this case completes the study of the diffusion for Hamiltonian (1.1)+(1.2). All considerations about the unperturbed Hamiltonian are exactly the same described in Section 2.1 and we do not repeat here.

We begin by describing the inner dynamics and a brief description of the resonant region. In Section 3.2, we describe the scattering maps and their geometrical properties. In Section 3.3, we prove our theorem of diffusion. Finally, we describe a new kind of scattering maps in Section 3.4 and the new possibilities of study with them.

3.1 Inner dynamics

The inner dynamics is derived from the restriction of H_ε in (3.1) and its equations to $\tilde{\Lambda}$, that is,

$$K(I,\varphi,s) = \frac{I^2}{2}+\varepsilon\left(a_1\cos\varphi+a_2\cos(\varphi-s)\right), \tag{3.2}$$

and differential equations

$$\dot{\varphi} = I \qquad \dot{s} = 1 \qquad \dot{I} = \varepsilon\left(a_1\sin\varphi+a_2\sin(\varphi-s)\right). \tag{3.3}$$

Note that in this case the inner dynamics is slightly more complicated than in Chapter 2 where there was just one resonance, namely, in $I=0$. In the current case we have two resonant regions of size $\mathcal{O}(\sqrt{\varepsilon})$ where secondary KAM tori appear. To describe these regions, we use normal forms as in [DLS06].

Consider the autonomous extended Hamiltonian

$$\overline{K}(I, A, \varphi, s) = \frac{I^2}{2} + A + \varepsilon \left(a_1 \cos\varphi + a_2 \cos(\varphi - s)\right), \tag{3.4}$$

with associated differential equations

$$\begin{aligned} \dot{\varphi} =& I & \dot{I} =& \varepsilon \left(a_1 \sin\varphi + a_2 \sin(\varphi - s)\right) \\ \dot{s} =& 1 & \dot{A} =& -\varepsilon a_2 \sin(\varphi - s). \end{aligned}$$

This system is equivalent to the system represented by (3.2)+(3.3). We wish to eliminate the dependence on the angle variables. Consider a change of variables ε-close to the identity

$$(\varphi, s, I, A) = g(\phi, \sigma, J, B) = (\phi, \sigma, J, B) + \mathcal{O}(\varepsilon)$$

such that it is the one-time flow for a Hamiltonian εG, i.e., $g = g_{t=1}$, where g_t is solution of

$$\frac{dg_t}{dt} = J_2 \nabla \varepsilon G \circ g_t, \text{ where } J_2 \text{ is the symplectic matrix } \begin{pmatrix} 0 & 1 \\ -1 & 0 \end{pmatrix}.$$

Composing $\overline{K}$ with g and expanding in a Taylor series around $t = 0$, one obtains

$$\overline{K} \circ g = \overline{K} + \left\{\overline{K}, \varepsilon G\right\} + \frac{1}{2}\left\{\left\{\overline{K}, \varepsilon G\right\}, \varepsilon G\right\} + \ldots,$$

where $\{\cdot\}$ is the Poisson bracket. Using the expansion (3.4) of $\overline{K}$, the equation above can be written as

$$\begin{aligned} \overline{K} \circ g = \frac{J^2}{2} + B + \varepsilon \left(a_1 \cos\phi + a_2 \cos(\phi - \sigma) + \left\{\frac{J^2}{2} + B, G\right\}\right) \\ + \frac{\varepsilon^2}{2}\left\{\left\{\frac{J^2}{2} + B, G\right\}, G\right\} + \mathcal{O}(\varepsilon^3). \end{aligned} \tag{3.5}$$

We want to find G such that $a_1 \cos\phi + a_2 \cos(\phi - \sigma) + \left\{\frac{J^2}{2} + B, G\right\} = 0$, or equivalently,

$$J\frac{\partial G}{\partial \phi} + \frac{\partial G}{\partial \sigma} = a_1 \cos\phi + a_2 \cos(\phi - \sigma).$$

Given $a < b < 1$, consider any function $\Psi \in C^\infty(\mathbb{R})$ satisfying $\Psi(x) = 1$ for $x \in [-a, a]$ and $\Psi(x) = 0$ for $|x| \geq b$ and introduce

$$G(J, B, \phi, \sigma) := \frac{a_1}{J}\left(1 - \Psi(J)\right)\sin\phi + \frac{a_2}{J - 1}\left(1 - \Psi(J - 1)\right)\sin(\phi - \sigma),$$

Substituting the above function $G(J, B, \phi, \sigma)$ in (3.5) we have

$$\overline{K} \circ g = \frac{J^2}{2} + B + \mathcal{O}(\varepsilon^2), \tag{3.6}$$

for $J, J-1 \notin [-b, b]$. For $J \in [-a, a]$,

$$\overline{K} \circ g = \frac{J^2}{2} + B + \varepsilon a_1 \cos\phi + \mathcal{O}(\varepsilon^2). \tag{3.7}$$

Finally, for $J - 1 \in [-a, a]$,

$$\overline{K} \circ g = \frac{J^2}{2} + B + \varepsilon a_2 \cos(\phi - \sigma) + \mathcal{O}(\varepsilon^2). \tag{3.8}$$

From (3.7) and (3.8), one sees that on $J = 0$ and $J = 1$ there are resonances of first order in ε with a pendulum-like behavior.

Coming back to the original variables, three kinds of invariant tori are obtained. For the first order resonance $I = 0$, there is a positive $\overline{a}$ such that the invariant tori are given by $F^0(I, \varphi, s) =$ constant with

$$F^0(I, \varphi, s) = \frac{I^2}{2} + \varepsilon a_1 \cos\varphi + \mathcal{O}(\varepsilon^2). \tag{3.9}$$

for $I \in [-\overline{a}, \overline{a}]$.

Analogously, for the first order resonance $I = 1$, with

$$F^1(I, \varphi, s) = \frac{(I-1)^2}{2} + \varepsilon a_2 \cos(\varphi - s) + \mathcal{O}(\varepsilon^2),$$

for $I - 1 \in [-\overline{a}, \overline{a}]$.

Remark 32. As commented in [DLS06], there exists a *secondary* resonance in $I = 1/2$, but the size of the gap in its resonant region is much smaller than the size of gaps in resonant regions associated to $I = 0$ and $I = 1$.

Remark 33. For Hamiltonian (1.5) with $r \neq 1$, the resonances take place in $I = 0$ and $I = 1/r$.

From (3.6), on the non-resonant region the invariant tori has equations $F^{\mathrm{nr}}(I) =$ constant with

$$F^{\mathrm{nr}}(I) = \frac{I^2}{2} + \mathcal{O}(\varepsilon^2).$$

An illustration of the inner dynamics is displayed in Figure 3.1.

3.2 Scattering map

We are going to explore the properties of the scattering maps of Hamiltonian (3.1). The notion of scattering map on a NHIM was introduced in [DLS00]. Let W be an open set of $[-I^*, I^*] \times \mathbb{T}^2$ such that the invariant manifolds of the NHIM $\tilde{\Lambda}$ introduced in (1.3) intersect

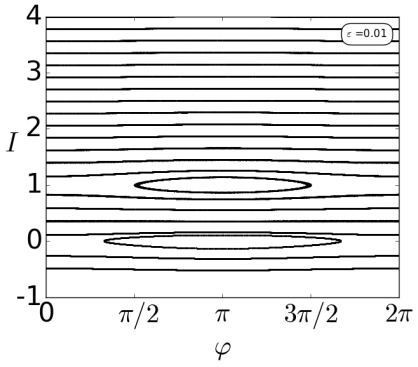

Fig. 3.1: Plane $\varphi \times I$ of inner dynamics for $\mu = 0.75$ and $\varepsilon = 0.01$.

transversally along a homoclinic manifold $\Gamma = \{\tilde{z}(I, \varphi, s; \varepsilon), (I, \varphi, s) \in W\}$ so that for any $\tilde{z} \in \Gamma$ there exist unique $\tilde{x}_{+,-} = \tilde{x}_{+,-}(I, \varphi, s; \varepsilon) \in \tilde{\Lambda}$ such that $\tilde{z} \in W^s_\varepsilon(x_-) \cap W^u_\varepsilon(\tilde{x}_+)$. Let

$$H_{+,-} = \bigcup \{\tilde{x}_{+,-}(I, \varphi, s; \varepsilon) : (I, \varphi, s) \in W\}.$$

The scattering map associated to Γ is the map

$$\begin{array}{rcl} S : H_- & \longrightarrow & H_+ \\ \tilde{x}_- & \longmapsto & S(\tilde{x}_-) = \tilde{x}_+. \end{array}$$

For the characterization of the scattering maps, it is required to select the homoclinic manifold Γ and this is done using the Poincaré-Melnikov theory. From [DH11, DLS06], we have the following proposition (compare with Chapter 2, Prop. 5)

Proposition 34. *Given $(I, \varphi, s) \in [-I^*, I^*] \times \mathbb{T}^2$, assume that the real function*

$$\tau \in \mathbb{R} \longmapsto \mathcal{L}(I, \varphi - I\,\tau, s - \tau) \in \mathbb{R} \tag{3.10}$$

has a non degenerate critical point $\tau^* = \tau^*(I, \varphi, s)$, where

$$\mathcal{L}(I, \varphi, s) := \int_{-\infty}^{+\infty} (f(q_0(\sigma)) - f(0))\, g(\varphi + I\sigma, s + \sigma; 0) d\sigma.$$

Then, for $0 < \varepsilon$ small enough, there exists a unique transversal homoclinic point $\tilde{z}$ to $\tilde{\Lambda}_\varepsilon$ of Hamiltonian (1.1)*, which is ε-close to the point*

$$\tilde{z}^*(I, \varphi, s) = (p_0(\tau^*), q_0(\tau^*), I, \varphi, s) \in W^0(\tilde{\Lambda}) :$$

$$\tilde{z} = \tilde{z}(I, \varphi, s) = (p_0(\tau^*) + O(\varepsilon), q_0(\tau^*) + O(\varepsilon), I, \varphi, s) \in W^u(\tilde{\Lambda_\varepsilon}) \pitchfork W^s(\tilde{\Lambda_\varepsilon}).$$

The function $\mathcal{L}$ is called the *Melnikov potential* of Hamiltonian (1.1). For the concrete Hamiltonian (3.1) it takes the form

$$\mathcal{L}(I, \varphi, s) = A_1(I) \cos\varphi + A_2(I) \cos(\varphi - s), \tag{3.11}$$

where

$$A_1(I) = \frac{2\pi I a_1}{\sinh(\pi I/2)} \quad \text{and} \quad A_2(I) = \frac{2\pi(I-1)a_2}{\sinh(\pi(I-1)/2)}.$$

The homoclinic manifold Γ is characterized by the function $\tau^*(I,\varphi,s)$. Once a $\tau^*(I,\varphi,s)$ is chosen, which under the conditions of Proposition 34, is locally smoothly well defined, by the geometric properties of the scattering map, see [DH09, DH11, DLS08], the scattering map has the explicit local form

$$S(I,\varphi,s) = \left(I + \varepsilon\frac{\partial L^*}{\partial\varphi}(I,\varphi,s) + \mathcal{O}(\varepsilon^2), \varphi - \varepsilon\frac{\partial L^*}{\partial I}(I,\varphi,s) + \mathcal{O}(\varepsilon^2), s\right),$$

where

$$L^*(I,\varphi,s) = \mathcal{L}(I,\varphi - I\tau^*(I,\varphi,s), s - \tau^*(I,\varphi,s)). \tag{3.12}$$

Notice that the variable s is fixed under the scattering map. As a consequence, see [DH11], introducing the variable

$$\theta = \varphi - Is$$

and defining the *reduced Poincaré function*

$$\mathcal{L}^*(I,\theta) := L^*(I,\varphi - Is, 0) = L^*(I,\varphi,s), \tag{3.13}$$

in the variables (I,θ), the scattering map has the simple form

$$\mathcal{S}(I,\theta) = \left(I + \varepsilon\frac{\partial\mathcal{L}^*}{\partial\theta}(I,\theta) + \mathcal{O}(\varepsilon^2), \theta - \varepsilon\frac{\partial\mathcal{L}^*}{\partial I}(I,\theta) + \mathcal{O}(\varepsilon^2)\right),$$

so up to $\mathcal{O}(\varepsilon^2)$ terms, $\mathcal{S}(I,\theta)$ is the ε times flow of the *autonomous* Hamiltonian $-\mathcal{L}^*(I,\theta)$. In particular, the iterates under the scattering map follow the level curves of $\mathcal{L}^*$ up to $\mathcal{O}(\varepsilon^2)$.

3.2.1 Crests and NHIM lines

We have seen that the function τ^* plays a central role in our study. Therefore, we are interested in finding the critical points $\tau^* = \tau^*(I,\varphi,s)$ of function (3.10). For our concrete case (3.11), τ^* is a solution of

$$IA_1(I)\sin(\varphi - I\tau^*) + (I-1)A_2(I)\sin(\varphi - s - (I-1)\tau^*) = 0. \tag{3.14}$$

This equation can be viewed from two equivalently geometrical viewpoints. The first one is that to find $\tau^* = \tau^*(I,\varphi,s)$ satisfying (3.14) for any $(I,\varphi,s) \in [-I^*, I^*]\times\mathbb{T}^2$ is the same as to look for the extrema of $\mathcal{L}$ on the *NHIM line*

$$R(I,\varphi,s) = \{(I, \varphi - I\tau, s - \tau) : \tau \in \mathbb{R}\}. \tag{3.15}$$

Remark 35. Since $(\varphi,s) \in \mathbb{T}^2$, $R(I,\varphi,s)$ is a closed line if $I \in \mathbb{Q}$ and it is a dense line on $\{I\}\times\mathbb{T}^2$ if $I \notin \mathbb{Q}$.

The other viewpoint is that, fixing (I, φ, s), a solution τ^* of (3.14) is equivalent to finding intersections between a NHIM line (3.15) and a curve defined by

$$IA_1(I)\sin\varphi + (I-1)A_2(I)\sin(\varphi - s) = 0.$$

These curves are called *crests*, and in a general way can be defined as follows.

Definition 36. [DH11] We define by *Crests* $\mathcal{C}(I)$ the curves on (I, φ, s), $(\varphi, s) \in \mathbb{T}^2$, such that

$$\frac{\partial \mathcal{L}}{\partial \tau}(I, \varphi - I\tau, s - \tau)|_{\tau=0} = 0, \tag{3.16}$$

or equivalently,

$$I\frac{\partial \mathcal{L}}{\partial \varphi}(I, \varphi, s) + \frac{\partial \mathcal{L}}{\partial s}(I, \varphi, s) = 0.$$

As in our case $\mathcal{L}(I, \varphi - I\tau, s - \tau) = A_1(I)\cos(\varphi - I\tau) + A_2(I)\cos(\varphi - s - (I-1)\tau)$, equation (3.16) takes the form (3.16). Introducing

$$\sigma = \varphi - s, \tag{3.17}$$

equation (3.16) can be rewritten as

$$\mu\alpha(I)\sin\varphi + \sin\sigma = 0, \tag{3.18}$$

for $I \neq 1$, where

$$\mu = \frac{a_1}{a_2} \quad \text{and} \quad \alpha(I) = \frac{I^2\sinh(\frac{\pi}{2}(I-1))}{(I-1)^2\sinh(\frac{\pi I}{2})}. \tag{3.19}$$

From now on, when we refer to crests $\mathcal{C}(I)$ we mean the set of points (I, φ, σ) satisfying equation (3.18). See an illustration in Fig. 3.3.

Remark 37. In Chapter 2 the crests were described on the plane (φ, s), whereas now such curves lie on the plane (φ, σ). Besides, differently from the cases studied in [DH11] and in Chapter 2, the function $\alpha(I)$ introduced in (3.19) is not defined for all I. More precisely, it is not defined for $I = 1$. For this value of I, equation (3.18) is not adequate, and one has to use (3.16) to check that for $I = 1$ the crests are just two vertical straight lines on the plane (φ, σ) given by $\varphi = 0$ and $\varphi = \pi$.

Remark 38. For Hamiltonian (1.5) and $r \in (0, 1)$, $\alpha_r(I)$ is not defined for $I = 1/r$ and is given by

$$\alpha_r(I) = \frac{I^2\sinh\left(\frac{\pi}{2}(rI-1)\right)}{(rI-1)^2\sinh\left(\frac{\pi I}{2}\right)}. \tag{3.20}$$

We are interested in understanding the behavior of these crests because, as we have seen in[DH11] and Chapter 2, their intersection with the NHIM lines determine the existence and behavior of scattering maps.

From (3.18), when $|\alpha(I)| < 1/|\mu|$, σ can be written as a function of φ for all $\varphi \in \mathbb{T}$ on the crest $\mathcal{C}(I)$. On the other hand, if $|\alpha(I)| > 1/|\mu|$, φ can be written as a function of σ for all $\sigma \in \mathbb{T}$. These two conditions give us two kinds of crests: *horizontal* for $|\alpha(I)| < 1/|\mu|$ and *vertical* for $|\alpha(I)| > 1/|\mu|$. These names are due to their forms on the plane (φ, σ). We consider the same characterization used in Chapter 2:

- For $|\alpha(I)| < 1/|\mu|$, there are two horizontal crests $\sigma = \xi_{\mathrm{M,m}}(I, \varphi)$

$$\mathcal{C}_{\mathrm{M,m}}(I) = \{(I, \varphi, \xi_{\mathrm{M,m}}(I, \varphi)) : \varphi \in \mathbb{T}\},$$

$$\begin{aligned} \xi_{\mathrm{M}}(I, \varphi) &= -\arcsin(\mu\alpha(I)\sin\varphi) \qquad \mod 2\pi \\ \xi_{\mathrm{m}}(I, \varphi) &= \arcsin(\mu\alpha(I)\sin\varphi) + \pi \qquad \mod 2\pi. \end{aligned} \tag{3.21}$$

- For $|\alpha(I)| > 1/|\mu|$, there are two vertical crests $\varphi = \eta_{\mathrm{M,m}}(I, \sigma)$

$$\mathcal{C}_{M,m}(I) = \{(I, \eta_{M,m}(I, \sigma), \sigma) : \sigma \in \mathbb{T}\},$$

$$\begin{aligned} \eta_{M}(I, \sigma) &= -\arcsin(\sin\sigma/(\mu\alpha(I))) \qquad \mod 2\pi \\ \eta_{m}(I, \sigma) &= \arcsin(\sin\sigma/(\mu\alpha(I))) + \pi \qquad \mod 2\pi. \end{aligned}$$

Remark 39. $|\alpha(I)| = 1/|\mu|$ is a singular or bifurcation case. In this case, the crests are straight lines and are not differentiable in $\varphi = \pi/2$ and $\varphi = 3\pi/2$. See Fig. 2.6.

Remark 40. The crest containing the point $(\varphi, \sigma) = (0, 0)$ will be denoted by $\mathcal{C}_{\mathrm{M}}(I)$ and the crest containing the point $(\varphi, \sigma) = (\pi, \pi)$ by $\mathcal{C}_{\mathrm{m}}(I)$.

Note that the function $|\alpha(I)|$ is not bounded, indeed

$$\lim_{I \to 1} |\alpha(I)| = +\infty.$$

This implies that for any μ there exists a neighborhood U of $I = 1$ such that for all $I \in U$ the crests are vertical. On the other hand, since $\alpha(0) = 0$ there exists a neighborhood V of $I = 0$ such that for all $I \in V$ the crests are horizontal. We notice here a remarkable difference with the Hamiltonians studied in [DH11] and Chapter 2, where, for $|\mu| \leq 0.97$, all the crests are horizontal for all I.

Now take a look at the properties of the function $\alpha(I)$ introduced in (3.19) to describe under which conditions in μ the crests are horizontal or vertical. First of all, observe that for $I \neq 1$, $\alpha(I)$ is smooth and $\alpha'(I) \neq 0$, and for $I = 1$ $\alpha(I)$ is not bounded, indeed it has a vertical asymptote

$$\lim_{I \to 1^-} \alpha(I) = -\infty \qquad \text{and} \qquad \lim_{I \to 1^+} \alpha(I) = +\infty.$$

Given a $\mu \neq 0$, since $\alpha(0) = 0$, there exists a unique $I_c \in (0, 1)$ such that $|\alpha(I)| = 1/|\mu|$. So, the crests are horizontal for $I \in [0, I_c)$ and vertical for $I \in (I_c, 1)$.

Others important limits are

$$\lim_{I \to -\infty} \alpha(I) = \exp(\pi/2) \qquad \text{and} \qquad \lim_{I \to +\infty} \alpha(I) = \exp(-\pi/2).$$

The first limit implies that $|\alpha(I)| < \exp(\pi/2)$ for $I \in (-\infty, 0)$. Thus, if $\exp(\pi/2) \leq 1/|\mu|$ the crests are horizontal for $I \in (-\infty, 0)$. Otherwise, if $1/|\mu| < \exp(\pi/2)$, there exists a unique $I_\mathrm{l} \in (-\infty, 0)$ such that $|\alpha(I)| = 1/|\mu|$ and the crests are vertical for $I \in (-\infty, I_\mathrm{l})$ and horizontal for $I \in (I_\mathrm{l}, 0)$.

The second limit implies that $|\alpha(I)| > \exp(-\pi/2)$ for $I \in (1, +\infty)$. Then, if $\exp(-\pi/2) \geq 1/|\mu|$, the crests are vertical for $I \in [1, +\infty)$. if $\exp(-\pi/2) < 1/|\mu|$, there exists a unique $I_\mathrm{r} \in (1, +\infty)$, such that the crests are vertical for any I in $[1, I_\mathrm{r})$ and horizontal for $I \in (I_\mathrm{r}, +\infty)$.

Summarizing, for $1/|\mu| \geq \exp(\pi/2)$, crests are horizontal for $I \in (-\infty, I_\mathrm{c}) \cup (I_\mathrm{r}, +\infty)$ and vertical for $I \in (I_\mathrm{c}, I_\mathrm{r})$. For $\exp(-\pi/2) < 1/|\mu| < \exp(\pi/2)$, crests are horizontal for $I \in (I_\mathrm{l}, I_\mathrm{c}) \cup (I_\mathrm{r}, +\infty)$ and vertical for $I \in (-\infty, I_\mathrm{l}) \cup (I_\mathrm{c}, I_\mathrm{r})$. Finally, if $1/|\mu| < \exp(-\pi/2)$, crests are horizontal for $I \in (I_\mathrm{l}, I_\mathrm{c})$ and vertical for $I \in (-\infty, I_\mathrm{l}) \cup (I_{\mathrm{c},+\infty})$.

Remark 41. For $r \in (0, 1)$, $\alpha_r(I)$ (3.20) is not bounded on a neighborhood of the resonance $I = 1/r$, i.e., $\lim_{I \to 1/r^-} \alpha_r(I) = -\infty$ and $\lim_{I \to 1/r^+} \alpha_r(I) = +\infty$. The same behavior takes place for $r = 1$ and close to $I = 1$. On the other hand, for $I \to \pm\infty$, $\alpha_r(I)$ has the same behavior as in the case for $r = 0$, $\lim_{I \to \pm\infty} \alpha_r(I) = 0$. This implies that for any value of μ, for I close enough to $I = 1/r$ the crests are vertical, and for $|I|$ large enough the crests are horizontal.

Example To illustrate this discussion, we present a concrete example. Taking $\mu = 0.5$, we have $\exp(-\pi/2) < 1/\mu = 2 < \exp(\pi/2)$. In this case we have $I_\mathrm{l} \approx -1.807$, $I_\mathrm{c} \approx 0.701$ and $I_\mathrm{r} \approx 1.367$. The crests are horizontal in $(-1.807, 0.701) \cup (1, 367, +\infty)$ and vertical in $(-\infty, -1.807) \cup (0.701, 1.367)$. We emphasize that this scenario is very different from the case in Chapter 2. There, for $\mu = 0.5$ the crests are horizontal for all I.

Now, we are going to focus on the transversality of the intersection between NHIM lines $R(I, \varphi, s)$ and crests $\mathcal{C}(I)$. On the plane (φ, σ) the NHIM lines can be written as

$$R_I(\varphi, \sigma) = \{(\varphi - I\tau, \sigma - (I-1)\tau), \tau \in \mathbb{R}\}, \tag{3.22}$$

so that its slope is $(I-1)/I$ in such plane. Therefore, there exists an intersection between NHIM lines and crests that is not transversal if, and only if, there exists a tangent vector of $\mathcal{C}(I)$ at a point that is parallel to $(I, I-1)$, or, using the parameterizations,

$$\frac{\partial \xi}{\partial \varphi}(I, \varphi) = \frac{I-1}{I} \qquad \text{or} \qquad \frac{\partial \eta}{\partial \sigma}(I, \sigma) = \frac{I}{I-1}.$$

Considering a *horizontal* parameterization of $\mathcal{C}(I)$, the tangency condition is equivalent to

$$\frac{\pm\alpha(I)\mu\cos\varphi}{\sqrt{1-\mu^2\alpha^2(I)\sin^2\varphi}} = \frac{I-1}{I}.$$

Therefore, there exists a φ satisfying the above condition if, and only if,

$$|\beta(I)| \geq \frac{1}{|\mu|}, \quad \text{where} \quad \beta(I) = \frac{I\alpha(I)}{I-1}$$

and φ takes the form

$$\varphi = \pm\arctan\left(\sqrt{\frac{\beta(I)^2-(1/\mu)^2}{(1/\mu)^2-\alpha(I)^2}}\right).$$

In an analogous way, for a *vertical* parameterization $\eta(I,\sigma)$, there are tangencies if, and only if,

$$|\beta(I)| \leq \frac{1}{|\mu|} \qquad \text{with} \qquad \sigma = \pm\arctan\left(\left|\frac{I-1}{I}\right|\sqrt{\frac{(1/\mu)^2-\beta(I)^2}{\alpha(I)^2-(1/\mu)^2}}\right).$$

Remark 42. Observe that in both cases, horizontal and vertical crests, there are tangencies if, and only if,

$$\left(|\alpha(I)| - \frac{1}{|\mu|}\right)\left(|\beta(I)| - \frac{1}{|\mu|}\right) < 0.$$

The function $|\beta(I)|$ is smooth in $\mathbb{R}\setminus\{1\}$ and $d\,|\beta(I)|\,/dI = 0$ only for $I = 0$. Besides, we have (see Figs. 3.2(a) and 3.2(b))

$$\lim_{I\to 1}|\beta(I)| = +\infty, \qquad \lim_{I\to-\infty}|\beta(I)| = \exp(\pi/2) \quad \text{and} \quad \lim_{I\to+\infty}|\beta(I)| = \exp(-\pi/2).$$

Therefore, there are three possibilities:

- for $1/|\mu| \geq \exp(\pi/2)$, there exist $I_0 \in (1/2,1)$ and $I_+ \in (1,+\infty)$ such that I_0 and I_+ are solutions of $|\beta(I)| - 1/|\mu| = 0$. Besides, $|\beta(I)| < 1/|\mu|$ for $I \in (-\infty, I_0)\cup(I_+,+\infty)$ and $|\beta(I)| > 1/|\mu|$ for $I \in (I_0,1)\cup(1,I_+)$.

- for $\exp(-\pi/2) < 1/|\mu| < \exp(\pi/2)$, there exist $I_- \in (-\infty,0)$, $I_0 \in (0,1)$ and $I_+ \in (1,+\infty)$ such that I_-, I_0 and I_+ are solutions of $|\beta(I)| - 1/|\mu| = 0$. Besides, $|\beta(I)| < 1/|\mu|$ for $I \in (I_-,I_0)\cup(I_+,+\infty)$ and $|\beta(I)| > 1/|\mu|$ for $I \in (-\infty,I_-)\cup(I_0,1)\cup(1,I_+)$.

- For $1/|\mu| \leq \exp(-\pi/2)$, there exist $I_- \in (-\infty,0)$ and $I_0 \in (0,1/2)$ such that I_- and I_0 are solutions of $|\beta(I)| - 1/|\mu| = 0$. Besides, $|\beta(I)| < 1/|\mu|$ for $I \in (I_-,I_0)$ and $|\beta(I)| > 1/|\mu|$ for $I \in (-\infty,I_-)\cup(I_0,1)\cup(1,\infty)$.

Putting together this description of $|\beta(I)|$ with the study about vertical and horizontal crests and adding that

$$\begin{aligned} |\beta(I)| < |\alpha(I)| \quad & \forall I \in (-\infty, 0) \cup (0, 1/2); \\ |\beta(I)| > |\alpha(I)| \quad & \forall I \in (1/2, 1) \cup (1, +\infty); \\ |\beta(0)| = |\alpha(0)| = 0 \quad & |\beta(1/2)| = |\alpha(1/2)| = 1 \end{aligned}$$

we can state the proposition below.

Proposition 43. *Consider the two crests $\mathcal{C}(I)$ defined by* (3.18) *and the NHIM line $R_I(\varphi, \sigma)$ defined in* (3.15) *for Hamiltonian* (3.1).

- *For $|\mu| \leq \exp(-\pi/2)$, there exist $I_b < I_a < I_A < I_B$ such that*
  - *for $I < I_b$ or $I_B < I$, $\mathcal{C}(I)$ are horizontal and intersect transversally any $R_I(\varphi, \sigma)$;*
  - *for $I_b \leq I < I_a$ or $I_A < I \leq I_B$, the crests $\mathcal{C}(I)$ are horizontal, but now, there exist tangencies between $\mathcal{C}(I)$ and two NHIM lines $R_I(\varphi, \sigma)$;*
  - *for $I_a < I < I_A$, the crests $\mathcal{C}(I)$ are vertical and intersect transversally any $R_I(\varphi, \sigma)$.*
- *For $\exp(-\pi/2) < |\mu| < \exp(\pi/2)$ there exist $I_b < I_a < I_c \leq I_C < I_A < I_B$ such that*
  - *for $I < I_b$ or $I_C < I < I_A$, $\mathcal{C}(I)$ are vertical and intersect transversally any $R_I(\varphi, \sigma)$;*
  - *for $I_b \leq I < I_a$, the crests $\mathcal{C}(I)$ are vertical and there exist tangencies between $\mathcal{C}(I)$ and two NHIM lines $R_I(\varphi, \sigma)$;*
  - *for $I_a < I < I_c$ or $I_B < I$, $\mathcal{C}(I)$ are horizontal and intersect transversally any $R_I(\varphi, \sigma)$;*
  - *for $I_A \leq I \leq I_B$, the crests $\mathcal{C}(I)$ are horizontal and there exist tangencies between $\mathcal{C}(I)$ and two NHIM lines $R_I(\varphi, \sigma)$;*
  - *for $I_c \leq I \leq I_C$, if $I_c < 1/2$, the crests $\mathcal{C}(I)$ are vertical and there exist tangencies between $\mathcal{C}(I)$ and $R_I(\varphi, \sigma)$. If $I_c = 1/2$, from the properties of $\alpha(I)$ and $\beta(I)$ this interval is just one point. If $I_c > 1/2$, the crests $\mathcal{C}(I)$ are horizontal and there exist tangencies.*
- *For $|\mu| \geq \exp(\pi/2)$ there exist $I_b < I_a < I_A < I_B$ such that*
  - *for $I < I_b$ or $I_B < I$, $\mathcal{C}(I)$ are vertical and intersect transversally any $R_I(\varphi, \sigma)$;*
  - *for $I_b \leq I < I_a$ or $I_A < I \leq I_B$, the crests $\mathcal{C}(I)$ are vertical and there exist tangencies between $\mathcal{C}(I)$ and two NHIM lines $R_I(\varphi, \sigma)$;*
  - *for $I_a < I < I_A$, the crests $\mathcal{C}(I)$ are horizontal and intersect transversally any $R_I(\varphi, \sigma)$.*

Remark 44. Note that we are not considering the singular case $|\alpha(I)| = 1/|\mu|$ described in Remark 39.

Example Again, to illustrate this proposition, we take the case with $\mu = 0.5$, see Fig. 3.2(a). In this case, we have $|\beta(I)| = 1/\mu$ for $I \approx -2.942$, 0.595, 1.85 and

- for $I \in (-\infty, -2.942) \cup (0.701, 1) \cup (1, 1.367) \Rightarrow \begin{cases} |\alpha(I)| > 1/|\mu| \Rightarrow \text{vertical crests} \\ |\beta(I)| > 1/|\mu| \Rightarrow \text{no tangencies} \end{cases}$
- for $I \in [-2.942, -1.807) \Rightarrow \begin{cases} |\alpha(I)| > 1/|\mu| & \Rightarrow \text{vertical crests} \\ |\beta(I)| \leq 1/|\mu| & \Rightarrow \text{tangencies} \end{cases}$
- for $I \in (-1.807, 0.595) \cup (1.85, +\infty) \Rightarrow \begin{cases} |\alpha(I)| < 1/|\mu| & \Rightarrow \text{horizontal crests} \\ |\beta(I)| < 1/|\mu| & \Rightarrow \text{no tangencies} \end{cases}$
- for $I \in [0.595, 0.701) \cup (1.367, 1.85] \Rightarrow \begin{cases} |\alpha(I)| < 1/|\mu| & \Rightarrow \text{horizontal crests} \\ |\beta(I)| \geq 1/|\mu| & \Rightarrow \text{tangencies} \end{cases}$

Once more, we compare with the Hamiltonian (1.6) studied in Chapter 2. For Hamiltonian (1.6) and $\mu = 0.5$ there is no tangency, but for Hamiltonian (3.1) we can find tangencies for horizontal and vertical crests. Indeed, for Hamiltonian (1.6) and any $0 < |\mu| < 0.625$ there is no tangency, whereas for any $\mu \neq 0$ there are tangencies for Hamiltonian (3.1).

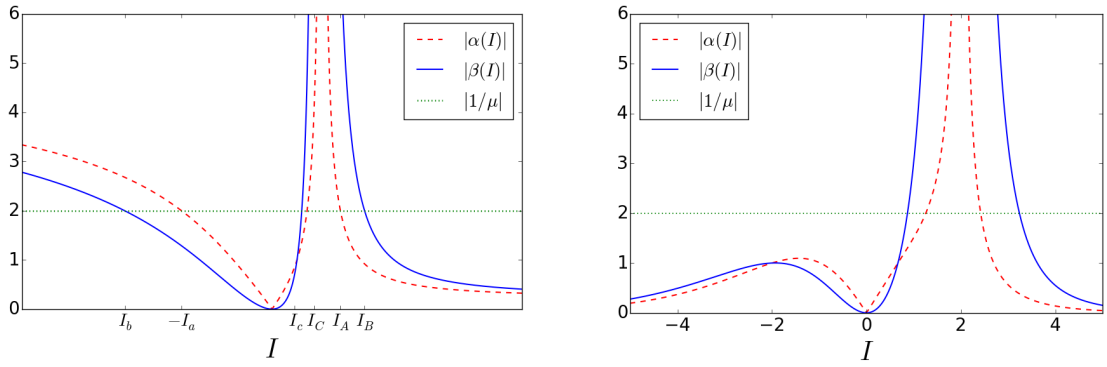

(a) $|\alpha(I)|$ and $|\beta(I)|$:$\mu = 0.5$, $I_b \approx -2.942$, $I_a \approx -1.807$, $I_c \approx 0.595$, $I_C \approx 0.701$, $I_A \approx 1.367$ and $I_B \approx 1.85$

(b) $|\alpha_r(I)|$ and $|\beta_r(I)|$: $\mu = 0.5$ and $r = 0.5$.

Fig. 3.2: $|\alpha(I)|$ and $|\beta(I)|$: Behavior of the crests and tangencies.

Remark 45. For $r \in (0, 1)$ in Hamiltonian (1.5), $\beta_r(I)$ is defined by $\beta_r(I) = I\alpha_r(I)/(rI - 1)$. In this case, $\lim_{I \to 1/r} |\beta_r(I)| = +\infty$ and $\lim_{I \to \pm\infty} |\beta_r(I)| = 0$. In Fig. 3.2(b), a comparison between the functions $\alpha_r(I)$, $\beta_r(I)$ and the straight line $1/|\mu|$ for $r = 1/2$ is displayed.

For each crest, where it is well defined, there exists, at least, a value τ^* such that

$$(\varphi - I\tau^*, \sigma - (I-1)\tau^*) = (\varphi - I\tau^*, \xi(I, \varphi - I\tau^*)) \text{ or } (\eta(I, \sigma - (I-1)\tau^*), \sigma - (I-1)\tau^*),$$

which means that $R_I(\varphi, \sigma) \cap \mathcal{C}(I) \neq \emptyset$. This intersection is intrinsically associated to a homoclinic orbit to the NHIM. To make a choice about how to take such τ^* is to choose in which homoclinic manifold Γ the homoclinic points $\tilde{z}^*$ lie. Even more, it is to choose what scattering map we are going to use.

3.2.2 Construction of scattering maps

We have now several goals. First, to explain, given (I,θ), how to find the intersection between one of the NHIM lines and one of the two crests, and consequently, to define the function τ^*. Second, to show how each crest can give rise to many scattering maps. And third, to explain the different scattering maps or combinations of them that can be defined.

Let us first study the intersection between NHIM lines and crests. From the definition of the function $\tau^* = \tau^*(I,\varphi,s)$ in equation (3.14) and the definition of a NHIM line $R(I,\varphi,s)$ in (3.15) and a crest $\mathcal{C}(I)$ in Definition 36, it turns out that

$$R(I,\varphi,s) \cap \mathcal{C}(I) = \{(I, \varphi - I\tau^*(I,\varphi,s), s - \tau^*(I,\varphi,s))\}\,.$$

Moreover, from the equation satisfied by the function τ^*, one can get (see Eq. (2.15) in Chapter 2) that for any γ

$$\tau^*(I,\varphi - I\gamma, s-\gamma) = \tau^*(I,\varphi,s) - \gamma.$$

In particular, for the change (3.17) $s = \varphi - \sigma$ and $\gamma = \varphi - \sigma$ one gets

$$\tau^*(I,\varphi,\varphi-\sigma) = \tau^*(I,\theta) + \varphi - \sigma, \tag{3.23}$$

where $\theta = \varphi - Is = (1-I)\varphi + I\sigma$. In the variables (I,φ,σ), taking into account the expression (3.22) for the NHIM lines $R(I,\varphi,\varphi-\sigma)$ and again equation (3.14) satisfied by $\tau^*(I,\varphi,s)$, we have that

$$\begin{aligned} R(I,\varphi,\varphi-\sigma) \cap \mathcal{C}(I) &= \{(I, \varphi - I\tau^*(I,\varphi,\varphi-\sigma), \sigma - (I-1)\tau^*(I,\varphi,\varphi-\sigma))\} \\ &= \{(I, \theta - I\tau^*(I,\theta), \theta - (I-1)\tau^*(I,\theta))\}\,, \end{aligned}$$

where (3.23) has been used, and $\theta = (1-I)\varphi + I\sigma$.

From a geometrical point of view, to find an intersection between a NHIM line and a crest, one throws from a point (θ,θ) on the plane (φ,σ) a straight line with slope $(I-1)/I$, until it touches the crest $\mathcal{C}(I)$. The function $\tau^*(I,\theta)$ is the time spent to go from a point (θ,θ) in the diagonal $\sigma = \varphi$ up to $\mathcal{C}(I)$ with a velocity vector $\mathbf{v} = -(I, I-1)$, see Fig. 3.3.

One has to decide the direction for τ^* using the idea explained above. For example, if we are on a point on the straight line $\sigma = \varphi$, we have to decide if we go up or go down along the NHIM line, i.e., to look for a negative or a positive $\tau^*(I,\theta)$ (to look at the past or the future). In both cases we are going to detect an intersection with the desired crest, but, in general, different choices give rise to different scattering maps, because we are looking for different homoclinic invariant manifolds Γ.

To show another difference between scattering maps from the choice of τ^* we begin by introducing each kind of scattering map. The first one is inspired in [DH11] and Chapter 2 for $|\mu| < 0.97$. In these cited cases all scattering maps studied were associated to one of the horizontal crests like in (3.21). In the same way, we can separate completely the scattering maps associated to the horizontal crests from the scattering maps associated to the vertical crests. Notice that the scattering maps associated to horizontal crests are defined only for

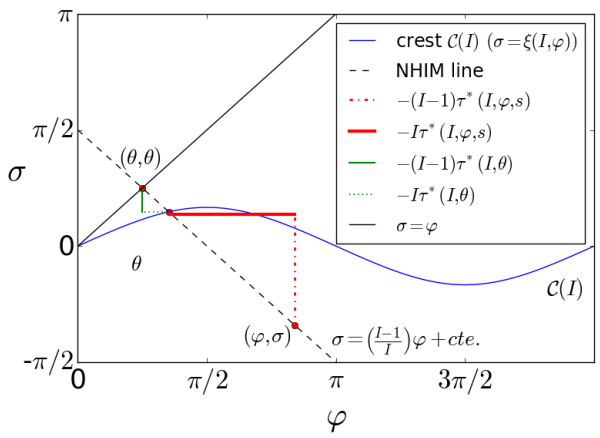

Fig. 3.3: Finding $\tau^*(I,\theta)$ using the straight line $\sigma=\varphi$.

values of I satisfying $|\alpha(I)|<1/|\mu|$ whereas the scattering maps associated to the vertical crests are defined only for values of I satisfying $|\alpha(I)|>1/|\mu|$.

As noted previously, crests are vertical in a neighborhood of $I=1$ for any value of μ. Therefore, close to $I=1$ there is no scattering map associated to a horizontal crest. Analogously, since $|\alpha(0)|=0$, crests are horizontal in a neighborhood of $I=0$ for any value of μ and, therefore, there is no scattering map associated to a vertical crest close to $I=0$. This implies that these "horizontal" or "vertical" scattering maps are just locally defined, in other words, they are not defined on the whole plane (θ,I). This motivates to define *global scattering maps*. Global scattering maps are important because they describe the outer dynamics for large intervals of I and are defined as follows

Definition 46. A scattering map $\mathcal{S}(I,\theta)$ is called a *global scattering map* if it is defined on all $\theta\in\mathbb{T}$ for any fixed I.

Note that $\mathcal{S}(I,\theta)$ is a global scattering map as long as $\tau^*(I,\theta)$ is a global function, i.e., defined on all $\theta\in\mathbb{T}$ for any fixed I. If $\tau^*(I,\theta)$ is smoothly defined, the same will happen to $\mathcal{S}(I,\theta)$. Tangencies between NHIM lines and crests, as well as discontinuities in their intersections give rise to non-smooth scattering maps.

Remark 47. For instance, in Chapter 2 devoted to the Hamiltonian (1.6), it was proven that for $0<\mu=a_1/a_2<0.625$, there exist two different global scattering maps. Let us add that for $0.625\leq\mu<0.97$, due to the existence of tangencies between the NHIM lines and the crests, there appear two or six scattering maps, see Section 2.2.2. Such *multiple* scattering maps are indeed piecewise smooth global scattering maps, see Figs. 2.9–2.11. Their discontinuities lie along the *tangency locus* and were avoided there to construct diffusion paths, just for the sake of simplicity.

For Hamiltonian (3.1), to extend scattering maps which are in principle only locally defined we have now two options: to combine a scattering map associated to a horizontal

crest with a scattering map associated to a vertical crest or to extend the previously called "horizontal" or "vertical" scattering maps. Although the first option may provide a global scattering map, they may appear complex discontinuity sets which give rise to a complicated phase space.

The second option is to apply the same idea used in Chapter 2 when we defined the scattering map "with holes". When $|\alpha(I)| > 1/|\mu|$, the horizontal crests are no longer defined for all $\varphi \in \mathbb{T}$, indeed, they become vertical crests defined for all $\sigma \in \mathbb{T}$. Nevertheless, the vertical crests are formed by pieces of horizontal crests. This implies that even for these values of I we can use ξ given in (3.21) to parameterize some intersections between $R(I, \varphi, \sigma)$ and $\mathcal{C}(I)$. As we can see in Fig. 3.4, the vertical and horizontal crests $\mathcal{C}_{\mathrm{M}}$ are very close in a neighborhood of $\varphi = 0$. When we have a bifurcation from horizontal to vertical crests (or vice versa), it is natural just to change the parameterization from ξ_{M} to η_{M} for these values of φ. With this choice the orbits of the scattering map are continuous for θ close to 0 or 2π. The same happens with ξ_{m} and η_{m} for values of φ close to π. Scattering maps associated to horizontal crests for values of I satisfying $|\mu\alpha(I)| < 1$ are defined for all $\varphi \in \mathbb{T}$. The extension of them to values of I for $\varphi \in \mathbb{T}$ such that $|\mu\alpha(I)\sin\varphi| < 1$ are called *extended scattering maps*.

Definition 48. A scattering map $\mathcal{S}(I, \theta)$ is called an *extended scattering map* if it is associated to horizontal crests for which $|\mu\alpha(I)| < 1$, and is continuously extended to the pieces of the vertical crests where they behave as horizontal crests, that is, for the values φ such that $|\mu\alpha(I)\sin\varphi| < 1$.

Since we have already seen in Proposition 43 that there exist tangencies between NHIM lines and crests for any value of μ, there are no global scattering maps for Hamiltonian (3.1). However, there exist extended scattering maps with a domain large enough to provide diffusion paths.

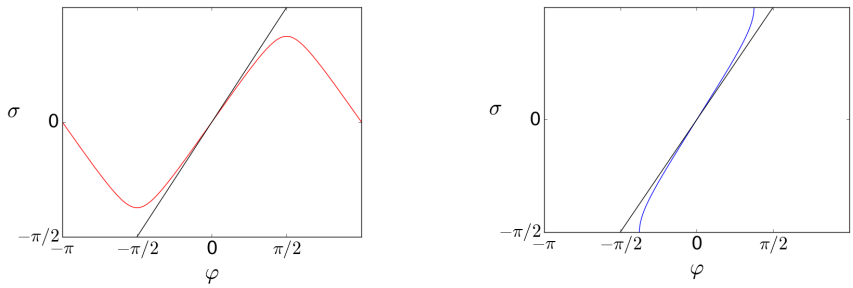

(a) A piece of $\xi_{\mathrm{M}}(I, \varphi)$ for $I = 0.68$. (b) A piece of $\eta_{\mathrm{M}}(I, \sigma)$ for $I = 0.72$.

Fig. 3.4: Comparison between $\xi_{\mathrm{M}}(I, \varphi)$ and $\eta_{\mathrm{M}}(I, \sigma)$ for $\mu = 0.5$, $I = 0.68$ and $I = 0.72$ respectively.

To illustrate the current scenario we will display the level curves of the reduced Poincaré function $\mathcal{L}^*(I, \theta)$ defined in (3.13), which up to $\mathcal{O}(\varepsilon^2)$ contain orbits of the scattering map $\mathcal{S}(I, \theta)$. We begin by considering $\mu = 0.6$ and the horizontal crest $\mathcal{C}_{\mathrm{M}}(I)$. In Fig. 3.5(a) we display the scattering map built using τ^* defined by the first intersection between $R_I(\varphi, \sigma)$

and $\mathcal{C}_{\mathrm{M}}(I)$ from $\sigma = \varphi$ going down along $R_I(\varphi, \sigma)$. In Fig.3.5(b), we use a similar idea, but now, form $\sigma = \varphi$ going up along $R_I(\varphi, \sigma)$. Alternatively, if we choose τ^* with minimal absolute value, independently of going up or down, we obtain the scattering map plotted on Fig. 3.5(c). In this last case, there are orbits of the scattering maps that are not smooth in $\theta = \pi$. This happens because we change the homoclinic manifold Γ, so we are using, indeed, two different scattering maps. In Chapter 2 we chose scattering maps associated to a function τ^* with the minimal absolute value, which were called *primary* scattering maps. This example show us that is not enough to say what crest is associated to a scattering map, but it is also necessary to make explicit the criterion used for τ^* (going up or down along the NHIM lines, or choosing a minimal $|\tau^*|$).

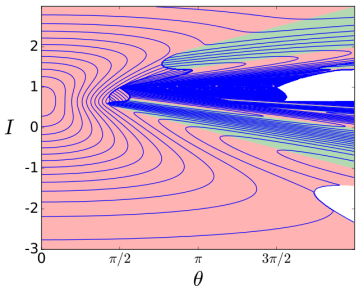

(a) Going down along the NHIM lines $R_I(\varphi, \sigma)$.

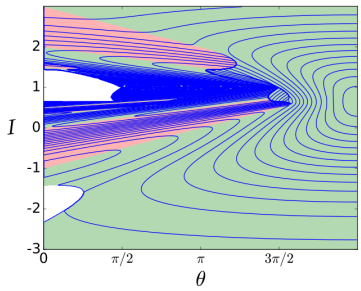

(b) Going up along the NHIM lines $R_I(\varphi, \sigma)$.

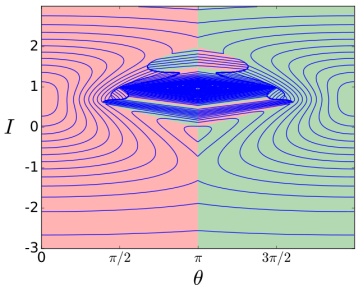

(c) Minimal absolute value of τ^*.

Fig. 3.5: Different phase space of scattering maps $\mathcal{S}(I, \theta)$ associated to the same horizontal crest $C_{\mathrm{M}}(I)$, for $\mu = 0.6$ and $\varepsilon = 0.01$. The orbits of scattering maps are represented by the blue lines which are, up to $\mathcal{O}(\varepsilon^2)$, level sets of the reduced Poincaré function $\mathcal{L}^*(I, \theta)$. In the red zones the values of I on such orbits decrease, in the green one the values of I increase. The white regions are regions where $|\mu\alpha(I)\sin\varphi| > 1$ is satisfied.

The next lemma is a good example about the criteria for $\tau^*(I, \theta)$ and its consequences, and is used to prove Proposition 51. Before, a new notation is introduced. An *even* subindex k is assigned to the branches $\mathcal{C}_k(I)$ of $\mathcal{C}_{\mathrm{M}}(I)$ when considering σ, $\varphi \in \mathbb{R}$

$$\xi_k(I, \varphi) = -\arcsin\left(\alpha(I)\mu\sin\varphi\right) + k\pi \quad \text{and} \quad \eta_k = -\arcsin\left(\frac{\sin\sigma}{\alpha(I)\mu}\right) + k\pi$$

and an *odd* subindex k to the branches $\mathcal{C}_k(I)$ of $\mathcal{C}_{\rm m}(I)$ when considering σ, $\varphi \in \mathbb{R}$

$$\xi_k(I,\varphi) = \arcsin\left(\alpha(I)\mu\sin\varphi\right) + k\pi \quad \text{and} \quad \eta_k = \arcsin\left(\frac{\sin\sigma}{\alpha(I)\mu}\right) + k\pi.$$

We notice that the crests $\mathcal{C}(I)$ are naturally defined for $(\varphi,\sigma) \in \mathbb{T}^2$ and give rise to two different crests $\mathcal{C}_{\rm M}(I)$, $\mathcal{C}_{\rm m}(I)$ (except for the singular case $|\mu\alpha(I)| = 1$). When we run now over real values of φ, σ, we may have an *infinite* number of crests $\mathcal{C}_k(I)$, where even (odd) values of k are assigned to the branches of $\mathcal{C}_{\rm M}(I)$ ($\mathcal{C}_{\rm m}(I)$). Among them, we are going to use $\mathcal{C}_0(I)$, $\mathcal{C}_1(I)$ and $\mathcal{C}_2(I)$.

Lemma 49. *Let $\mathcal{L}_0^*$ and $\mathcal{L}_2^*$ be reduced Poincaré functions associated to the same crest $\mathcal{C}(I)$, where for $\mathcal{L}_0^*$ we look at the first intersection points "under" $\sigma = \varphi$, that is, with $\mathcal{C}_0(I)$, and for $\mathcal{L}_2^*$ we look at the first intersection points "over" $\sigma = \varphi$, that is, with $\mathcal{C}_2(I)$. Then we have*

$$\frac{\partial\mathcal{L}_0^*}{\partial\theta}(I,\theta) = -\frac{\partial\mathcal{L}_2^*}{\partial\theta}(I,2\pi-\theta). \tag{3.24}$$

Remark 50. We say "under" $\sigma = \varphi$ and "over" $\sigma = \varphi$ for intersection points going down or up along $R_I(\varphi,\sigma)$, respectively on $(\varphi,\xi_0(I,\varphi))$ and $(\varphi,\xi_2(I,\varphi))$, because when the horizontal crest $\mathcal{C}_{\rm M}(I)$ is defined for all $\varphi \in \mathbb{T}$ the graphs $(\varphi,\xi_0(I,\varphi))$ of $\mathcal{C}_0(I)$ and $(\varphi,\xi_2(I,\varphi))$ of $\mathcal{C}_2(I)$ are under and over the straight line $\sigma = \varphi$.

Proof. Let $\mathcal{L}^*$ be a reduced Poincaré function (3.13)-(3.11), then

$$\frac{\partial\mathcal{L}^*}{\partial\theta}(I,\theta) = \frac{A_1(I)\sin(\theta - I\tau^*(I,\theta))}{I-1}.$$

So, equation (3.24) is satisfied if, and only if

$$\sin(\theta - I\tau_0^*(I,\theta)) = \sin(\theta - I(-\tau_2^*(I,2\pi-\theta))). \tag{3.25}$$

We assume that the crest is horizontal and given by the graph of $\xi_{\rm M}$, the other cases are analogous. Indeed, we are going to use

$$\xi_0(I,\varphi) = -\arcsin(\mu\alpha(I)\sin\varphi) \quad \text{and} \quad \xi_2(I,\varphi) = \xi_0(I,\varphi) + 2\pi. \tag{3.26}$$

This implies that the intersection point "under" $\sigma = \varphi$ is a point on the curve parameterized by $\xi_0(I,\varphi)$. Otherwise, the intersection "over" $\sigma = \varphi$ is a point on the curve parameterized by $\xi_2(I,\varphi)$. As the slope of the NHIM lines is $(I-1)/I$, given a point (θ,θ), we obtain

$$\frac{\xi_2(I,\theta - I\tau_2^*(I,\theta)) - \theta}{\theta - I\tau_2^*(I,\theta) - \theta} = \frac{I-1}{I},$$

which can be rewritten as

$$\frac{2\pi + \xi_0(I,\theta - I\tau_2^*(I,\theta)) - \theta}{-I\tau_2^*(I,\theta)} = \frac{I-1}{I}.$$

From this equation, we obtain an expression for $\tau_2^*(I,\theta)$

$$\tau_2^*(I,\theta) = \frac{-\left(2\pi + \xi_0(I, \theta - I\tau_2^*(I,\theta)) - \theta\right)}{I-1}.$$

From the expressions of $\tau_2^*(I,\theta)$ above and (3.26),

$$\tau_2^*(I, 2\pi - \theta) = \frac{\left(\xi_0(I, \theta - I\left(-\tau_2^*(I, 2\pi - \theta)\right)) + \theta\right)}{I-1},$$

and therefore

$$\theta - (I-1)(-\tau_2^*(I,2\pi-\theta)) = \xi_0(I, \theta - (I-1)(-\tau_2^*(I,2\pi-\theta))),$$

which implies that $-\tau_2^*(I,2\pi-\theta)$ is a time of intersection between the NHIM line and the curve parameterized by ξ_0. In the case that there exists only one intersection point, this implies

$$\tau_0^*(I,\theta) = \tau_2^*(I,2\pi-\theta).$$

So, condition (3.25) is satisfied. □

Proposition 51. *Let $\mathcal{S}_1(I,\theta)$ be the scattering map associated to the graphs of ξ_1 and η_1 of $\mathcal{C}_1(I)$. Assuming $a_1, a_2 > 0$, for any I there exists a θ_+ such that $\dot{I} > 0$ for $\theta \in (\pi, \theta_+)$. Moreover, $\theta_+ \geq 3\pi/2$ for $I \notin (-1/2, 1/2)$.*

Proof. We have

$$\dot{I} = \frac{\partial \mathcal{L}^*}{\partial \theta}(I,\theta) = \frac{A_1(I)\sin(\theta - I\tau^*(I,\theta))}{I-1} = -\frac{A_2(I)\sin(\theta-(I-1)\tau^*(I,\theta)}{I}. \tag{3.27}$$

where $A_1(I)$ and $A_2(I)$ are positive, because a_1, $a_2 > 0$. Notice that $\mu = a_1/a_2 > 0$.

Note that as $(I, \varphi = \pi, \theta = \pi)$ is always on the crest $\mathcal{C}_{\rm m}(I)$, $\tau^*(I,\pi) = 0$ for all I.

Consider first the case of horizontal crests ($|\alpha(I)\mu| < 1$).

a) For $I < 0$, the function $\alpha(I)$ introduced in (3.19) satisfies $\alpha(I) > 0$, and from (3.21), $\sin(\xi_1(I,\varphi))\sin\varphi = -\mu\alpha(I)\sin\varphi \leq 0$. Take $\theta = \frac{3\pi}{2}$; since $I < 0$, the slope $m = (I-1)/I$ of the NHIM lines is greater than 1. Therefore, $3\pi/2 - I\tau_1^*(I, 3\pi/2) \in (\pi, 3\pi/2)$. This implies that for any $\theta \in (\pi, 3\pi/2)$, $\theta - I\tau_1^*(I,\theta) \in (\pi, 3\pi/2)$, so $\sin(\theta - I\tau_1^*) < 0$. From (3.27), $\dot{I} > 0$.

b) For $0 < I < 1$, $\alpha(I) < 0$, so $\sin\xi_1(I,\varphi)\sin\varphi \geq 0$. Besides, $m < 0$, so if we look for θ_* satisfying

$$\begin{aligned} \theta - I\tau &= 2\pi \\ \theta - (I-1)\tau &= \pi, \end{aligned} \tag{3.28}$$

we have that for any $\theta \in (\pi, \theta_*)$, $\theta - I\tau_1^* \in (\pi, 2\pi)$. By solving (3.28) and defining $\theta_+ := \theta_*$, we obtain $\theta_+ = (2-I)\pi$. Then, $\sin(\theta - I\tau_1^*(I,\theta)) < 0$ and therefore $\dot{I} > 0$ for any $\theta \in (\pi, \theta_+ = (2-I)\pi)$. In particular, $\theta_+ < 3\pi/2$ if, and only if, $I \in (1/2, 1)$.

c) For $I > 1$, one more time $\alpha(I) > 0$ and $\sin\xi_1(I,\varphi)\sin(\varphi) < 0$, but now $0 < m = 1 - 1/I < 1$. We first fix $\theta = 3\pi/2$ and search for I such that

$$\frac{3\pi}{2} - I\tau^*(I, 3\pi/2) = 0$$
$$\frac{3\pi}{2} - (I-1)\tau^*(I, 3\pi/2) = \pi.$$

We obtain $I = 3/2$, so $\theta - I\tau_1^*(I,\theta) \in (0,\pi)$ for any $I \geq 3/2$ and $\theta \in (\pi, \theta_+ = 3\pi/2)$. Consequently, $\sin(\theta - I\tau_1^*(I,\theta)) > 0$ and $\dot{I} > 0$. For the values of $I \in (1, 3/2)$ we change the strategy. We look for θ_* such that

$$\theta - I\tau^*(I,\theta) = 0$$
$$\theta - (I-1)\tau^*(I,\theta) = \pi.$$

We have $\theta_* = \pi I$ and $\theta - I\tau_1^*(I,\theta_*) \in (0,\pi)$ for any $I \in (1,3/2)$ and $\theta \in (\pi, \theta_*)$, so $\dot{I} > 0$. Note that $\theta_* < 3\pi/2$ and we can define $\theta_+ := \theta_*$.

Observe that for $I = 1$ the crests are vertical, and for $I = 0$, $\theta = \theta - I\tau_1^*(I,\theta)$, and $\dot{I} > 0$ for $\theta \in (\pi, 3\pi/2)$.

Consider now the case of vertical crests ($|\alpha(I)\mu| > 1$).

a) For $I < 0$, $\sin\eta_1(I,\sigma)\sin\sigma = -\mu\alpha(I)\sin^2\sigma \leq 0$ and $m > 1$. We fix $\theta = 3\pi/2$ and look for I such that

$$3\pi/2\pi - I\tau^* = \pi$$
$$3\pi/2 - (I-1)\tau^*(I, 3\pi/2) = 0.$$

We obtain $I = -1/2$ and therefore, $\sin(\theta - (I-1)\tau_1^*(I,\theta)) > 0$ for $I \in (-\infty, -1/2)$ and $\theta \in (\pi, 3\pi/2)$. Consequently, $\dot{I} > 0$ from (3.27). For $I \in (-1/2, 0)$, we have that $\theta_+ = (1-I)\pi$ satisfies

$$\theta - I\tau^*(I,\theta_+) = \pi$$
$$\theta_+ - (I-1)\tau^*(I,\theta_+) = 0.$$

Therefore, $\sin(\theta - (I-1)\tau_1^*)(I,\theta) > 0$ and $\dot{I} > 0$ for any $\theta \in (\pi, \theta_+)$.

b) For $0 < I < 1$ $\sin\eta_1(I,\sigma)\sin\sigma \geq 0$ and $m < 0$. $\theta_+ = (I+1)\pi$ satisfies

$$\theta - I\tau^*(I,\theta_+) = \pi$$
$$\theta_+ - (I-1)\tau^*(I,\theta_+) = 2\pi.$$

So, $\sin(\theta - (I-1)\tau_1^*(I,\theta)) > 0$ and $\dot{I} > 0$ for any $\theta \in (\pi, \theta_+)$. Note that $\theta_+ < 3\pi/2$ for $I \in (0, 1/2)$.

c) Finally, for $I > 1$, $\sin\eta_1(I,\sigma)\sin\sigma \leq 0$. We have that $\theta - (I-1)\tau_1^*(I,\theta) \in (\pi, 2\pi)$, so $\sin(\theta - (I-1)\tau_1^*(I,\theta)) < 0$ and $\dot{I} > 0$ for any $\theta \in (\pi, 3\pi/2)$.

For $I = 0$ the crests are horizontal. For $I = 1$, $\theta = \theta - (I-1)\tau_1^*(I,\theta)$, so $\dot{I} > 0$ for $\theta \in (\pi, 2\pi)$. □

Remark 52. If $a_1 < 0$, we have that there exists a θ_- such that $\dot{I} > 0$ for any $\theta \in (\theta_-, \pi)$.

Remark 53. An analogous proposition holds for $\mathcal{S}_2(I,\theta)$, the scattering map associated to the graphs of ξ_2 and η_2 of $\mathcal{C}_2(I)$. In such case, there is a θ_+ such that $\dot{I} \geq 0$ for any $\theta \in (\theta_+, 2\pi)$ where $\theta \geq 3\pi/2$ for $I \in (1/2, 3/2)$.

Note that this proposition leads us to ensure the diffusion in an analogous way to the one used to prove Theorem 25. Next, the diffusion mechanism is stated and the Arnold diffusion is proven.

3.3 Arnold Diffusion

In this section we are going to complete our goal proving the existence of global instability or Arnold diffusion, that is, Theorem 1.

We begin by presenting some general geometrical properties of the scattering maps that we have to take into account to prove the theorem of diffusion. The first one reduces the study of scattering maps to positive values of μ. More precisely, we have the lemma below

Lemma 54. *The scattering map for a value of μ and $s = \pi$, associated to the intersection between $R(I,\varphi,s)$ and $C_m(I)$ ($C_M(I)$) has the same geometrical properties as the scattering map for $-\mu$ and $s = 0$, associated to the intersection between $R_\theta(I)$ and $C_M(I)$ ($C_m(I)$), i.e.,*

$$S^{\mu}_{m(M)}(I,\varphi,\pi) = S^{-\mu}_{M(m)}(I,\varphi,0) = \mathcal{S}^{-\mu}_{M(m)}(I,\theta)$$

Proof. First, we look for τ^*_{m} such that the NHIM segment $R(I,\varphi,s)$ intersects the crest $C_{\mathrm{m}}(I)$. If we fix $s = \pi$, we have from (3.11) and (3.12):

$$\begin{aligned} L^*_{\mu,\mathrm{m}}(I,\varphi,\pi) =& A_1(I)\cos(\varphi - I\tau^*_{\mathrm{m}}(I,\varphi,\pi)) \\ &+ A_2(I)\cos(\varphi - \pi - (I-1)\tau^*_{\mathrm{m}}(I,\varphi,\pi)). \end{aligned} \tag{3.29}$$

Besides, τ^* satisfies

$$\mu\alpha(I)\sin(\varphi - I\tau^*_{\mathrm{m}}) + \sin(\varphi - \pi - (I-1)\tau^*_{\mathrm{m}}) = 0,$$

or

$$-\mu\alpha(I)\sin(\varphi - I\tau^*_{\mathrm{m}}) + \sin(\varphi - (I-1)\tau^*_{\mathrm{m}}) = 0.$$

We have that $\varphi - \pi - (I-1)\tau^*_{\mathrm{m}} \pmod{2\pi} = \xi_{\mathrm{m}}(I, \varphi - I\tau^*_{\mathrm{m}})$ with $\pi/2 \leq \xi_{\mathrm{m}} \leq 3\pi/2$. Then, for each τ^*_{m} there exists a $K \in \mathbb{Z}$ such that

$$\frac{\pi}{2} < \varphi - \pi - (I-1)\tau^*_{\mathrm{m}} + 2\pi K < \frac{3\pi}{2}.$$

This implies

$$\frac{3\pi}{2} < \varphi - (I-1)\tau_{\mathrm{m}}^* + 2\pi K \quad \text{and} \quad \varphi - (I-1)\tau_{\mathrm{m}}^* + 2\pi(K-1) < \frac{\pi}{2}.$$

Therefore,

$$\varphi - (I-1)\tau_m^* \pmod{2\pi} < \frac{\pi}{2} \quad \text{or} \quad \varphi - (I-1)\tau_m^* \pmod{2\pi} > \frac{3\pi}{2}.$$

We can conclude that $\varphi - (I-1)\tau_m^* \pmod{2\pi} = \xi_{\mathrm{M}}(I, \varphi - I\tau_{\mathrm{m}}^*)$. Therefore $\tau_{\mathrm{m}}^*(I,\varphi,\pi)$ for μ is equal to $\tau_{\mathrm{M}}^*(I,\varphi,0)$ for $-\mu$. From (3.29), $L_{\mu,\mathrm{m}}^*(I,\varphi,\pi)$ satisfies

$$\begin{aligned} L_{\mu,\mathrm{m}}^*(I,\varphi,\pi) &= A_1(I)\cos(\varphi - \tau_{\mathrm{M}}^*(I,\varphi,0)) + (-A_2(I))\cos(\varphi - (I-1)\tau_{\mathrm{M}}^*(I,\varphi,0)) \\ &= L_{-\mu,\mathrm{M}}^*(I,\varphi,0). \end{aligned}$$

Since $L_{\mu,\mathrm{m}}^*(\cdot,\cdot,\pi)$ and $L_{-\mu,\mathrm{M}}^*(\cdot,\cdot,0)$ coincide, their derivatives too and this implies that

$$S_{\mathrm{m}}^{\mu}(I,\varphi,\pi) = S_{\mathrm{M}}^{-\mu}(I,\varphi,0) = \mathcal{S}_{\mathrm{M}}^{-\mu}(I,\theta).$$

□

From now on, just to simplify the exposition, a_1 and a_2 are considered positive. The same strategy used in Chapter 2, Section 2.3, is applied to prove the existence the diffusion: we combine the scattering map in an interval of θ where $\dot{I} > 0$ and the inner map to build a diffusion pseudo-orbit. Then we apply shadowing results to get the existence of a diffusion orbit.

Since $I = 0$ and $I = 1$ are resonance values, the application of the inner map must be more careful, because in these resonance regions, for some orbits, the value of I decreases in order $\mathcal{O}(\sqrt{\varepsilon})$, i. e., the tori cannot be considered flat. We study the transversality between the foliations of invariant sets of the inner and the scattering map in resonant and non-resonant regions and its image under the scattering map $\mathcal{S}$. For more details and a more general case, the reader is referred to [DH09].

Consider the resonant region associated to $I = 0$. In such region, the tori can be approximated by $F^0(I,\varphi)$ given in (3.9). The tranversality between invariant sets of the inner and the scattering map holds if the gradient vectors of the level curves of F^0 and $\mathcal{L}^*$ are not parallel vectors, or equivalently,

$$\left\{F^0(I,\theta), \mathcal{L}^*(I,\theta)\right\} \neq 0,$$

where $\{,\}$ is the Poisson bracket,

$$\left\{F^0, \mathcal{L}^*\right\} = \frac{\partial F^0}{\partial \theta}\frac{\partial \mathcal{L}}{\partial I} - \frac{\partial F^0}{\partial I}\frac{\partial \mathcal{L}}{\partial \theta}.$$

From (3.9), the partial derivatives of F^0 are

$$\frac{\partial F^0}{\partial I} = I \quad \text{and} \quad \frac{\partial F^0}{\partial \theta} = -\varepsilon a_1 \sin\theta,$$

and since $\mathcal{L}^*(I,\theta) = A_1(I)\cos(\theta - I\tau^*(I,\theta)) + A_2(I)\cos(\theta - (I-1)\tau^*(I,\theta))$, we have the partial derivatives given by

$$\frac{\partial \mathcal{L}^*}{\partial \theta} = \frac{A_1(I)\sin(\theta - I\tau^*)}{I-1},$$

$$\begin{aligned}\frac{\partial \mathcal{L}^*}{\partial I} =& A_1'(I)\cos(\theta - I\tau^*) + A_2'(I)\cos(\theta - (I-1)\tau^*) \\ &+ A_1(I)\tau^*\sin(\theta - I\tau^*) + A_2(I)\tau^*\sin(\theta - (I-1)\tau^*).\end{aligned}$$

Note that if $|I| > \mathcal{O}(\varepsilon)$, $\partial F^0/\partial I$ dominates $\partial F^0/\partial\theta$, so the Poisson bracket above can be reduced to

$$\left\{F^0, \mathcal{L}^*\right\} \simeq -\frac{\partial F^0}{\partial I}\frac{\partial \mathcal{L}}{\partial \theta} = \frac{-IA_1(I)\sin(\theta - I\tau^*)}{I-1}$$

Expanding $\sin(\theta - I\tau^*)$ in Taylor's series around $I = 0$, we have

$$\sin(\theta - I\tau^*) = \sin\theta + \mathcal{O}(I),$$

which implies $\{F^0, \mathcal{L}^*\} = 0$ if, and only if, $\theta \approx 0, \pi$, assuming that $\mathcal{O}(I)$ is small enough.

Now, we consider $I = \mathcal{O}(\varepsilon)$ and look at the intersections between the NHIM lines and the graph of ξ_1. Note that as the value of I is close to 0 we can assume that the crests are horizontal. Using Taylor's series we can write

$$\begin{aligned}\sin(\theta - I\tau^*) &= \sin\theta + \mathcal{O}(I) \qquad & \cos(\theta - I\tau^*) &= \cos\theta + \mathcal{O}(I) \\ \sin(\theta - (I-1)\tau^*) &= \mathcal{O}(I) \qquad & \cos(\theta - (I-1)\tau^*) &= -1 + \mathcal{O}(I).\end{aligned}$$

This implies

$$\begin{aligned}\left\{F^0, \mathcal{L}^*\right\} =& -\frac{IA_1(I)\sin\theta}{I-1} - \varepsilon a_1\sin\theta\,(A_1'(I)\cos\theta - A_2'(I) \\ &+ A_1(I)\tau^*\sin\theta) + \mathcal{O}(I^2, \varepsilon I).\end{aligned} \tag{3.30}$$

Taylor expanding the functions $A_1(I)$, $A_1'(I)$ and $A_2'(I)$ around $I = 0$, we obtain

$$A_1(I) = 4a_1 + \mathcal{O}(I^2),\ A_1'(I) = \mathcal{O}(I) \text{ and } A_2'(I) = a_2\pi(\pi\coth\pi/2 - 2)\mathrm{csch}(\pi/2) + \mathcal{O}(I)$$

Plugging these expressions in (3.30), we set

$$\begin{aligned}\left\{F^0, \mathcal{L}^*\right\} =& -\frac{4a_1 I\sin\theta}{I-1} - \varepsilon a_1\sin\theta\,[a_2\pi(\pi\coth\pi/2 - 2)\mathrm{csch}(\pi/2) \\ &+ 4a_1(\pi - \theta)\sin\theta] + \mathcal{O}(I^2, I\varepsilon).\end{aligned}$$

Therefore,

$$\begin{aligned}\left\{F^0, \mathcal{L}^*\right\} = 0 \Leftrightarrow & a_1\sin\theta\left[\frac{-4I}{I-1} - \varepsilon a_2\pi\left(\pi\coth\left(\frac{\pi}{2}\right) - 2\right)\mathrm{csch}\left(\frac{\pi}{2}\right)\right) \\ &+ \varepsilon 4(\pi - \theta)\sin\theta] = 0.\end{aligned}$$

In other words, we do not have transversality if, and only if, $\theta = 0, \pi$ or satisfies

$$(\pi - \theta)\sin\theta = \frac{I}{\varepsilon a_1} + \frac{\pi(\coth \pi/2 - 2)\mathrm{csch}\pi/2)}{4},$$

which is not an horizontal curve in the plane (θ, I) and is transversal to an invariant torus of the inner dynamics.

For the other resonant region $I = 1$, F^1 is very similar. Assuming $I - 1 = \mathcal{O}(\varepsilon)$, we have

$$\left\{F^1, \mathcal{L}^*\right\} = a_2 \sin\theta \left\{4\left(\frac{I-1}{I}\right) - \varepsilon\left[\pi a_1(2 - \pi\coth(\pi/2))\mathrm{csch}(\pi/2) + 4a_2\sin\theta\right]\right\}.$$

Applying the same methodology, we obtain an analogous result for the other resonant region F^1. In short, we conclude that the image $\mathcal{S}(\mathcal{T}_i)$ of an invariant torus $\mathcal{T}_i$ of the inner map under the scattering map intersects tranversally another invariant torus $\mathcal{T}_{i+1}$ of the inner map.

Finally, in the non-resonant region, we notice that

$$\{F^{\mathrm{nr}}, \mathcal{L}^*\} = -\frac{\partial F^{\mathrm{nr}}}{\partial I}\frac{\partial \mathcal{L}^*}{\partial \theta} = -\frac{IA_1(I)\sin(\theta - I\tau^*)}{I-1},$$

just the same expression as the one for the resonance $I = 0$, so the transversality between invariant sets of the inner and the scattering map follows.

Now, a constructive proof of Theorem 1 is presented. This proof is similar to the proof presented in Subsection 2.3.2 of Chapter 2, but now, there is no any piece of "highway" or fast vertical lines where $|I|$ is large. So, the inner map is applied more times.

3.3.1 Proof of Theorem 1

Proof. We consider $r = 1$ in Hamiltonian (1.5). First of all we have to choose what scattering map we use. This choice depends on the sign of μ as explained in Lemma 54. Assuming $\mu > 0$, we take $\mathcal{S}_1(I, \theta)$, the global scattering map associated to the graphs of ξ_1 and η_1. If $a_1 > 0$, by Proposition 51 for any I there exists an interval $\theta \in (\pi, \theta_+)$ where $\dot{I} > 0$. Define H_{r} the set $(\rho, \theta_+) \times [-I^*, I^*]$, where $\rho = \pi + \delta$ is such that $\pi < \rho < \theta_+$ and the transversality between NHIM lines and $\mathcal{L}_1^*$ holds. We first construct a pseudo-orbit $\{(I_i, \theta_i) : i = 0, \ldots, N_1\} \subset H_{\mathrm{r}}$ with $I_0 = -I^*$ and θ_{N_1} as close as possible to ρ. Note that all these points lie in the same level curve of $\mathcal{L}_1^*$, that is, $\mathcal{L}_1^*(I_0, \theta_0) = \mathcal{L}_1^*(I_i, \theta_i)$, $i = 1, \ldots, N_1$. Applying the inner dynamics, we get $(I_{\mathrm{N}_1+1}, \theta_{\mathrm{N}_1+1}) = \phi_{t_{N_1}}(I_{\mathrm{N}_1}, \theta_{\mathrm{N}_1})$ with $\theta_{\mathrm{N}_1+1} \in (\rho, \theta_+)$ and then we construct a pseudo-orbit $\{(I_i, \theta_i) : i = N_1 + 1, \ldots, N_1 + M_1\} \subset \mathcal{L}_1^*(I_{\mathrm{N}_1+1}, \theta_{\mathrm{N}_1+1}) = l_{\mathrm{N}_1+1}$ with $\theta_i \in (\rho, \theta_{\mathrm{N}_1+1})$, $\theta_+ - \theta_{\mathrm{N}_1+\mathrm{M}_1} = \mathcal{O}(\varepsilon^2)$. Applying the inner dynamics, we get $(I_{\mathrm{N}_1+\mathrm{M}_1+1}, \theta_{\mathrm{N}_1+\mathrm{M}_1+1}) = \phi_{t_{\mathrm{N}_1+\mathrm{M}_1}}(I_{\mathrm{N}_1+\mathrm{M}_1}, \theta_{\mathrm{N}_1+\mathrm{M}_1})$ with $\theta_{\mathrm{N}_1+\mathrm{M}_1+1} \in (\rho, \theta_+)$. Recursively, we construct a pseudo-orbit $\{(I_i, \theta_i) : i = \mathrm{N}_1 + 1, \ldots, \mathrm{N}_2\}$ such that $I_{\mathrm{N}_2} \geq I^*$. In the same way, as in the proof of Teorem 25, we can apply shadowing techniques of [FM00, FM03, GLS14], due to the fact that the inner dynamics is simple enough to satisfy

the required hypothesis of these references, to prove the existence of a diffusion trajectory. If $a_{10} < 0$, changing H_{r} to $H_{\mathrm{l}} = (\theta_+, \pi)$ all the previous reasoning applies.

Considering Remark 33, Remark 38, Remark 41 and Remark 45, for any $r \in (0, 1)$, an equivalent diffusion result is readily obtained. And, finally, the case for $r = 0$ is proved in Theorem 25 in Chapter 2.

□

3.4 Piecewise smooth global scattering maps

In this section, the geometric freedom of the choice of τ^* is explored. Until now, only two different scattering maps have been used to build a global one, and this was enough to ensure diffusion. But, with this approach, finding a diffusion pseudo-orbit is not always easy enough and this pseudo-orbit can be also complicated. This depends simply on the "aspect" of the scattering map obtained.

We now suggest a new criterion to choose τ^*: to take the minimal value for $|\tau^*|$ for any (θ, I). This provides us with a piecewise smooth global scattering map with a good property: the phase space of this scattering map which is $\mathcal{O}(\varepsilon^2)$-close to the level sets of the reduced Poincaré function $\mathcal{L}^*(I, \theta)$ associated to the chosen τ^* is simpler and "cleaner" than the phase spaces of other scattering maps displayed up to now. By a cleaner scattering map, we mean that we can easily identify and understand the orbits of the scattering maps, except for a small region which contains the tangency locus.

Besides, the zones where the value of I is increased or decreased under the scattering map is well behaved. I decreases for $\theta \in (0, \pi)$ (the red region on all pictures in Fig. 3.6) and I increases for $\theta \in (\pi, 2\pi)$ (the green region on all pictures in Fig. 3.6). So it is easy to infer that for finding a diffusion pseudo-orbit it is enough to build a combination between the inner map and this scattering map restricted to $(\pi, 2\pi)$, for example if an increased value of I is wished. The same idea used in the proof of Theorem 1.

Observe that the scattering maps we are now considering are a mix of the scattering maps studied previously. As an example, we illustrate the scattering map obtained for $\mu = 0.9$. Such scattering map can be divided into three regions and in each region, the scattering map coincides with a scattering map studied before.

In Fig. 3.7, for regions I ($0 < \theta < \pi/2$), II ($\pi/2 < \theta < 3\pi/2$) and III ($3\pi/2 < \theta < 2\pi$) the scattering map has the following correspondence:

I Extended scattering map $\mathcal{S}_0(I, \theta)$ associated to the horizontal $\mathcal{C}_{\mathrm{M}}(I)$ "under" $\sigma = \varphi$.

II Extended scattering map $\mathcal{S}_1(I, \theta)$ associated to the horizontal $\mathcal{C}_{\mathrm{m}}(I)$.

III Extended scattering map $\mathcal{S}_2(I, \theta)$ associated to the horizontal $\mathcal{C}_{\mathrm{M}}(I)$ "over" $\sigma = \varphi$.

If extended scattering maps are not considered and we just use scattering maps associated to horizontal and vertical crests, one can see that these scattering maps can be divided into 6 regions, i.e., they can be viewed as a combination of up to 6 scattering maps.

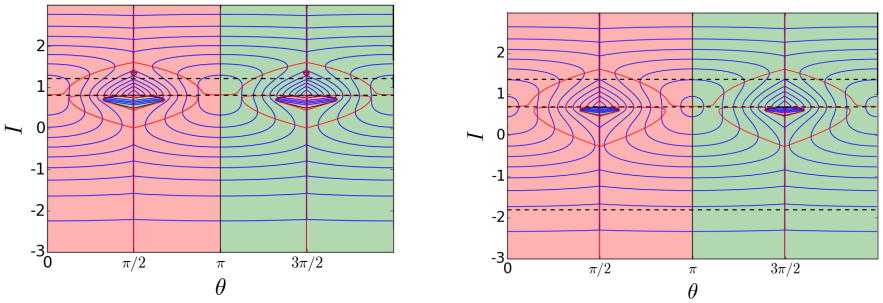

(a) Piecewise scattering map for $\mu = 0.3$.

(b) Piecewise scattering map for $\mu = 0.5$.

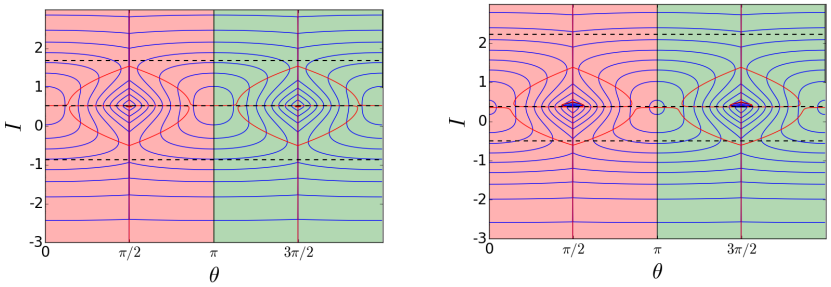

(c) Piecewise scattering map for $\mu = 0.9$.

(d) Piecewise scattering map for $\mu = 1.5$.

Fig. 3.6: Examples of piecewise smooth global scattering maps. The orbits of scattering maps are represented by the blue lines. In the red zones the values of I on such orbits decrease, in the green one the values of I increase.

Another property of these scattering maps is the loss of differentiability on the straight lines $\theta = \pi/2$ and $\theta = 3\pi/2$. The vector field associated to the Hamiltonian $-\mathcal{L}_i^*$ defined around these discontinuity lines behaves as the vector fields studied in non-smooth dynamics theory. More precisely, we can find regions with slide and unstable slide behavior [Fil88]. In a future work, we envisage to design special pseudo-orbits along these discontinuity lines using such theory. Note that these pseudo-orbits would be very similar to the "highways" defined in 2.3 of Chapter 2, so in principle, one can expect fast and simple diffusion along these discontinuity lines.

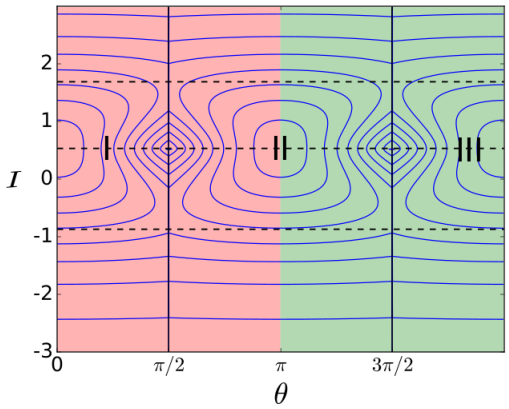

Fig. 3.7: A piecewise smooth global scattering map divided into 3 regions. The vertical black lines are the boundaries of the domains of smooth scattering maps.

Chapter 4

A case of 3+1/2 degrees of freedom

After a study about an *a priori* unstable Hamiltonian system with $2 + 1/2$ degrees of freedom, a natural question is what happens for a similar system with more degrees of freedom. In this chapter, we try to answer, at least partially, this question. Partially because we consider a particular case for $3 + 1/2$ degrees of freedom.

We are going to consider a generalization of the Hamiltonian considered in Chapters 2 and 3, which is given by the *a priori unstable* Hamiltonian with $3+1/2$ degrees of freedom

$$H_\varepsilon(p, q, I_1, I_2, \varphi_1, \varphi_2, s) = \pm \left(\frac{p^2}{2} + \cos q - 1 \right) + h(I_1, I_2) + \varepsilon f(q)\, g(\varphi_1, \varphi_2, s), \tag{4.1}$$

where $f(q) = \cos q$, $h(I_1, I_2) = \Omega_1 I_1^2/2 + \Omega_2 I_2^2/2$ and

$$g(\varphi_1, \varphi_2, s) = a_1 \cos \varphi_1 + a_2 \cos \varphi_2 + a_3 \cos(k \cdot \varphi - s),$$

with $k = (k_1, k_2) \in \mathbb{Z}^2$ and $(\varphi_1, \varphi_2) \in \mathbb{T}^2$.

Remark 55. In [DLS16], the authors dealt with $k = (1, 1)$ as an example for their results.

In this thesis, we restrict our attention to the case with $k = (0, 0)$. There are two main reasons for this restriction: First, this system is a direct generalization of Hamiltonian (2.1)+(2.3) in Chapter 2. So, for this Hamiltonian, we can expect to find a similar behavior of the crests, the existence of global scattering maps and, moreover, the existence of highways. Besides, we have a well-known case to compare with the new results obtained. The second reason is that it is much easier to handle it because we reduced the number of parameters and its inner dynamics is simplified.

Therefore, from now on, we are always assume

$$g(\varphi_1, \varphi_2, s) = a_1 \cos \varphi_1 + a_2 \cos \varphi_2 + a_3 \cos s. \tag{4.2}$$

For a simpler notation, we denote $I = (I_1, I_2)$ and $\varphi = (\varphi_1, \varphi_2)$.

4.1 Unperturbed case

In the unperturbed case ($\varepsilon = 0$), such system is the Hamiltonian system with Hamiltonian

$$H_0(p, q, I, \varphi, s) = \pm \left(\frac{p^2}{2} + \cos q - 1 \right) + h(I),$$

and equations

$$\begin{aligned} \dot{q} &= p & \dot{p} &= \sin q \\ \dot{\varphi}_1 &= \omega_1 & \dot{I}_1 &= 0 \\ \dot{\varphi}_2 &= \omega_2 & \dot{I}_2 &= 0 \\ \dot{s} &= 1, \end{aligned}$$

where $\omega_i = \Omega_i I_i$, $i = 1, 2$. This system consists of a pendulum plus two rotors. From the equations above, I_1 and I_2 are constants and the flow has the form

$$\Phi_t(p, q, I, \varphi) = (p(t),\, q(t), I, \varphi + t\omega),$$

where $\omega = (\omega_1, \omega_2)$. And we have an invariant set (on the extend phase space)

$$\mathcal{T}_I = \{(0, 0, I, \varphi, s); \varphi, s \in \mathbb{T}^3\}.$$

In this case, the NHIM is

$$\tilde{\Lambda} = \{(0, 0, I, \varphi, s) : (I, \varphi, s) \in \mathbb{R}^2 \times \mathbb{T}^3\}, \tag{4.3}$$

4.2 Inner dynamics

The inner dynamics is derived from the restriction of the Hamiltonian (4.1) and its equations to $\tilde{\Lambda}$, given in (4.3), i.e.,

$$K_\varepsilon(I, \varphi, s) = h(I) + \varepsilon \left(a_1 \cos \varphi_1 + a_2 \cos \varphi_2 + a_3 \cos s \right)$$

and its equations

$$\begin{aligned} \dot{\varphi}_1 &= \omega_1 & \dot{I}_1 &= \varepsilon a_1 \sin \varphi_1 \\ \dot{\varphi}_2 &= \omega_2 & \dot{I}_2 &= \varepsilon a_2 \sin \varphi_2 \\ \dot{s} &= 1. \end{aligned}$$

Note that the inner dynamics is integrable, with first integrals

$$F_1(I_1, \varphi_1) = \frac{\Omega_1 I_1^2}{2} + a_1 \left(\cos \varphi_1 - 1 \right) \text{ and } F_2(I_2, \varphi_2) = \frac{\Omega_2 I_2^2}{2} + a_2 \left(\cos \varphi_2 - 1 \right)$$

in involution. The inner dynamics is just the product in the spaces (I_1, φ_1), (I_2, φ_2) of the dynamics described in Fig. 2.2, so there are two resonances centered at $I_1 = 0$ and $I_2 = 0$.

Remark 56. There is a double resonance in $I_1 = I_2 = 0$. The study of the dynamics close to double resonances is a very hard problem, and it is out of the scope of this work. For a interested reader we give some references for about it [Nek77, Las93, CGS03, LMS03, FGL05, LGF09, KZ12, GSV13] . As, in our case, the double resonance is just the point $I = (0, 0)$ and we simply avoid it.

4.3 Scattering map

4.3.1 Definition of scattering map

We are going to explore the properties of the scattering maps of Hamiltonian (4.1)+(4.2). The notion of scattering map on a NHIM was introduced in Chapter 2, Subsection sub:Meln pot and crests. Let W be an open set of $[-I_1^*, I_1^*] \times [-I_2^*, I_2^*] \times \mathbb{T}^3$ such that the invariant manifolds of the NHIM $\tilde{\Lambda}$ introduced in (4.3) intersect transversally along a homoclinic manifold $\Gamma = \{\tilde{z}(I, \varphi, s; \varepsilon), (I, \varphi, s) \in W\}$ and for any $\tilde{z} \in \Gamma$ there exists an unique $\tilde{x}_{+,-} = \tilde{x}_{+,-}(I, \varphi, s; \varepsilon) \in \tilde{\Lambda}$ such that $\tilde{z} \in W^s_\varepsilon(x_-) \cap W^u_\varepsilon(\tilde{x}_+)$. Let

$$H_{+,-} = \bigcup \{\tilde{x}_{+,-}(I, \varphi, s; \varepsilon) : (I, \varphi, s) \in W\}.$$

The scattering map associated to Γ is the map

$$\begin{array}{rcl} S : H_- & \longrightarrow & H_+ \\ \tilde{x}_- & \longmapsto & S(\tilde{x}_-) = \tilde{x}_+. \end{array}$$

For the characterization of the scattering maps, it is required to select the homoclinic manifold Γ and this be done using the Poincaré-Melnikov theory. Again, from [DLS06, DH11], we have the following proposition

Proposition 57. *Given $(I, \varphi, s) \in [-I_1^*, I_1^*] \times [-I_1^*, I_1^*] \times \mathbb{T}^3$, assume that the real function*

$$\tau \in \mathbb{R} \longmapsto \mathcal{L}(I, \varphi - \tau\omega,\, s - \tau) \in \mathbb{R} \tag{4.4}$$

has a non degenerate critical point $\tau^* = \tau^*(I, \varphi, s)$, where $\omega = (\omega_1, \omega_2)$ and

$$\mathcal{L}(I, \varphi, s) := \int_{-\infty}^{+\infty} (f(q_0(\rho)) - f(0))\, g(\varphi + \rho\omega, s + \rho; 0) d\rho.$$

Then, for $0 < \varepsilon$ small enough, there exists a unique transversal homoclinic point $\tilde{z}$ to $\tilde{\Lambda}_\varepsilon$ of Hamiltonian (4.1), which is ε-close to the point $\tilde{z}^*(I, \varphi, s) = (p_0(\tau^*), q_0(\tau^*), I, \varphi, s) \in W^0(\tilde{\Lambda})$:

$$\tilde{z} = \tilde{z}(I, \varphi, s) = (p_0(\tau^*) + O(\varepsilon), q_0(\tau^*) + O(\varepsilon), I, \varphi, s) \in W^u(\tilde{\Lambda_\varepsilon}) \pitchfork W^s(\tilde{\Lambda_\varepsilon}).$$

The function $\mathcal{L}$ is called the *Melnikov potential* of Hamiltonian (4.1). The Melnikov potential takes the form

$$\mathcal{L}(I,\varphi,s) = A_1\cos\varphi_1 + A_2\cos\varphi_2 + A_3\cos s, \tag{4.5}$$

where

$$A_i := A(\omega_i) = \frac{2\pi\omega_i a_i}{\sinh(\pi\omega_i/2)}, \quad i=1,2 \quad \text{and } A_3 = \frac{2\pi a_3}{\sinh(\pi/2)} \tag{4.6}$$

The homoclinic manifold Γ is characterized by the function $\tau^*(I,\varphi,s)$. Once a function $\tau^*(I,\varphi,s)$ is chosen, by the geometric properties of the scattering map, see [DLS08, DH09, DH11], the scattering map has the explicit form

$$S(I,\varphi,s) = \left(I \ + \varepsilon\nabla_\varphi L^* + (\mathcal{O}(\varepsilon^2),\mathcal{O}(\varepsilon^2)), \varphi - \varepsilon\nabla_I L^* + (\mathcal{O}(\varepsilon^2),\mathcal{O}(\varepsilon^2)), s\right),$$

where

$$L^* = L^*(I,\varphi,s) = \mathcal{L}(I,\varphi-\tau^*(I,\varphi,s)\omega, s-\tau^*(I,\varphi,s)). \tag{4.7}$$

Notice that the variable s is fixed under the scattering map. As a consequence [DH11], introducing the variable

$$\theta = \varphi - s\,\omega$$

and defining the *reduced Poincaré function*

$$\mathcal{L}^*(I,\theta) := L^*(I,\varphi - s\omega, 0) = L^*(I,\varphi,s), \tag{4.8}$$

in the variables (I,θ) the scattering map has the simple form

$$\mathcal{S}(I,\theta) = \left(I + \varepsilon\frac{\partial\mathcal{L}^*}{\partial\theta}(I,\theta) + \mathbf{O}(\varepsilon^2), \theta - \varepsilon\frac{\partial\mathcal{L}^*}{\partial I}(I,\theta) + \mathbf{O}(\varepsilon^2)\right), \tag{4.9}$$

where $\mathbf{O}(\varepsilon^2) = (\mathcal{O}(\varepsilon^2),\mathcal{O}(\varepsilon^2))$. So up to $\mathcal{O}(\varepsilon^2)$ terms, $\mathcal{S}(I,\theta)$ is the ε times flow of the *autonomous* Hamiltonian $-\mathcal{L}^*(I,\theta)$. In particular, the iterates under the scattering map follow the level curves of $\mathcal{L}^*$ up to $\mathcal{O}(\varepsilon^2)$.

4.3.2 Crests and NHIM lines

We have seen that the function τ^* plays a central role in our study. Therefore, we are interested in finding the critical points $\tau^* = \tau^*(I,\varphi,s)$ of function (4.4) or, for our concrete case (4.5), τ^* solution of

$$\frac{\partial\mathcal{L}}{\partial\tau}(I,\varphi-\omega\tau,s-\tau) = \omega_1 A_1\sin(\varphi_1-\omega_1\tau) + \omega_2 A_2\sin(\varphi_2-\omega_2\tau) + A_3\sin(s-\tau). \tag{4.10}$$

This equation can be viewed from two equivalently geometrical viewpoints. The first one is that to find $\tau^* = \tau^*(I,\varphi,s)$ satisfying (4.10) for any $(I,\varphi,s) \in [-I_1^*, I_1^*]\times[-I_2^*, I_2^*]\times\mathbb{T}^3$ is the same as to look for the extrema of $\mathcal{L}$ on the *NHIM line*

$$R(I,\varphi,s) = \{(I,\varphi-\tau\omega, s-\tau) : \tau\in\mathbb{R}\}. \tag{4.11}$$

The other viewpoint is that, fixing (I, φ, s), a solution τ^* of (4.10) is equivalent to finding intersections between a NHIM line (4.11) and a surface defined by

$$\omega_1 A_1 \sin\varphi_1 + \omega_2 A_2 \sin\varphi_2 + A_3 \sin s = 0. \tag{4.12}$$

These surfaces are called *crests*, and in a general way can be defined by

Definition 58. [DH11] We define by *Crests* $\mathcal{C}(I)$ the surfaces on (I, φ, s), $(\varphi, s) \in \mathbb{T}^3$, such that

$$\frac{\partial \mathcal{L}}{\partial \tau}(I, \varphi - \tau\omega, s - \tau)|_{\tau=0} = 0,$$

or equivalently,

$$\omega \cdot \frac{\partial \mathcal{L}}{\partial \varphi}(I, \varphi, s) + \frac{\partial \mathcal{L}}{\partial s}(I, \varphi, s) = 0.$$

Note that equation (4.12) can be rewritten as

$$\alpha_1(I_1)\mu_1 \sin\varphi_1 + \alpha_2(I_2)\mu_2 \sin\varphi_2 + \sin s = 0 \tag{4.13}$$

where, for $i = 1, 2$,

$$\mu_i = \frac{a_i}{a_3} \quad \text{and} \quad \alpha_i(I_i) = (\omega_i)^2 \frac{\sinh(\pi/2)}{\sinh(\omega_i \pi/2)}. \tag{4.14}$$

Observe that α_i is well defined for any value of I_i. To understand the intersection between NHIM lines and the crests $\mathcal{C}(I)$, first we need to study how these surfaces look like for different values of μ_i and ω_i, for $i = 1, 2$.

Remark 59. With Eq. (4.13) we wish to emphasize the similarity between such crests with the crests studied in Chapters 2 and 3, in Sections 2.2 and 3.2 respectively.

As explained before, when we have introduced the crests, we are interested in their geometrical behavior. For this purpose, we study their possible parameterization. One can see from (4.13) that if

$$|\alpha_1(I_1)\mu_1 \sin\varphi_1 + \alpha(I_2)\mu_2 \sin\varphi_2| \leq 1 \tag{4.15}$$

we can write s as a function of φ_1 and φ_2, more exactly

$$s = \begin{cases} \xi_{\mathrm{M}}(I, \varphi) = \arcsin\left(\alpha_1(I_1)\mu_1 \sin\varphi_1 + \alpha_2(I_2)\mu_2 \sin\varphi_2\right) \mod 2\pi \\ \xi_{\mathrm{m}}(I, \varphi) = -\arcsin\left(\alpha_1(I_1)\mu_1 \sin\varphi_1 + \alpha_2(I_2)\mu_2 \sin\varphi_2\right) + \pi \mod 2\pi. \end{cases}$$

In accordance with the notation used in Chapters 2 and 3, in Sections 2.2 and 3.2 respectively, the crests $\mathcal{C}(I)$ are formed by two surfaces, they are parameterized by $\xi_{\mathrm{M}}(I, \varphi)$ and $\xi_{\mathrm{m}}(I, \varphi)$ and are called *horizontal* crests. From expression of the function $\alpha_i(I_i)$ given in (4.14), we have $|\alpha_i(I_i)| < 1.03$. This implies

$$|\alpha_1(I_1)\mu_1 \sin\varphi_1 + \alpha_2(I_2)\mu_2 \sin\varphi_2| \leq 1.03(|\mu_1| + |\mu_2|).$$

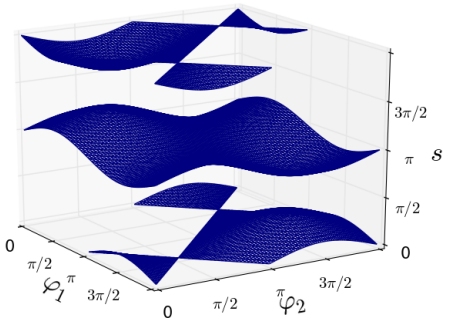

Fig. 4.1: *Horizontal Crests* $\mathcal{C}(I)$: $\mu_1 = \mu_2 = 0.4$ and $\omega_1 = \omega_2 = 1$.

Therefore, if

$$|\mu_1| + |\mu_2| \leq 1/1.03 \approx 0.97,$$

the two surfaces of the crests $\mathcal{C}(I)$ are horizontal for any value of I_1 and I_2.

If condition (4.15) is not satisfied, s cannot be written as a function of φ_1 and φ_2, then we have two possibilities: a) we can write φ_i as a function of φ_j and s, or b) the projection of the crests $\mathcal{C}(I)$ on each plane ((φ_1, φ_2) , (φ_1, s) and (φ_2, s)) has holes.

Case a) is only possible if $\left| \frac{\alpha(I_j)\mu_j}{\alpha_i(I_i)\mu_i} \sin\varphi_j + \frac{\sin s}{\alpha_i(I_i)\mu_i} \right| \leq 1$. Then, the crests $\mathcal{C}(I)$ are formed by two surfaces, they are called *vertical* crests and can be parameterized by

$$\varphi_i = \begin{cases} \eta_{\mathrm{M},i}(I, \varphi_j, s) = \arcsin\left(\frac{1}{\alpha_i(I_i)\mu_i} \left(\sin s - \alpha_j(I_j)\mu_j \sin\varphi_j \right) \right) \\ \eta_{\mathrm{m},i}(I, \varphi_j, s) = -\arcsin\left(\frac{1}{\alpha_i(I_i)\mu_i} \left(\sin s - \alpha_j(I_j)\mu_j \sin\varphi_j \right) \right) + \pi. \end{cases}$$

In case b), Eq. (4.12) defines a unique surface for any crest $\mathcal{C}(I)$, see Fig. 4.2(b). Note that for horizontal and vertical crests $\mathcal{C}(I)$ are formed by two surfaces that can be parameterized separately. In case b), $\mathcal{C}(I)$ is called *unseparated* crest.

To write φ_i as a function of φ_j and s $|\mu_i|$ is needed to be greater than 0.97. In fact, suppose that there exists an I such that $\varphi_i = \varphi_i(\varphi_j, s)$. From Eq. (4.12), we have

$$\sin\varphi_i = -\left(\frac{A_j(I_j)\omega_j \sin\varphi_j}{A_i(I_i)\omega_i} + \frac{A_3 \sin s}{A_i(I_i)\omega_i} \right),$$

for any φ_j and s with $\left| \frac{A_j(I_j)\omega_j \sin\varphi_j}{A_i(I_i)\omega_i} + \frac{A_3 \sin s}{A_i(I_i)\omega_i} \right| \leq 1$. In particular for $\varphi_j = 0$ and $s = \pi/2$, so

$$\left| \frac{A_3}{A_i(I_i)\omega_i} \right| \leq 1, \quad \text{or equivalentely} \quad \left| \frac{1}{\alpha_i(I_i)\mu_i} \right| \leq 1.$$

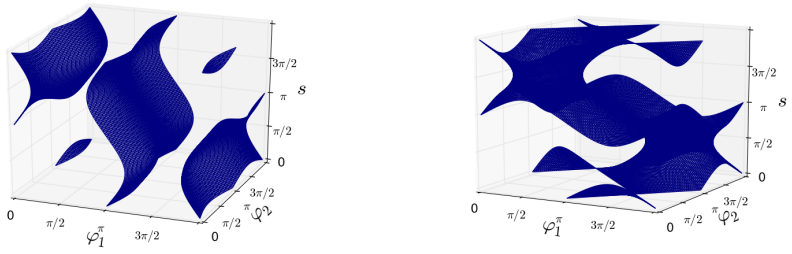

(a) *Vertical Crests* $\mathcal{C}(I)$: $\mu_1 = 1.7, \mu_2 = 0.4$ and $\omega_1 = \omega_2 = 1$.

(b) *Unseparated Crest* $\mathcal{C}(I)$: $\mu_1 = 0.7$, $\mu_2 = 0.7$ and $\omega_1 = \omega_2 = 1$.

Fig. 4.2: Different kinds of Crests

Therefore, we obtain

$$0.97 \approx \frac{1}{1.03} < \left| \frac{1}{\alpha_i(I_i)} \right| \leq |\mu_i| .$$

As a consequence, if $|\mu_1| + |\mu_2| > 0.97$, but $|\mu_1|, |\mu_2| < 0.97$ then there are no vertical crests, only horizontal or unseparated crest.

Tangency condition

We now explore the existence of tangency between the crests $\mathcal{C}(I)$ and the lines $R(I, \varphi, s)$. The crests are a family of surfaces, so there exists a tangency such tangency if a tangent vector of the straight line $R(I, \varphi, s)$ lies on the bundle tangent of one of these surfaces.

The vector tangent of $R(I, \varphi, s)$ at any point is $v = -(\omega_1, \omega_2, 1)$. Consider the function $F_I : \mathbb{T}^3 \mapsto \mathbb{R}$,

$$F_I(\varphi, s) = \alpha_1(I_1)\mu_1 \sin\varphi_1 + \alpha_2(I_2)\mu_2 \sin\varphi_2 + \sin s,$$

we note that the crests $\mathcal{C}(I)$ can be defined as $(\varphi, s) \in \mathbb{T}^3$ such that $F_I(\varphi, s) = 0$. Fixing a point $\mathbf{p} = (\varphi, s)$ in $\mathcal{C}(I)$, the normal vector of $\mathcal{C}(I)$ at the point $\mathbf{p}$ is

$$\nabla F_I(\mathbf{p}) = (\alpha_1(I_1)\mu_1 \cos\varphi_1, \alpha_2(I_2)\mu_2 \cos\varphi_2, \cos s).$$

The vector v lies on the tangent space of the crests at the point $\mathbf{p}$ if, and only if $\nabla F(\mathbf{p}) \cdot v = 0$. This condition is equivalent to

$$\alpha_1(I_1)\omega_1\mu_1 \cos\varphi_1 + \alpha_2(I_2)\omega_2\mu_2 \cos\varphi_2 + \cos s = 0. \tag{4.16}$$

From (4.13) and (4.16), there is tangency between a horizontal crest $\mathcal{C}(I)$ and the NHIM lines $R(I, \varphi, s)$ for φ_1 and φ_2 satisfying

$$(\omega_1\alpha_1(I_1)\mu_1 \cos\varphi_1 + \omega_2\alpha_2(I_2)\mu_2 \cos\varphi_2)^2 + (\alpha_1(I_1)\mu_1 \sin\varphi_1 + \alpha_2(I_2)\mu_2 \sin\varphi_2)^2 = 1$$

Denote by

$$f_I(\varphi) = \left(\omega_1\alpha_1(I_1)\mu_1\cos\varphi_1 + \omega_2\alpha_2(I_2)\mu_2\cos\varphi_2\right)^2 + \left(\alpha_1(I_1)\mu_1\sin\varphi_1 + \alpha_2(I_2)\mu_2\sin\varphi_2\right)^2.$$

Note that, if there are values of μ_1 and μ_2 such that $f_I(\varphi) < 1$ for any I, there is no tangency. As commented before, $|\alpha_i(I_i)| < 1.03$ From (4.14), we obtain $|\alpha_i(I_i)\omega_i| < 1.6$. This implies

$$\begin{aligned} f_I(\varphi) &< (1.6)^2\left(|\mu_1\cos\varphi_1| + |\mu_2\cos\varphi_2|\right)^2 + (1.03)^2\left(|\mu_1\sin\varphi_1| + |\mu_2\sin\varphi_2|\right)^2 \\ &< 1.6^2\,|\mu_1|^2 + 1.6^2\,|\mu_2|^2 + 2\,|\mu_1|\,|\mu_2|\left(1.6^2\,|\cos\varphi_1|\,|\cos\varphi_2| + 1.03^2\,|\sin\varphi_1|\,|\sin\varphi_2|\right) \\ &< 1.6^2(|\mu_1| + |\mu_2|)^2. \end{aligned}$$

It is enough to require $|\mu_1| + |\mu_2| < 1/1.6 = 0.625$ to ensure $f_I(\varphi) < 1$ for any value of I. It is easy to verify that if $|\mu_1| + |\mu_2| > 1/1.6$ there are a I and a φ such that $f_I(\varphi) > 1$.

Proposition 60. *Consider the crest $\mathcal{C}(I)$ defined by* (58) *and the NHIMlines $R(I,\varphi,s)$ defined in* (4.11).

a) For $|\mu_1| + |\mu_2| > 0.625$ the crests are horizontal and the intersections between any crest and any NHIMline are transversal.

b) For $0.625 \le |\mu_1| + |\mu_2| \le 0.97$ the two crests $\mathcal{C}(I)$ are still horizontal, but for some value of I there are NHIMlines which are tangent to the crests.

c) For $0.97 < |\mu_1| + |\mu_2|$ and $|\mu_1|, |\mu_2| < 0,97$, the crests $\mathcal{C}(I)$ are horizontal or unseparated and for some value of I there are NHIMlines which are tangent to the crests.

d) For For $0.97 < |\mu_1| + |\mu_2|$ and $0.97 < |\mu_i|$, The crests $\mathcal{C}(I)$ can be horizontal, vertical or unseparated and for some value of I there are NHIMlines which are tangent to the crests.

4.3.3 Symmetry of the scattering map

Proposition 61. *a) The reduced Poincaré function $\mathcal{L}_0^*(I,\theta)$ is an even function in the variable I, that is, $\mathcal{L}_0^*(I,\theta) = \mathcal{L}_0^*(-I,\theta)$, and consequently the image of $\mathcal{S}_0(I,\theta)$ is geometrically symmetric in this variable I.*

b) The reduced Poincaré function $\mathcal{L}_0^*(I,\theta)$ is symmetric with respect to the straight line $\theta = (\pi,\pi)$, that is, $\mathcal{L}_0^*(I,\theta) = \mathcal{L}_0^*(I,2\pi-\theta)$, where $2\pi - \theta = (2\pi,2\pi) - (\theta_1,\theta_2)$, and consequently the image of $\mathcal{S}_0(I,\theta)$ is geometrically symmetric with respect to $\theta = (\pi,\pi)$.

Proof. a) From (4.5), (4.7) and (4.8), we have

$$\mathcal{L}^*(I,\theta) = A_1\cos(\theta_1 - \omega_1\tau^*(I,\theta)) + A_2\cos(\theta_2 - \omega_2\tau^*(I,\theta)) + A_3\cos(-\tau^*(I,\theta)).$$

From (4.6), it is to verify that A_i is an even function, and therefore,

$$\mathcal{L}^*(-I,\theta) = A_1\cos(\theta_1+\omega_1\tau^*(-I,\theta)) + A_2\cos(\theta_2+\omega_2\tau^*(-I,\theta)) + A_3\cos(-\tau^*(-I,\theta)). \tag{4.17}$$

From (4.12) and (4.12), $\tau^*(I,\theta)$ is the solution of

$$\omega_1 A_1\sin(\theta_1-\omega_1\tau) + \omega_2 A_2\sin(\theta_2-\omega_2\tau) + A_3\sin(-\tau) = 0. \tag{4.18}$$

Analogously, $\tau^*(-I,\theta)$ is the solution of

$$-\omega_1 A_1\sin(\theta_1+\omega_1\tau) - \omega_2 A_2\sin(\theta_2+\omega_2\tau) + A_3\sin(-\tau) = 0.$$

Note that the above equation can be written as

$$\omega_1 A_1\sin(\theta_1-\omega_1(-\tau))\omega_2 A_2\sin(\theta_2-\omega_2(-\tau)) + A_3\sin(-(-\tau)) = 0. \tag{4.19}$$

From the local uniqueness of the solution of (4.18) and (4.19) we can conclude $\tau_j^*(I,\theta) = -\tau_{-j}^*(-I,\theta)$, so $\tau_0^*(I,\theta) = -\tau_0^*(-I,\theta)$ Applying this equality in (4.17), we obtain

$$\mathcal{L}_0^*(-I,\theta) = A_1\cos(\theta_1-\omega_1\tau_0^*(I,\theta)) + A_2\cos(\theta_2-\omega_2\tau_0^*(I,\theta)) + A_3\cos(\tau_0^*(I,\theta)).$$

Therefore, $\mathcal{L}_0^*(I,\theta) = \mathcal{L}_0^*(-I,\theta)$.

Let $(I^+,\theta^+) = \mathcal{S}_0(I,\theta)$ and $(I^-,\theta^-) = \mathcal{S}_0^{-1}(-I,\theta)$, where $\mathcal{S}_0^{-1}$ is the inverse image of the scattering map. We are going to prove that $I^+ = -I^-$ and $\theta^+ = \theta^-$. From (4.9) we have

$$I^+ = I + \varepsilon\frac{\partial\mathcal{L}_0^*}{\partial\theta}(I,\theta) + \mathcal{O}(\varepsilon^2) \quad \text{and} \quad \theta^+ = \theta - \varepsilon\frac{\partial\mathcal{L}_0^*}{\partial I}(I,\theta) + \mathcal{O}(\varepsilon^2).$$

On the other hand, it is easy to verify that $\mathcal{S}_0^{-1}(-I,\theta)$ is

$$I^- = -I + (-\varepsilon)\frac{\partial\mathcal{L}_0^*}{\partial\theta}(-I,\theta) + \mathcal{O}(\varepsilon^2) \quad \text{and} \quad \theta^- = \theta - (-\varepsilon)\frac{\partial\mathcal{L}_0^*}{\partial I}(-I,\theta) + \mathcal{O}(\varepsilon^2).$$

Now, we use the fact that $\mathcal{L}_0^*(I,\theta) = \mathcal{L}_0^*(-I,\theta)$, and so

$$\begin{aligned} I^- &= -I + (-\varepsilon)\frac{\partial\mathcal{L}_0^*}{\partial\theta}(I,\theta) + \mathcal{O}(\varepsilon^2) = -I^+ \\ \theta^- &= \theta - (-\varepsilon)\left(-\frac{\partial\mathcal{L}_0^*}{\partial I}(I,\theta)\right) + \mathcal{O}(\varepsilon^2) = \theta^+. \end{aligned}$$

b) Analogously to the above case, $\tau^*(I,2\pi-\theta)$ is the solution of

$$\omega_1 A_1\sin(2\pi-\theta_1-\omega_1\tau) + \omega_2 A_2\sin(2\pi-\theta_2-\omega_2\tau) + A_3\sin(-\tau) = 0.$$

Or, equivalently,

$$\omega_1 A_1 \sin(\theta_1 - \omega_1(-\tau)) + \omega_2 A_2 \sin(\theta_2 - \omega_2(-\tau)) + A_3 \sin(-(-\tau)) = 0.$$

This implies $\tau^*(I,\theta) = -\tau^*(I, 2\pi - \theta)$.

As the related scattering map depends on which interval the function $\tau^*(I,\theta)$ belongs, we can write $\tau_j^*(I,\theta) = -\tau_{-j}^*(I, 2\pi - \theta)$, $j \in \mathbb{Z}$. Therefore, we have $\tau_0^*(I,\theta) = -\tau_0^*(I, 2\pi - \theta)$. Using this equality and the 2π periodicity of the cosine,

$$\begin{aligned}
\mathcal{L}_0^*(I, 2\pi - \theta) &= A_1 \cos(-\theta_1 + \omega_1 \tau_0^*(I,\theta)) + A_2 \cos(-\theta_2 + \omega_2 \tau_0^*(I,\theta)) + A_3 \cos(\tau_0^*(I,\theta)) \\
&= A_1 \cos(\theta_1 - \omega_1 \tau_0^*(I,\theta)) + A_2 \cos(\theta_2 - \omega_2 \tau_0^*(I,\theta)) + A_3 \cos(-\tau_0^*(I,\theta)) \\
&= \mathcal{L}_0^*(I,\theta).
\end{aligned}$$

Let $(I^+, \theta^+) = \mathcal{S}_0(I, 2\pi - \theta)$ and $(I^-, \theta^-) = \mathcal{S}_0^{-1}(I,\theta)$, where $\mathcal{S}_0^{-1}$ is the inverse image of the scattering map. We want to prove $I^- = I^+$ and $\theta^+ = 2\pi - \theta^-$.

From (4.9) we have

$$\begin{aligned}
I^+ &= I + \varepsilon \frac{\partial \mathcal{L}_0^*}{\partial \theta}(I, 2\pi - \theta) + \mathcal{O}(\varepsilon^2) = I + \varepsilon \left(-\frac{\partial \mathcal{L}_0^*}{\partial \theta}(I,\theta) \right) + \mathcal{O}(\varepsilon^2) \\
&= I + (-\varepsilon) \frac{\partial \mathcal{L}_0^*}{\partial \theta}(I,\theta) + \mathcal{O}(\varepsilon^2) = I^-.
\end{aligned}$$

In the same way,

$$\begin{aligned}
\theta^+ &= (2\pi - \theta) - \varepsilon \frac{\partial \mathcal{L}_0^*}{\partial I}(I, 2\pi - \theta) + \mathcal{O}(\varepsilon^2) \\
&= 2\pi - \left[\theta - (-\varepsilon) \frac{\partial \mathcal{L}_0^*}{\partial I}(I,\theta) + \mathcal{O}(\varepsilon^2) \right] = 2\pi - \theta^-.
\end{aligned}$$

□

Theorem 62 (The general diffusion)**.** *Consider the Hamiltonian* (4.1)+(4.2)*. Assume* $a_1 a_2 a_3 \neq 0$ *and* $|a_1/a_3| + |a_2/a_3| < 0.625$*. Then, for every* $\delta < 1$ *there exists* $\varepsilon_0 > 0$ *such that for every* $0 < |\varepsilon| < \varepsilon_0$*, given* $I_\pm \in \mathcal{I}^* \setminus \{(0,0)\}$*, there exists an orbit* $\tilde{x}(t)$ *and* $T > 0$*, such that*

$$\begin{aligned}
|I(\tilde{x}(0)) - I_-| &\leq C\delta \\
|I(\tilde{x}(T)) - I_+| &\leq C\delta
\end{aligned}$$

Proof. Consider first the case that $I_{2-} = I_{2+}$ so that I_-, I_+ are joined by a horizontal line $\gamma : [0, t^*] \to \mathbb{R}^2$ such that $\gamma(0) = I_-$, $\gamma(t^*) = I_+$, $I_{1-} < I_{1+}$ and $\gamma(t) \neq (0,0)$ for $t \in [0, t^*]$. Given a positive δ, define the finite open covering of the image of the curve γ

$$\bigcup_{i=0}^{N} B_\delta(\gamma(t_i)),$$

where $B_\delta(\gamma(t_i)) = \{p \in \mathbb{R}^2 : \|\gamma(t_i) - p\|_\infty < \delta\}$.

Let $I^i \in B_\delta(\gamma(t_i))$ and $I^i \notin B_\delta(\gamma(t_{i+1}))$. This implies $I_1^i < \gamma_1(t_i) < \gamma_1(t_{i+1})$. We take the vector $u^i = \gamma(t_{i+1}) - I^i$. We want to find a vector v^i satisfying

$$v_1^i u_1^i > 0 \quad \text{and} \quad v_2^i u_2^i > 0.$$

Assume $u_2^i > 0$ ($u_1^i = \gamma_1(t_{i+1}) - I_1^i > 0$). In this case we wish $v_j > 0$, $j = \{1, 2\}$. This implies $I_2^i < \gamma_2(t_i) = \gamma_2(t_{i+1})$. Since

$$v^i = \dot{I}(I^i, \theta^*) = \big(-A_1(I_1)\sin(\theta_1^* - \omega_1^i \tau^*(I^i, \theta^*), -A_2(I_2)\sin(\theta_2^* - \omega_2^i \tau^*(I^i, \theta^*))\big)$$

and assuming a_1, $a_2 > 0$, $v_j > 0$ if, and only if, $\theta_j^* - \omega_j^i \tau^*(I^i, \theta^*) \in (\pi, 2\pi)$.

Since the initial values (I^i, θ^i), we want to use the inner dynamics to displace θ^i to a point $\theta^* \in (\pi, 2\pi)^2$. The inner dynamics is very simple and as Chapter 2 we are going to assume that it is horizontal, i.e., it is described by the equations

$$\dot{I}_j = 0 \quad \text{and} \quad \dot{\varphi}_j = \omega_j, \quad j = 1, 2.$$

And therefore, $\varphi(t) = \omega t + \varphi(0)$. So, we wish to prove the existence of a t^* such that

$$\theta(t^*) - \omega^i \tau^*(I^i, \theta(t^*)) \in (\pi, 2\pi)^2,$$

where $\theta(t) = \theta^i + \omega^i t$.

Define $\psi_j(t) = \theta_j^i(t) - \omega_j^i \tau^*(I^i, \theta(t))$. Without loss of generality we can assume $\omega_1^i \geq \omega_2^i$, we have

$$\psi_2 = \frac{\omega_2^i}{\omega_1^i}\psi_1 + \bar{\psi},$$

where $\bar{\psi} = \theta_2^i - \omega_2^i \theta_1^i / \omega_1^i$. For $\omega_2^i/\omega_1^i \in \mathbb{R} \setminus \mathbb{Q}$, $(\psi_1, \psi_2(\psi_1))$ is dense in $\mathbb{T}^2$, then there exists a t^* such that $(\psi_1(t^*), \psi_2(t^*)) \in (\pi, 2\pi)$.

For $\omega_2^i/\omega_1^i = p/q \in \mathbb{Q}$, $q, p \in \mathbb{Z}$, assume without loss of generality $q\,p > 0$, this implies $0 < \ p/q \leq \ 1$. Now, we look at $\psi_2(\psi_1) = 2\pi p \psi_1/q + \bar{\psi}$ as a rotation by the angle $2\pi p/q$ of C on the S^1. So, we write

$$r_l(\bar{\psi}) = \frac{2\pi p}{q} l + \bar{\psi}.$$

We want to prove that for any $\bar{\psi}$ there exists a $l \in \mathbb{N}$ such that $r_l(\bar{\psi}) \in (\pi, 2\pi]$, so that the straight lines $(\psi_1, \psi_2(\psi_1))$ intersects $(\pi, 2\pi)^2$.

Suppose by contradiction that $r_l(\bar{\psi}) \in (0, \pi]$, $l \in \mathbb{N}$. Note that $r_l(\bar{\psi})$ is a q-periodic function. This implies that there exists a $l' \in \mathbb{N} \setminus 0$ such that $r_{l'}(\bar{\psi}) = \bar{\psi}$. Therefore, if $\bar{\psi} \in (\pi, 2\pi]$ we obtain a contradiction. So, assume $\bar{\psi} \in (0, \pi]$ and consider the orbit $\mathcal{O} = \big\{0, r_1(\bar{\psi}), \ldots, r_{q-1}(\bar{\psi})\big\}$. For $q \neq 1$, if we sort the points of the orbit we have to obtain q equidistant points in S^1. Impossible if $r_l(\bar{\psi}) \in (0, \pi]$, $l \in \{0, \ldots, q-1\}$.

For $q = 1$, $\omega_1^i = \omega_2^i$ and it is easy to verify that $(\psi_1, \psi_2(\psi_1))$ does not intersect $(\pi, 2\pi]^2$ only for $\bar{\psi} = \pi$. We first prove the case that it does not happen.

We want to prove for any $k \in \{0, \ldots, N\}$, I^k is δ-close to the curve γ. We have

$$I^{i+1} = I^i + \varepsilon v^i + \mathcal{O}(\varepsilon^2). \tag{4.20}$$

So, I^{i+1} is δ-close to γ if the following conditions are satisfied

$$I_2^{i+1} < \gamma_2(t_i) + \delta \quad \text{and} \quad I_1^{i+1} < \gamma_1(t_{i+1}) + \delta.$$

From (4.20) and if we consider only the terms of the first order, these conditions are equivalent to

$$\varepsilon < \frac{\gamma_2(t_i) - I_2^i + \delta}{v_2^i} \quad \text{and} \quad \varepsilon < \frac{\gamma_1(t_{i+1}) - I_1^i + \delta}{v_1^i}.$$

Note that $\gamma_2(t_i) - I_2^i < \delta$ and $\gamma(t_{i+1}) - I_1^i > \delta$. Besides, $v_1^i, v_2^i \leq \|v^i\|_\infty$. Therefore, it is enough to require

$$\varepsilon < \frac{\gamma_2(t_i) - I_2^i + \delta}{\|v^i\|_\infty}. \tag{4.21}$$

Define $\varepsilon_i = \sup\left\{\varepsilon : \varepsilon < \frac{\gamma_2(t_i) - I_2^i + \delta}{\|v^i\|_\infty}\right\}$,we obtain for any $0 < \epsilon \leq \varepsilon_i$, I^{i+1} is δ-close to γ. For $u_2 \leq 0$, (4.21) takes the form

$$\varepsilon < \frac{I_2^i - \gamma_2(t_i) + \delta}{\|v^i\|_\infty}.$$

Now we wish to obtain a similar result for any iterate of scattering map. Observe that $\|v^i\|_\infty < 4a$, for any i and $a = \max\{a_1, a_2\}$. Therefore, the result is hold if we consider

$$\varepsilon < \frac{\delta}{4a}.$$

That is, we take $\varepsilon_0 = \sup\left\{\varepsilon : 0 < \varepsilon < \frac{\delta}{4a}\right\}$, and thus for any $\varepsilon < \varepsilon_0$ we obtain a pseudo-orbit δ-close to γ.

Now we come back to the case where $\omega_1^i = \omega_2^i$ and $\bar{\psi} = \pi$. In this case $(\psi_1, \psi_2(\psi_1))$ intersects just $((0,\pi) \times (\pi, 2\pi)) \bigcup ((\pi, 2\pi) \times (0, \pi))$. Now, we consider a finite open cover of the image of the straight line γ given by

$$\bigcup_{i=0}^{N} B_{\delta/2}(\gamma(t_i)),$$

where $B_{\delta/2}(\gamma(t_i)) = \{p \in \mathbb{R}^2 : \|\gamma(t_i) - p\|_\infty < \delta/2\}$. As $u_1^i, u_2^i > 0$, we take $v_1^i > 0$ and $v_2^i < 0$. The image of the scattering map in the variable I is given by

$$I_1^{i+1} = I_1^i + \varepsilon v_1^i + \mathcal{O}(\varepsilon^2) \quad \text{and} \quad I_2^{i+1} = I_2^i + \varepsilon v_2^i + \mathcal{O}(\varepsilon^2). \tag{4.22}$$

The problem is when $I_2^{i+1} < \gamma_2(t_i) - \delta$. From (4.22),

$$I_2^{i+1} > \gamma_2(t_i) - \delta \Leftrightarrow \delta > \gamma_2(t_i) - I_2^i - v_2^i \varepsilon_2^i + \mathcal{O}(\varepsilon^2).$$

As $I^i \in B_\delta(\gamma(t_i))$, we have $\gamma_2(t_i) - I_2^i < \delta/2$. Besides, $\|v^i\|_\infty < 4a$. Therefore,

$$I_2^{i+1} > \gamma_2(t_i) - \delta \Leftrightarrow \delta/2 > 4a\varepsilon.$$

Or explicitly, $I_2^{i+1} < \gamma_2(t_i) - \delta$ for any ε satisfying

$$\varepsilon < \frac{\delta}{8a}.$$

We prove now that this situation is not invariant, we mean, it is not possible in our purpose to obtain $\omega_1^{i+1} = \omega_2^{i+1}$ and $\theta_2^{i+1} - \theta_1^{i+1} = \pi$. We have

$$\begin{aligned}\theta_2^{i+1} - \theta_1^{i+1} &= \theta_2^i - \varepsilon v_2^i - \theta_1^i + \varepsilon v_1^i + \mathcal{O}(\varepsilon^2) \\ &= \pi - \varepsilon\left(v_2^i - v_1^i\right) + \mathcal{O}(\varepsilon^2).\end{aligned}$$

Then, $\theta_2^{i+1} - \theta_1^{i+1} = 0$ if, and only if, $-\varepsilon\left(v_2^i - v_1^i\right) + \mathcal{O}(\varepsilon^2) = 2\pi K$, $K \in \mathbb{Z}$. Since $v_1^i v_2^i < 0$, $K \neq 0$. From the definition of v^i, we have

$$v_1^i = -A_1(I_1)\sin(\theta_1 - \omega_1\tau^*(I^i, \theta^i)) \quad \text{and} \quad v_2^i = -A_2(I_2)\sin(\theta_2 - \omega_2\tau^*(I^i, \theta^i))$$

From $\omega_1^i = \omega_2^i$ and $\theta_2^i = \theta_1^i + \pi$, we obtain $A_2(I_1) = a_2 A_1(I_1)/a_1$ and

$$v_2^i - v_1^i = \left(\frac{a_2 + a_1}{a_1}\right) A_1(I_1)\sin(\theta_1 - \omega_1\tau^*(I, \theta)).$$

Therefore

$$\varepsilon\left|v_2^i - v_1^i\right| < \frac{\delta}{8a} 4(|a_1| + |a_2|) < \delta.$$

So, $-\varepsilon\left(v_2^i - v_1^i\right) + \mathcal{O}(\varepsilon^2) = 2\pi K$ is satisfied only for a *delta* satisfying

$$\delta > 2\pi + \mathcal{O}(\varepsilon^2).$$

But this δ is too big and it is out our interest.

For vertical lines, the same result can be stated *mutatis mutandis*.

For a more general case, that is, C^1-curve $\gamma : [0, t^*] \to \mathbb{R}^2$ such that $\gamma(0) = I_-$, $\gamma(t^*) = I_+$, we take a stairstep curve γ_{step}, a combination of horizontal and vertical lines, in a such way that γ_{step} is a good enough approximation of γ, where "good enough" we mean, the result is hold for γ applying the above results (for horizontal and vertical lines) for γ_{step}.

Using the shadowing lemmas of [FM00, FM03, GLS14] we obtain the desired orbit. □

4.4 Highways

In analogy with Definition 22, in Chapter 2, we define a Highway as an invariant set $\mathcal{H} = \{(I, \Theta(I))\}$ of the Hamiltonian given by the reduced Poincaré function $\mathcal{L}^*(I, \theta)$ which

is contained in the level energy $\mathcal{L}^*(I,\theta) = A_3$. It is therefore a Lagrangian manifold, that is, $\Theta(I)$ is gradient function, i.e., there exists a function $F(I)$ such that $\Theta(I) = \nabla F(I)$. As Θ is a gradient function, it has to satisfy the following condition

$$\frac{\partial \Theta_1}{\partial I_2} = \frac{\partial \Theta_2}{\partial I_1}.$$

This condition is equivalent to

$$\frac{\partial^2 F}{\partial I_2 \partial I_1} = \frac{\partial^2 F}{\partial I_1 \partial I_2}.$$

Proposition 63. *Consider the Hamiltonian* (4.1)+(4.2). *Assume* $a_1 a_2 a_3 \neq 0$ *and* $|a_1/a_3|+|a_2/a_3| < 0.625$. *For* I_1 *and* I_2 *close to infinity, the function* F *takes the asymptotic form*

$$\begin{aligned} F(I) = \frac{3\pi}{2}(I_1+I_2) - \sum_{i=1,2} \frac{2a_i \sinh(\pi/2)}{\pi^4 \Omega_i} \left(\pi^3\omega_i^3 + 6\pi^2\omega_i^2 + 24\pi\omega_i + 48\right) e^{-\pi\omega_i/2} \\ + \mathcal{O}(\omega_1^2\omega_2^2 e^{\pi(\omega_1+\omega_2)/2}), \end{aligned} \tag{4.23}$$

Proof. Assume a candidate of a function $F(I)$ given by (4.23), such that $\Theta = \nabla F(I)$. $\Theta(I)$ has to satisfy the energy level for highways in the reduced Poincaré function

$$\begin{aligned} A_1(I_1)\cos(\Theta_1 - \omega_1\tau^*(I,\Theta)) + A_2(I_2)\cos(\Theta_2 - \omega_2\tau^*(I,\Theta)) \\ + A_3\left(\cos(-\tau^*(I,\Theta)) - 1\right) = 0, \end{aligned} \tag{4.24}$$

and $\tau^*(I,\theta)$ has to satisfy the equation of the crest

$$\begin{aligned} \omega_1 A_1(I_1)\sin(\Theta_1 - \omega_1\tau^*(I,\Theta)) + \omega_2 A_2(I_2)\sin(\Theta_2 - \omega_2\tau^*(I,\Theta)) \\ + A_3\sin(-\tau^*(I,\theta)) = 0. \end{aligned} \tag{4.25}$$

We want to write their version for I_1 and I_2 close to infinity. Using (4.23) we notice that $\Theta_i = \Theta_i(I)$ takes the form

$$\Theta_i = 3\pi/2 - a_i \sinh(\pi/2)\omega_i^3 e^{-\pi\omega_i/2} + \mathcal{O}(\omega_1^2\omega_2^2 e^{\pi(\omega_1+\omega_2)/2}).$$

This implies

$$\cos(\Theta_i - \omega_i\tau^*) = -a_i \sinh(\pi/2)\omega_i^3 e^{-\pi\omega_i/2} - \omega_i\tau_\infty^* + \mathcal{O}(\omega_1^2\omega_2^2 e^{\pi(\omega_1+\omega_2)/2})$$

and

$$\sin(\Theta_i - \omega_i\tau^*) = -1 + \mathcal{O}(\omega_i^6 e^{-\pi\omega_i}),$$

Besides,

$$\cos(-\tau^*(I,\Theta)) = 1 - \frac{\tau_\infty^{*2}}{2} + \mathcal{O}(\tau_\infty^{*4}), \quad \sin(-\tau^*) = -\tau_\infty^* + \mathcal{O}(\tau_\infty^*),$$

where τ_∞^* is an asymptotic approximation of τ^* that we are going to estimate below. First, we notice that the functions $A_1(I_1)$ and $A_2(I_2)$ can be approximated by

$$A_i(I_i) = 4\pi a_i\omega_i e^{-\pi\omega_i/2}\left(1 + e^{-2\pi\omega_i} + \dots\right) = 4\pi a_i\omega_i e^{-\pi\omega_i/2} + \mathcal{O}\left(\omega_i e^{-5\pi\omega_i/2}.\right)$$

From (4.13), the function $\tau^*(I,\Theta)$ satisfies

$$-\tau^*(I,\Theta) = -\arcsin\left(\frac{A_1(I_1)\omega_1}{A_3}\sin(\Theta_1-\omega_1\tau^*(I,\Theta)) + \frac{A_2(I_2)\omega_2}{A_3}\sin(\Theta_2-\omega_2\tau^*)\right),$$

and therefore,

$$\tau^*_\infty \approx \sum_{i=1,2} 2a_i\sinh(\pi/2)\omega_i^2 e^{-\pi\omega_i/2} + \mathcal{O}\left(\omega_i e^{-5\pi\omega_i/2}\right).$$

Applying these estimates in Eq. (4.24) we obtain that the left hand of Eq. (4.24) satisfies

$$\begin{aligned}&\sum_{i=1,2}\Big\{4\pi a_i\omega_i e^{-\pi\omega_1/2}\Big[-a_i\sinh(\pi/2)\omega_i^3 e^{-\pi\omega_i/2} - \omega_i\left(2a_1\sinh(\pi/2)\omega_1^2 e^{-\pi\omega_1/2}\right.\\ &\left.+2a_2\sinh(\pi/2)\omega_2^2 e^{-\pi\omega_2/2}\right)\Big]\Big\} - \frac{A_3}{2}\left(\sum_{i=1,2}2a_i\sinh(\pi/2)\omega_i^2 e^{-\pi\omega_i/2}\right)^2\\ &+\mathcal{O}(\omega_1^2\omega_2^2 e^{-\pi(\omega_1+\omega_2)/2}) = \mathcal{O}(\omega_1^2\omega_2^2 e^{-\pi(\omega_1+\omega_2)/2}).\end{aligned}$$

In the same way, applying in Eq. (4.25) the estimates obtained, we have that the left hand of Eq. (4.25) satisfies

$$\begin{aligned}&-4\pi a_1\omega_1^2 e^{-\pi\omega_1/2} - 4\pi a_2\omega_2^2 e^{-\pi\omega_2/2} + A_3\left(\sum_{i=1,2}2a_i\sinh(\pi/2)\omega_i^2 e^{-\pi\omega_i/2}\right)\\ &+\mathcal{O}(\omega_1^2\omega_2^2 e^{-\pi(\omega_1+\omega_2)/2}) = \mathcal{O}(\omega_1^2\omega_2^2 e^{-\pi(\omega_1+\omega_2)/2}).\end{aligned}$$

Therefore, up to order $\mathcal{O}(\omega_1^2\omega_2^2 e^{-\pi(\omega_1+\omega_2)/2})$, the equation of the crest and the energy level of the reduced Poincaré function are satisfied. □

We finish this chapter with an explicit equation of the highway in a special case.

Proposition 64. *(Highways in a very special case) Consider the Hamiltonian* (4.1)+(4.2) *and* $a_1 = a_2 = a$ *satisfying* $2|a/a_3| < 0.625$ *and* $\Omega_1 = \Omega_2 = \Omega$.

Let $\mathcal{O} = \left\{(I^0,\theta^0),\dots,(I^N,\theta^N)\right\}$ *be an orbit in a highway,* $N \in \mathbb{N}$ *such that* $I_1^0 = I_2^0$ *and* $\theta_1^0 = \theta_2^0$. *Then,* $I_1^i = I_2^i = \bar{I}^i$ *and* $\theta_1^i = \theta_2^i = \bar{\theta}^i$ *for any* $i \in \{0,\dots,N\}$ *and can be described by*

$$\bar{\theta}_h(\bar{I}) = \begin{cases}\arccos\left(\frac{A_3(1-f_-(\bar{I}))}{A(\bar{I})}\right) + \bar{\omega}\arccos(f_-(\bar{I})), & \bar{I}\le 0;\\ \arccos\left(\frac{A_3(1-f_-(\bar{I}))}{A(\bar{I})}\right) - \bar{\omega}\arccos(f_-(\bar{I})), & I > 0;\end{cases}$$

or

$$\bar{\theta}_H(I) = \begin{cases}-\arccos\left(\frac{A_3(1-f_-(\bar{I}))}{A(\bar{I})}\right) - \bar{\omega}\arccos(f_-(\bar{I})), & \bar{I}\le 0;\\ -\arccos\left(\frac{A_3(1-f_-(\bar{I}))}{A(\bar{I})}\right) + \bar{\omega}\arccos(f_-(\bar{I})), & \bar{I} > 0;\end{cases},$$

where $f_-(\bar{I}) = \bar{\omega}A_3 - \sqrt{A_3^2 + (\bar{\omega}-1)\bar{I}^2A^2(\bar{I})}/\left[A_3(\bar{\omega}^2-1)\right]$ *and* $\bar{\omega} = \bar{I}\Omega_1$.

Proof. We have that the trajectories of the scattering map are given by the ε-time flow of the Hamiltonian $-\mathcal{L}^*(I,\theta)$ up to order $\mathcal{O}(\varepsilon^2)$. And such flow is given by the following differential equations:

$$\begin{aligned}\dot{I}_i &= -A_i(I_i)\sin(\theta_i - \omega_i\tau^*(I,\theta)) \\ \dot{\theta}_i &= -\Omega_i\frac{dA_i}{d\omega_i}(I_i)\left(\cos(\theta_i-\omega_i\tau^*) + \tau^*(I,\theta)A_i(I_i)\sin(\theta_i-\omega_i\tau^*(I,\theta))\right),\end{aligned} \tag{4.26}$$

for $i = 1, 2$. Assuming $\Omega_1 = \Omega_2 =: \Omega$ and $a_1 = a_2 =: a$ and taking initial conditions satisfying $I(0) = I^0$ and $\theta(0) = \theta^0$ where $I_1^0 = I_2^0$ and $\theta_1^0 = \theta_2^0$, the solution $(I(t), \theta(t))$ of (4.26) satisfies $\theta_1(t) = \theta_2(t)$ and $I_1(t) = I_2(t)$. Let $\mathcal{O} = \left\{(I^0,\theta^0),(I^1,\theta^1),\ldots,(I^N,\theta^N)\right\}$ be an orbit of the scattering map in a ε-time flow of the Hamiltonian $-\mathcal{L}^*(I,\theta)$ up to order $\mathcal{O}(\varepsilon^2)$, $N \in \mathbb{N}$. Therefore, $I_1^l = I_2^l$ and $\theta_1^l = \theta_2^l$ for any $l \in \{0,\ldots,N\}$. We simply denote $I_1 = I_2$ and $\theta_1 = \theta_2$.

If the orbit $\mathcal{O}$ is a highway, it has to satisfy two equations: the equation of the crests given in (4.12) and

$$\mathcal{L}^*(I,\theta) = A_3.$$

But now, as $I_1 = I_2 =: \bar{I}$, $\theta_1 = \theta_2 =: \bar{\theta}$, $\Omega_1 = \Omega_2$ and $a_1 = a_2$, these equations can be rewritten as

$$\begin{aligned}A(\bar{I})\cos(\bar{\theta} - \bar{\omega}\tau^*(\bar{I},\bar{\theta})) + A_3\cos(-\tau^*(\bar{I},\bar{\theta})) &= A_3 \\ \bar{\omega}A(\bar{\omega})\sin(\bar{\theta} - \bar{\omega}\tau^*(\bar{I},\bar{\theta})) + A_3\sin(-\tau^*(\bar{I},\bar{\theta})) &= 0,\end{aligned}$$

where $\bar{\omega} := \omega_1 = \omega_2$ and $A(\bar{I}) = 4\pi\bar{\omega}a/\sinh(\pi\bar{\omega}/2)$. From a similar approach used in Proposition 23, we obtain the crests are described by

$$\bar{\theta}_{\mathrm{h}}(\bar{I}) = \begin{cases}\arccos\left(\frac{A_3(1-f_-(\bar{I}))}{A(\bar{I})}\right) + \bar{\omega}\arccos(f_-(\bar{I})), & \bar{I} \le 0; \\ \arccos\left(\frac{A_3(1-f_-(\bar{I}))}{A(\bar{I})}\right) - \bar{\omega}\arccos(f_-(\bar{I})), & I > 0;\end{cases}$$

and

$$\bar{\theta}_{\mathrm{H}}(I) = \begin{cases}-\arccos\left(\frac{A_3(1-f_-(\bar{I}))}{A(\bar{I})}\right) - \bar{\omega}\arccos(f_-(\bar{I})), & \bar{I} \le 0; \\ -\arccos\left(\frac{A_3(1-f_-(\bar{I}))}{A(\bar{I})}\right) + \bar{\omega}\arccos(f_-(\bar{I})), & \bar{I} > 0;\end{cases},$$

where $f_-(\bar{I}) = \bar{\omega}A_3 - \sqrt{A_3^2 + (\bar{\omega}-1)\bar{I}^2A^2(\bar{I})}/\left[A_3(\bar{\omega}^2-1)\right]$. □

Chapter 5

Some open questions

5.1 Highways in piecewise smooth global scattering maps

As we showed in Section 3.4, in the piecewise smooth global scattering maps there exist two lines of discontinuity in the vector field of the scattering map. It seems that we can define two special orbits using the theory developed by [Fil88], such that these orbits lie on the lines of discontinuity and behave like the highways defined in Chapter 1.

In a future work we plan to perform numerical experiments to verify whether it is possible to find real orbits of the Hamiltonian behaving like these special orbits in this region of the phase space. After that we wish to exploit these orbits to obtain fast and simple diffusion.

5.2 About the case with 3 + 1/2 degrees of freedom

For the case studied in this thesis, i.e., the Hamiltonian system given by (4.1)+(4.2), in Proposition 63 we obtain an asymptotic approximation of the highways. A next step is to check that this approximation is good enough in order to continue globally those highways to obtain a global description.

Besides, here we have presented results for a restricted set of values of a_1 and a_2, more precisely, for a_1 and a_2 satisfying $|a_1| + |a_2| \leq 0.625$. And we have obtained similar results to the part of the results in Chapter 2. The next step is to eliminate this restriction over the values of a_1 and a_2 and to study the bifurcation of crests, the bifurcation of the scattering maps and the existence of the highways.

Finally, we expect to study the case of a complementary perturbation with respect to (4.2) to cover the complete family case, in an analogous way that we have done in Chapter 3.

5.3 About Shadowing lemmas

Taking into account our numerical experiments, the geometrical mechanisms used in our proof and our estimates for the time, we wish to understand the real role played by the inner map in this mechanism.

Our main question is: Is it really necessary to use the inner dynamics in the building of a pseudo-orbit to guarantee the existence of real orbit of the system?

In our theorems we were able to use the results of [FM00, FM03, GLS14]. In [GLS14] they proved a shadowing lemma for pseudo-orbits built by using a number of iterates of scattering map. But the result appears not to be very practical for fast diffusion.

In the ongoing work we plan to use numerical experiments to verify the existence of real orbits close to pseudo-orbits of a scattering map (or a combination of multiple scattering maps). Besides, in the future we wish to carry out an analytic approach as well.

5.4 Relation between the formulas of the scattering and separatrix maps

The separatrix map was introduced by Zaslavskii and Filonenko in [ZF68], and has been studied and developed in [Tre98, Tre02, Pif06, PT07, GKZ16, DT16]. Under certain conditions we believe that the formulas obtained in [Tre02] can be improved as

$$\begin{aligned}
I^* &= I + \varepsilon\partial_\varphi \mathcal{L}^*(I^*,\varphi,s) - \frac{\partial_\varphi\omega_0}{\lambda}\log\left|\frac{\kappa\,\omega_0}{\lambda}\right| + O_2\\
\varphi^* &= \varphi + \nu - \varepsilon\partial_I \mathcal{L}^*(I^*,\varphi,s) + \frac{\partial_I\omega_0}{\lambda}\log\left|\frac{\kappa\omega_0}{\lambda}\right| + O_1\\
h^* &= H_0 + \varepsilon\partial_s \mathcal{L}^*(I^*,\varphi,s) - \frac{\partial_s\omega_0}{\lambda}\log\left|\frac{\kappa\omega_0}{\lambda}\right| + O_2\\
s^* &= s + \bar{t}\frac{\partial_h\omega_0}{\lambda}\log\left|\frac{\kappa\omega_0}{\lambda}\right| + O_1,
\end{aligned}$$

where λ, κ and μ are functions of I^*, $\bar{t}$ is an integer.

$$\left|s + \bar{t} + \frac{\partial_h\omega_0}{\lambda}\log\left|\frac{\kappa\omega_0}{\lambda}\right|\right| < c^{-1}$$

and $O_1 = \boldsymbol{O}^{(\varepsilon^{\frac{1}{4}})}(\varepsilon^{\frac{7}{8}})\log^2\varepsilon$,$O_2 = \boldsymbol{O}^{(\varepsilon^{\frac{1}{4}})}(\varepsilon^{\frac{5}{4}})\log^2\varepsilon$ and $\mathcal{L}^*$ is a reduced Poincaré function. Since the *Scattering map* takes the explicit form

$$\mathcal{S}_\varepsilon(I,\theta) = \left(I + \varepsilon\,\frac{\partial}{\partial\theta}\mathcal{L}^*(I,\theta) + O(\varepsilon^2), \theta - \varepsilon\,\frac{\partial}{\partial I}\mathcal{L}^*(I,\theta) + O(\varepsilon^2)\right).$$

We expect to verify analytically and numerically these equations.

5.5 About the amount of diffusion trajectories

Along this thesis, we have proved along only the existence of "a" or "some" diffusing trajectories satisfying $I(0) < -I^*$, $I(T) > I^*$. It would be very important to verify, at least numerically, how many of such diffusion trajectories exist, depending on ε. This probably would amount to massive computations, but it would provide a better global understanding of the diffusion of the diffusion process that really takes place.

5.6 And more and more

There are several problems in Celestial Mechanics which give rise naturally to NHIMs, like the center manifolds associated to libration points of the elliptic restricted three body problem, spatial restricted three body problem, the same with Hill problem, double collision in the mentioned problems. There have been already some numerical approximations searching for diffusion, but we think that one can get better understanding searching systematically for crests and (symplectic) scattering maps.

Finally, for general Hamiltonian of $3 + 1/2$ d.o.f one expect to have to use *several* NHIMs, and combine thus different kinds of scattering maps plus the transition between the different NHIMs. This problem appears to be more difficult than the case of diffusion only along one NHIM considered in this thesis, but it is of course more general and deserves a deep attack.

Bibliography

[Arn63] V. I. Arnold. Proof of a theorem of A. N. Kolmogorov on the preservation of conditionally periodic motions under a small perturbation of the Hamiltonian. *Uspehi Mat. Nauk*, 18(5 (113)):13–40, 1963.

[Arn64] V. Arnold. Instability of dynamical systems with several degrees of freedom arnold. *Sov.Math. Doklady*, (5):581 – 585, 1964.

[BCV01] U. Bessi, L. Chierchia and E. Valdinoci. Upper bounds on Arnold diffusion times via Mather theory. *J. Math. Pures Appl. (9)*, 80(1):105–129, 2001.

[Ber10] P. Bernard. Arnold's diffusion: from the *a priori* unstable to the *a priori* stable case. In *Proceedings of the International Congress of Mathematicians. Volume III*, pages 1680–1700. Hindustan Book Agency, New Delhi, 2010.

[BKZ11] P. Bernard, V. Kaloshin and K. Zhang. Arnold diffusion in arbitrary degrees of freedom and crumpled 3-dimensional normally hyperbolic invariant cylinders. *arXiv preprint*, pages 1–58, 2011.

[BM11] A. Bounemoura and J.-P. Marco. Improved exponential stability for near-integrable quasi-convex Hamiltonians. *Nonlinearity*, 24(1):97–112, 2011.

[CDMR06] E. Canalias, A. Delshams, J. J. Masdemont and P. Roldan. The scattering map in the planar restricted three body problem. *Celestial Mechanics and Dynamical Astronomy*, 95(1):155–171, May 2006.

[CG94] L. Chierchia and G. Gallavotti. Drift and diffusion in phase space. *Ann. Inst. H. Poincaré Phys. Théor.*, 60(1):144, 1994.

[CG03] J. Cresson and C. Guillet. Periodic orbits and Arnold diffusion. *Discrete and Continuous Dynamical Systems*, 9(2):451–470, 2003.

[CGL16] M. J. Capinski, M. Gidea and R. de la Llave. Arnold diffusion in the planar elliptic restricted three-body problem: mechanism and numerical verification. *Nonlinearity*, 30(1):329, 2016.

[CGS03] P. M. Cincotta, C. M. Giordano and C. Simó. Phase space structure of multi-dimensional systems by means of the mean exponential growth factor of nearby orbits. *Physica D Nonlinear Phenomena*, 182:151–178, August 2003.

[Che17] C.-Q. Cheng. Dynamics around the double resonance. *Camb. J. Math.*, 5(2):153–228, 2017.

[Cre01] J. Cresson. The transfer lemma for Graff tori and Arnold diffusion time. *Discrete Contin. Dynam. Systems*, 7(4):787–800, 2001.

[Cre03] J. Cresson. Symbolic dynamics and Arnold diffusion. *Journal of Differential Equations*, 187(2):269 – 292, 2003.

[CY09] C.-Q. Cheng and J. Yan. Arnold diffusion in Hamiltonian systems: a priori unstable case. *J. Differential Geom.*, 82(2):229–277, 2009.

[DGR13] A. Delshams, M. Gidea and P. Roldán. Transition map and shadowing lemma for normally hyperbolic invariant manifolds. *Discrete & Continuous Dynamical Systems - A*, 33(1078-0947 2013 3 1089):1089, 2013.

[DGR16] A. Delshams, M. Gidea and P. Roldan. Arnold's mechanism of diffusion in the spatial circular restricted three-body problem: A semi-analytical argument. *Physica D: Nonlinear Phenomena*, 334(Supplement C):29 – 48, 2016. Topology in Dynamics, Differential Equations, and Data.

[DH09] A. Delshams and G. Huguet. Geography of resonances and Arnold diffusion in a priori unstable Hamiltonian systems. *Nonlinearity*, 22(8):1997–2077, 2009.

[DH11] A. Delshams and G. Huguet. A geometric mechanism of diffusion: rigorous verification in a priori unstable Hamiltonian systems. *J. Differential Equations*, 250(5):2601–2623, 2011.

[DLS00] A. Delshams, R. de la Llave and T. M. Seara. A geometric approach to the existence of orbits with unbounded energy in generic periodic perturbations by a potential of generic geodesic flows of $\mathbf{T}^2$. *Comm. Math. Phys.*, 209(2):353–392, 2000.

[DLS06] A. Delshams, R. de la Llave and T. M. Seara. A geometric mechanism for diffusion in Hamiltonian systems overcoming the large gap problem: heuristics and rigorous verification on a model. *Mem. Amer. Math. Soc.*, 179(844):viii+141, 2006.

[DLS08] A. Delshams, R. de la Llave and T. M. Seara. Geometric properties of the scattering map of a normally hyperbolic invariant manifold. *Adv. Math.*, 217(3):1096–1153, 2008.

[DLS16] A. Delshams, R. de la Llave and T. M. Seara. Instability of high dimensional hamiltonian systems: Multiple resonances do not impede diffusion. *Advances in Mathematics*, 294:689 – 755, 2016.

[DMR08] A. Delshams, J. J. Masdemont and P. Roldán. Computing the scattering map in the spatial hill's problem. *Discrete & Continuous Dynamical Systems - B*, 10(1531-3492 2008 2/3, September 455):455, 2008.

[DS97] A. Delshams and T. M. Seara. Splitting of separatrices in Hamiltonian systems with one and a half degrees of freedom. *Math. Phys. Electron. J.*, 3:Paper 4, 40, 1997.

[DS17a] A. Delshams and R. G. Schaefer. Arnold diffusion for a complete family of perturbations. *Regular and Chaotic Dynamics*, 22(1):78–108, 2017.

[DS17b] A. Delshams and R. G. Schaefer. Arnold diffusion for a complete family of perturbations with two independent harmonics. *ArXiv e-prints*, September 2017.

[DT16] M. N. Davletshin and D. V. Treschev. Arnold diffusion in a neighborhood of strong resonances. *Proc. Steklov Inst. Math.*, 295(1):63–94, 2016.

[FGL05] C. Froeschlé, M. Guzzo and E. Lega. Local and global diffusion along resonant lines in discrete quasi-integrable dynamical systems. *Celestial Mech. Dynam. Astronom.*, 92(1-3):243–255, 2005.

[Fil88] A. F. Filippov. *Differential equations with discontinuous righthand sides*, volume 18 of *Mathematics and its Applications (Soviet Series)*. Kluwer Academic Publishers Group, Dordrecht, 1988. ISBN 90-277-2699-X. Translated from the Russian.

[FM00] E. Fontich and P. Martín. Differentiable invariant manifolds for partially hyperbolic tori and a lambda lemma. *Nonlinearity*, 13(5):1561–1593, 2000.

[FM03] E. Fontich and P. Martín. Hamiltonian systems with orbits covering densely submanifolds of small codimension. *Nonlinear Anal.*, 52(1):315–327, 2003.

[GKZ16] M. Guardia, V. Kaloshin and J. Zhang. A second order expansion of the separatrix map for trigonometric perturbations of a priori unstable systems. *Comm. Math. Phys.*, 348(1):321–361, 2016.

[GLS14] M. Gidea, R. de la Llave and T. M. Seara. A general mechanism of diffusion in Hamiltonian systems: Qualitative results, 2014. Preprint, arXiv:1405.0866.

[GM17] M. Gidea and J.-P. Marco. Diffusion along chains of normally hyperbolic cylinders, 2017. Preprint, arXiv:1708.08314.

[GSV13] V. Gelfreich, C. Simó and A. Vieiro. Dynamics of $4D$ symplectic maps near a double resonance. *Phys. D*, 243:92–110, 2013.

[GT14] V. Gelfreich and D. Turaev. Arnold diffusion in a priory chaotic hamiltonian systems, 2014. Preprint, arXiv:1406.2945v2.

[KL08a] V. Kaloshin and M. Levi. An example of Arnold diffusion for near-integrable Hamiltonians. *Bull. Amer. Math. Soc. (N.S.)*, 45(3):409–427, 2008.

[KL08b] V. Kaloshin and M. Levi. Geometry of Arnold diffusion. *SIAM Rev.*, 50(4):702–720, 2008.

[KZ12] V. Kaloshin and K. Zhang. Normally hyperbolic invariant manifolds near strong double resonance. *ArXiv e-prints*, February 2012.

[KZ15] V. Kaloshin and K. Zhang. Arnold diffusion for smooth convex systems of two and a half degrees of freedom. *Nonlinearity*, 28(8):2699–2720, 2015.

[Las93] J. Laskar. Frequency analysis for multi-dimensional systems. Global dynamics and diffusion. *Phys. D*, 67(1-3):257–281, 1993.

[LGF09] E. Lega, M. Guzzo and C. Froeschlé. Measure of the exponential splitting of the homoclinic tangle in four-dimensional symplectic mappings. *Celestial Mech. Dynam. Astronom.*, 104(1-2):191–204, 2009.

[LM05] P. Lochak and J.-P. Marco. Diffusion times and stability exponents for nearly integrable analytic systems. *Cent. Eur. J. Math.*, 3(3):342–397, 2005.

[LMS03] P. Lochak, J.-P. Marco and D. Sauzin. On the splitting of invariant manifolds in multidimensional near-integrable Hamiltonian systems. *Mem. Amer. Math. Soc.*, 163(775):viii+145, 2003.

[LMS16] L. Lazzarini, J.-P. Marco and D. Sauzin. Measure and capacity of wandering domains in gevrey near-integrable exact symplectic systems, 2016. Preprint, arXiv:1507.02050. To appear in *Mem. Amer. Math. Soc.*

[Loc92] P. Lochak. Canonical perturbation theory: an approach based on joint approximations. *Russian Math. Surveys*, 47(6):57–133, 1992.

[LPS17] A. Luque and D. Peralta-Salas. Arnold diffusion of charged particles in ABC magnetic fields. *J. Nonlinear Sci.*, 27(3):721–774, 2017.

[Mar16] J.-P. Marco. Arnold diffusion for cusp-generic nearly integrable convex systems on $\mathbb{A}^3$, 2016. Preprint, arXiv:1602.02403.

[Mat12] J. N. Mather. Arnold diffusion by variational methods. In *Essays in mathematics and its applications*, pages 271–285. Springer, Heidelberg, 2012.

[Nek77] N. N. Nekhoroshev. An exponential estimate of the time of stability of nearly integrable Hamiltonian systems. *Russian Math. Surveys*, 32(6):1–65, 1977.

[Pif06] G. N. Piftankin. Diffusion speed in the Mather problem. *Nonlinearity*, 19(11):2617–2644, 2006.

[PT07] G. N. Piftankin and D. V. Treshchëv. Separatrix maps in Hamiltonian systems. *Uspekhi Mat. Nauk*, 62(2(374)):3–108, 2007.

[SB02] J. Stoer and R. Bulirsch. *Introduction to numerical analysis*, volume 12 of *Texts in Applied Mathematics*. Springer-Verlag, New York, third edition, 2002. ISBN 0-387-95452-X. Translated from the German by R. Bartels, W. Gautschi and C. Witzgall.

[Tre98] D. Treschev. Width of stochastic layers in near-integrable two-dimensional symplectic maps. *Phys. D*, 116(1-2):21–43, 1998.

[Tre02] D. Treschev. Multidimensional symplectic separatrix maps. *J. Nonlinear Sci.*, 12(1):27–58, 2002.

[Tre12] D. Treschev. Arnold diffusion far from strong resonances in multidimensional *a priori* unstable Hamiltonian systems. *Nonlinearity*, 25(9):2717–2757, 2012.

[ZF68] G. Zaslavskii and N. Filonenko. *Stochastic instability of trapped particles and conditions of applicability of the quasi-linear approximation*, volume 25. Soviet Phys. JETP, 1968.

[Zha11] K. Zhang. Speed of Arnold diffusion for analytic Hamiltonian systems. *Invent. Math.*, 186(2):255–290, 2011.